Towards closed-loop stimulation for stroke rehabilitation

Dissertation
der Mathematisch-Naturwissenschaftlichen Fakultät
der Eberhard Karls Universität Tübingen
zur Erlangung des Grades eines
Doktors der Naturwissenschaften
(Dr. rer. nat.)

vorgelegt von
Armin Walter
aus Bietigheim-Bissingen

Tübingen
2013

Tag der mündlichen Qualifikation:	27.01.2014
Dekan:	Prof. Dr. Wolfgang Rosenstiel
1. Berichterstatter:	Prof. Dr. Martin Bogdan
2. Berichterstatter:	Prof. Dr. Wolfgang Rosenstiel

Acknowledgements

I am grateful towards many people who supported and encouraged me throughout the making of this thesis and I would like to take this opportunity to thank them. First, I want to thank Prof. Dr. Wolfgang Rosenstiel for funding and supervising my work and giving me the opportunity to work in his department on this exciting project. I would like to especially thank Prof. Dr. Martin Bogdan for putting his faith in me. His encouragement, support and advice guided me through this work and is greatly appreciated.
A special thanks goes out to my coworkers in the Department of Computer Engineering and in particular the Neuroteam for their support throughout this time: Dr. Dominik Brugger, Dr. Michael Bensch and Dr. Alexander Roth for their help and encouraging discussions at the start of my work. Many thanks to Carina Walter, Markus Dobler, Dr. Martin Spüler and Thomas Kübler for our time together in the office, during many, many lunch breaks in the Mensa, team meetings and all those other activities - for the shared laughs and frustrations, stories and ideas that made the daily work so much easier. The same holds for the other members of the Neuroteam (Anita Dieckgraeff, Dirk Hettich, Enkelejda Kasneci, Jörg Peter, Katrin Sippel, Zahra Khanmirza), the Mensa regulars (Dennis Hospach, Stefan Müller, Werner Dreher) and all other colleagues at the TI.
I would like to thank the people at the Institute for Medical Psychology and Behavioural Neurobiology, in particular Prof. Dr. Niels Birbaumer, Dr. Ander Ramos-Murguialday and everyone involved in the Stroke project. Their guidance and support was invaluable for this work.
I am indebted to everyone who worked on the BCCI project and made this research possible with their commitment. In particular, my thanks go to the people at the Department of Neurosurgery (Prof. Dr. Alireza Gharabaghi, Dr. Georgios Naros, Dr. Florian Grimm and their students) for their hard work, their advice and the enlightening discussions and jokes during those long days, nights and weekends when experiments were planned and conducted.
I would like to thank all people who participated in the experiments, patient or healthy, technicians and students. Without them, this work would not have been possible.
However, without my family and friends who encouraged and supported me whenever I needed it and every once in a while pulled me out of research towards the other important things in life, I would not have been able to get through this time. Therefore, my greatest thanks goes to them.

Summary

The restoration of motor function to chronic stroke patients with a severe hand impairment is challenging, because no effective rehabilitation option exists. In recent years, brain-computer interfaces (BCIs) have shown potential to remedy this problem by decoding the patient's movement intention from the brain signal and translating it into movements of an orthosis. In addition, brain stimulation has been investigated for the treatment of a variety of neurological conditions, including stroke. Combining both approaches into a closed-loop stimulation system has been proposed to increase the effectiveness of this treatment approach. However, this has not been put into practice before, therefore it is unknown, if closed-loop paradigms can be realized for stroke patients.

In this thesis, closed-loop stimulation for stroke rehabilitation is studied for the first time. Two approaches for a closed-loop system are investigated: (i) Stimulation coupled to the movement intention of the patient and (ii) adaptation of stimulation parameters to control the shape of the evoked activity. The focus lies on 3 chronic stroke patients with a paralyzed left hand that had been implanted with epidural electrodes for electrocorticogram (ECoG) recording and electrical stimulation.

To implement intention-dependent stimulation for the first approach, one has to compensate for the distortions introduced by the stimulation after-effects into the brain signal in order to ensure reliable decoding of the movement intentions. Methods to solve this problem are presented and compared in this work. The MEMgap algorithm for spectral estimation in the presence of gaps in the signal is shown to allow an unbiased decoding of the movement intention. With these algorithms, the first bidirectional BCI system used for stroke rehabilitation was implemented.

The second approach, inspired by earlier work on visual neuroprosthetics, aims to reduce the variability of the evoked brain activity through adaptation of stimulation parameters to the ongoing brain activity. Experiments with stroke patients and healthy participants show that the brain activity preceding a stimulation pulse has a significant effect on the shape of the evoked activity but that the interaction of the stimulation intensity with the prestimulus brain activity in the generation of the evoked activity is too weak to make closed-loop stimulation for the stabilization of evoked activity promising. However, based on analysis of the dependency of stimulation-evoked neural activity on stimulation parameters and the brain activity at the moment of stimulation, novel electrophysiological markers for neural connectivity and for rehabilitation are proposed.

This work is one of the first studies on closed-loop stimulation in humans and in particular the first study where such a stimulation paradigm had been applied for stroke rehabilitation. It sets the basis for the use of brain-state-dependent stimulation for stroke rehabilitation and introduces analysis methods for stimulation-evoked potentials to monitor the rehabilitation process and to optimize future stimulation systems.

Zusammenfassung

Da für Schlaganfallpatienten mit Lähmungen der Hand momentan keine generell effektive Therapie existiert, ist die Entwicklung neuer Rehabilitationsverfahren ein wichtiges Ziel um die Effektivität der Physiotherapie zu verbessern. Relevante neue Entwicklungen für diese Arbeit sind kortikale Stimulation zur Erregung des Gehirngewebes und Gehirn-Computer-Schnittstellen (BCIs), die den Willen zur Bewegung der gelähmten Gliedmaße in Steuersignale für Orthesen umsetzen. In dieser Arbeit werden zwei Ansätze für die Kombination dieser Konzepte zu einem closed-loop System untersucht, das Stimulation in Abhängigkeit der aufgenommenen Hirnsignale und der daraus detektierten Intention des Patienten ermöglicht: (i) Zeitliche Kopplung der Stimulation an die Intention des Patienten, seine gelähmte Hand zu bewegen und (ii) Adaption der Stimulationsparameter zur Kontrolle der stimulationsevozierten Potentiale. Der Fokus dieser Arbeit liegt auf 3 Schlaganfallpatienten mit einer Lähmung der linken Hand, denen epidurale Elektroden zur Aufnahme des Elektrokortikogramms und zur elektrischen Stimulation implantiert wurden.

Für den ersten Ansatz muss sichergestellt werden, dass die Stimulationseffekte die Merkmalsextraktion zur Dekodierung der Bewegungsintention möglichst wenig stören. Daher werden in dieser Arbeit Methoden zur Spektralschätzung während Stimulation vorgeschlagen und verglichen. Dabei wird gezeigt, dass der MEMgap-Algorithmus für die Bestimmung autoregressiver Modelle bei lückenhaften Daten, verzerrungsfrei, und damit am besten für die Anwendung geeignet ist. Aus diesen Ergebnissen entstand das erste bidirektionale BCI, das zur Rehabilitation von chronischen Schlaganfallpatienten eingesetzt wurde.

Der zweite Ansatz, inspiriert durch Arbeiten zu visuellen Neuroprothesen, zielt darauf ab, die Variabilität der evozierten Potentialen durch die Anpassung von Stimulationsparametern an das gemessene Gehirnsignal zu verringern. Anhand von Experimenten mit Schlaganfallpatienten und gesunden Probanden wird gezeigt, dass die Hirnaktivität vor einem Stimulationspuls zwar einen signifikanten Einfluß auf die Form der evozierten Potentiale hat, dass aber die Interaktion zwischen der Stimulationsintensität, der Prä- und der Poststimulusaktivität nicht stark genug ausgeprägt ist, um ein closed-loop Stimulationssystem auf dieser Basis vielversprechend erscheinen zu lassen. Durch die Analyse der Abhängigkeit evozierter Potentiale von Stimulationsparametern und der Gehirnaktivität im Moment der Stimulation konnten aber neue elektrophysiologische Marker für neuronale Konnektivität und Rehabilitation vorgeschlagen werden.

Dies ist eine der ersten Arbeiten zur Anwendung von closed-loop Stimulation bei Menschen und das erste Mal, dass die Ableitung von Hirnsignalen und Hirnstimulation zur Rehabilitation gleichzeitig durchgeführt wurde. Sie legt das Fundament für weitere Studien zu bidirektionalen BCIs zur Schlaganfallrehabilitation und eröffnet durch die Analyse evozierter Potentiale neue Möglichkeiten um den Rehabilitationsprozess zu überwachen und neue Stimulationssysteme zu optimieren.

Contents

List of Figures

List of Tables

1 Introduction and motivation

Over the last two decades, the field of neural engineering has emerged at the frontier between neuroscience, biomedical engineering and computer science, aiming to restore or augment neural function. By building direct interfaces with neural tissue, this field shows promise to provide therapies for many neurological disorders. However, the human brain is nowhere near fully understood and the current state of knowledge about it only scratches the surface of the probably most complex "black box" in nature. Thus, the field of neural engineering is constantly evolving, driven both by new neuroscientific findings as well as by advances in hard- and software.
Numerous exciting devices are in development: Sensory neuroprostheses are envisioned to restore lost senses. The most prominent examples are cochlear implants which have found their way into clinical practice already and retinal implants, which are being investigated in clinical trials on their ability to restore at least basic vision. Brain-computer or brain-machine interfaces offer a way for paralyzed patients to regain the possibility to interact with their environment by allowing them for example to type letters or control robots. For the restoration of neuronal function, or neurorehabilitation, one attempts to repair neurological damage through the interaction of the patient with specialized devices. Neuromodulation through drugs or brain stimulation might be promising in this regard as it can directly alter neural activity.
Great challenges for all these applications are the individuality of each patient, the typically very large number of degrees of freedom in designing a suitable treatment paradigm and in general the limited understanding about the inner processes of the brain, how they contribute to the pathophysiology of the patient and how they can be influenced most effectively. These questions are typically studied in single cases or small patient groups, but the hope is to identify approaches which might generalize to the whole patient group or, when transfered to novel patient groups, leading to new treatment options for these patients.

In this thesis, the feasibility of such a knowledge transfer is investigated. It focuses on the application of closed-loop stimulation, inspired amongst others by a paradigm developed for a visual neuroprosthesis [23], to stroke patients for movement restoration. In typical fashion for neural engineering projects, as this approach has not been attempted before, this work is as much about solving algorithmic and technical challenges to apply closed-loop stimulation to stroke patients as it is about

gaining new insights into their brain function such that one might be able to derive treatment paradigms from it.

1.1. Stroke

A stroke is a cardiovascular accident in the brain which severs the blood supply to certain brain areas. Two types of stroke have to be distinguished: *Ischemic* stroke, the most common form, is responsible for about 90 % of all stroke cases [6]. It occurs because of the blockage of a blood vessel, for example due to a clot. *Hemorraghic* stroke, on the other hand, is less common and can follow the rupture of a blood vessel leading to bleeding in the brain. Brain tissue that had been supplied by the disrupted vessel with oxygen and nutrients is then at risk of receiving permanent damage or even cell death (a *lesion*), possibly leading to the loss of functions associated with the affected brain areas. Thus, the site of the lesion determines the symptoms following the stroke. Physical disabilities are very common, such as problems of moving muscles on one side of the body (hemiparesis) or difficulties of speaking.

Stroke is the leading cause of adult disability in the developed world and the third most common cause of death [103, 113]. In its "Atlas of Heart Disease and Stroke" [113], the World Health Organization (WHO) estimated a total number of 15 million stroke case worldwide each year with a mortality rate of one-third and puts the number of people permanently disabled by the stroke at 5 million per year. Following the stroke, 80 - 85 % of all survivors suffer at least temporarily from hemiparesis [45] and/or sensorimotor deficits in the upper arm [39], leading to a reduced quality of life [105]. Therefore, effective rehabilitation methods are needed to treat these patients.
Faster and more reliable rehabilitation would not only be in the interest of the patients. The current situation places an immense burden on families and the society as a whole in order to provide treatment options and/or long-term care for stroke survivors. Kolominsky-Rabas et al. [96] estimated the lifetime cost of ischemic stroke in Germany to be 40,000 - 45,000 € per case for a total of 108.6 billion € for the time period between 2006 and 2025. 37 % of this estimation were costs for rehabilitation. For the United States, the impact of new and recurring strokes on the health care system for the year 2007 alone was estimated at more than 62 billion $ [105]. Thus, the socioeconomic impact of improved therapies would be immense as well, especially considering that the aging process of the society will likely lead to an increase in the number of stroke cases in the future.

1.2. Stroke rehabilitation

In a review on the topic of motor recovery, Langhorne et al. [103] stated: "Motor recovery after stroke is complex and confusing". The established way to treat patients who suffer from movement impairments following stroke is physical therapy, where the patient, guided and encouraged by the therapist, performs exercises in addition to other interventions such as manual therapy over an extended period of time - at least several weeks, often months and years. Achieving functional recovery is especially challenging for the upper limb [82]. 6 months after the stroke, more than half of all stroke patients have persisting sensorimotor impairments in the arm [39] and only about 20 % of all stroke survivors with severe paresis of the upper limb achieve full recovery [102, 125]. One third of all stroke patients have poor to no hand function even one year after the stroke [27]. Thus, the current state of rehabilitation of upper limb function, in particular the hand, is not satisfactory [82].
A reason for this might be that hand and arm movements are less stereotypical than movements of lower extremities, thus it is easier to retrain gait and mobility than the coordinated movements of multiple joints necessary for effective upper limb function [105]. A multitude of novel techniques for rehabilitation have been developed and tested in recent years in randomized controlled trials (RCTs). In 2009, Langhorne et al. [103] reviewed RCTs of 19 methods on their effectiveness for lower limb, arm and hand recovery. Although they identified methods that consistently improve lower limb and arm function, no method achieved the same for hand function. For example, while robotics, constraint-induced movement therapy and functional electrostimulation of muscles are likely to be beneficial for arm function, the same methods did not consistently lead to an improvement of hand function. Thus, a patient in the chronic state several months after the stroke with persisting impairment of the hand function has at the moment no promising treatment option available except to continue with the classical rehabilitation approaches. Hence, novel technologies are needed to provide a new perspective for rehabilitation for patients with hand paralysis and also to further improve on recovery of the other limbs.

Recently, two new approaches have emerged that have shown promise in this regard: Brain-computer interfaces (BCIs) (e.g. [27, 65, 138]) and cortical stimulation (e.g. [1, 21, 79, 106]). BCIs for stroke rehabilitation use the phenomenon that the intention to perform a movement or just the visualization of a movement (*motor imagery*) can be decoded from the brain signal, even for intended or imagined movements of a paralyzed limb [7]. The result of the decoding (e.g. "Patient tries to move the paralyzed hand") can then be used to control a feedback device, such as an orthosis or a robot capable of moving the paralyzed hand of the patient [27, 65, 138], or for example visual feedback on a monitor [173]. Thus, the sensorimotor feedback loop of (i) intention to perform a movement, (ii) movement is performed, (iii) visual or haptic feedback of the movement, which was severed by the stroke, is reconnected

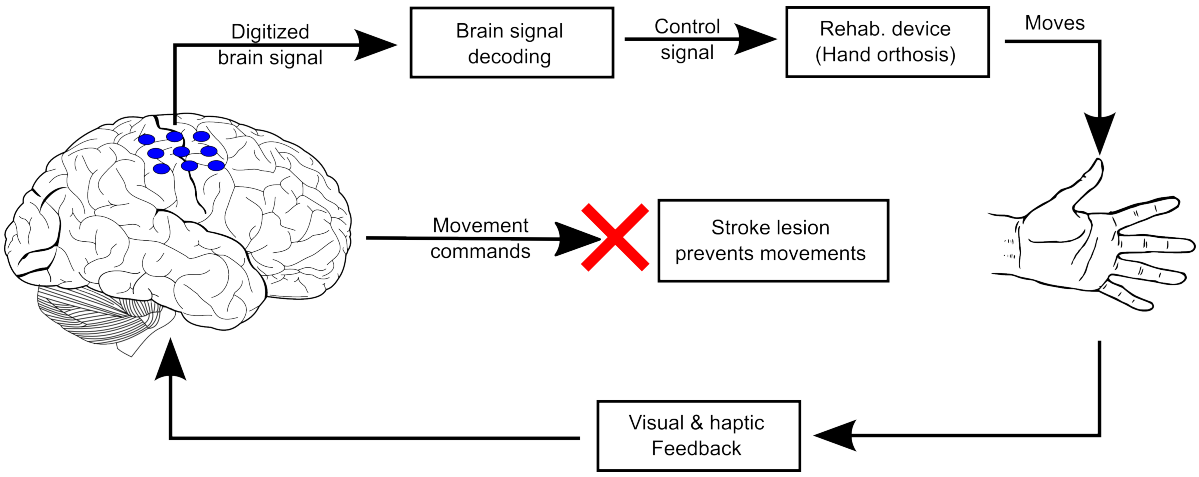

Figure 1.1.: Flow chart of the application of a BCI for hand movement rehabilitation. In this example, the connection between the brain and the muscles of the patient has been severed by the stroke, thus prohibiting the transmission of movement commands. However, by decoding the movement intention from neural signals, an orthosis can be controlled to move the hand of the patient in the desired manner.

using the BCI as a ”bypass” for the lesion (figure 1.1). Repeated training with such a feedback device might support the brain to use residual cortico-muscular connections more effectively through principles of Hebbian plasticity [138].

Cortical stimulation aims to (re-)activate cortical areas which had been associated with the now lost motor function, but have been damaged by the stroke. In contrast to the BCI approach, where there is only one (very recent) publication of a controlled study on its benefit [138], several systematic tests with the stimulation approach have been published in the last decade: Results from first clinical studies supported by Northstar Neuroscience (Seattle, WA) about the efficacy of cortical stimulation combined with physiotherapy for hand function recovery following stroke have been reported between 2006 and 2009 [21, 79, 106, 136]. Based on results from Phase I and II trials with 8 [21] and 24 patients [106], respectively, cortical stimulation was found to be safe and possibly beneficial for stroke rehabilitation because the improvement in motor function of stimulated patients was significantly better than for control groups. However, a Phase III study with 146 patients could not confirm these results.
Subsequently, the design of the study and the stimulation parameters have been reviewed critically to gain insights for future trials. In their examination of this clinical study, it has been suggested by Plow et al. [136] to consider, among other points, ”brain activity before or after stimulation”, state-dependency of stimulation effects and closed-loop systems to improve the combination of cortical stimulation and rehabilitation. Thus, a transition might be sensible from using only stimulation towards a combination of stimulation with brain signal recording and, in particular

for closed-loop systems, towards a real-time adjustment of stimulation parameters depending on the measured brain activity.

The concepts of brain-activity-dependent selection of stimulation parameters, decoding brain states and giving state-dependent feedback and in general closed-loop feedback stimulation are very similar to the basic parts of BCIs - the difference being, that current BCIs do not employ cortical stimulation in order to close the feedback loop. Instead, other external devices such as a computer screen or robots are used which rely on afferent sensory channels to relay information to the brain. Cortical stimulation is a direct afferent channel to the brain. Hence, the inspiration of this thesis is the idea that the principles of BCIs (online brain signal analysis, brain state decoding, closed-loop feedback), when transferred to cortical stimulation, could allow "smart", more effective stimulation paradigms for movement restoration, because stimulation parameters would be optimized to the patient and his/her brain activity [171]. However, to achieve this, one has to determine, which kinds of closed-loop stimulation systems are feasible and applicable to stroke patients.

1.3. Problem statement

In this thesis, two approaches are proposed that investigate more intelligent ways to deliver cortical stimulation by utilizing the ongoing brain activity for the selection of stimulation parameters (*closed-loop stimulation*). The first approach is based on the principle of brain state-dependent stimulation (BSDS) [85], adapted to the rehabilitation of stroke patients. The BSDS paradigm works by detecting attempts of the patient to move the paralyzed limb, interpreting the presence or absence of this intention as a brain state, then controlling rehabilitation devices and the cortical stimulation in reaction to the detected brain state. In its simplest form, the cortical stimulator can be switched on and off depending on whether the patient attempts a movement. Hence, the timing of the stimulation is adapted to the ongoing brain activity and the brain state decoded from it. The intended effect is that the stimuli are specifically associated by the brain with the desired state of an attempt to move the hand. The main challenge that has been solved by the algorithms developed in this thesis is to ensure that the brain state can be decoded reliably in the presence of the artifacts and other undesirable after-effects of simultaneously applied cortical stimulation.

The second approach is based on earlier animal studies by Brugger [23] who demonstrated that the variance of the stimulation-evoked brain activity can be reduced by an adaptation of the stimulation intensity to the ongoing brain activity. In the context of stroke rehabilitation this might be useful if one is able to define, which shape of the evoked activity will be most beneficial for recovery of the pa-

tient and then use adaptive stimulation to reliably evoke this particular waveform. The challenge for this approach, apart from the question of how to the define the target waveform, is the transfer of the results obtained in this earlier study with rats and invasive microelectrodes to human patients - not only because it is a step from an animal model to humans, but also because of the microelectrodes. These have not been applied before to human stroke patients, thus less invasive methods might be preferable. It is an open question whether closed-loop stimulation to control the shape of the evoked activity can also be realized for these patients when using recording and stimulation methods more suited to human patients such as electroencephalography (EEG) combined with transcranial magnetic stimulation (TMS) or electrocorticography (ECoG) combined with stimulation via epidural or subdural electrodes. A major prerequisite for the feasibility of such an adaptive stimulation paradigm is that there has to be a functional relationship between the ongoing brain activity, stimulation parameters and the evoked activity [23]. Thus, the main question addressed in this thesis for the second approach for closed-loop stimulation is whether such a functional relationship can be identified with these less invasive recording and stimulation methods to allow an adaptive stimulation system.

1.3.1. Structure of the thesis

The thesis is organized as follows: Chapter 2 gives an introduction into brain stimulation and electrophysiological recording techniques, open-loop and closed-loop stimulation systems, and the use of brain-computer interfaces (BCIs) and brain stimulation for stroke rehabilitation. Furthermore, a general introduction is given into classification and regression algorithms with a focus on Support Vector Machines (SVMs) because these are important throughout the thesis for decision making from brain signals. In chapter 3, the main research questions are reviewed and an introduction into the research framework, the patients and the experiments is given. In chapter 4, the approach of brain-state-dependent stimulation (BSDS) is introduced as a way to integrate cortical stimulation and BCIs to form a novel rehabilitation paradigm for stroke patients. With this approach, however, the problem of a robust detection of the intention of the patient in the presence of stimulation artifacts arises. Algorithms that tackle this problem are proposed and compared on their suitability for continuous brain state decoding with simultaneous brain stimulation. It is also shown, how the BSDS approach was put into practice and applied to the patients.
The feasibility of the second closed-loop approach of adaptive stimulation to control the evoked activity is studied in chapters 5 and 6. Here, the focus lies on the postulated existence of a functional relationship between the prestimulus activity, the stimulation parameters and the poststimulus brain activity. In chapter 5, experiments are described and analyzed where the stimulation parameters were kept constant in order to investigate the direct influence of the prestimulus activity on the stimulation-evoked signals. It is shown that the brain state at the moment of

stimulation significantly modulates the shape of the evoked activity, but that there is almost no direct influence of the prestimulus spectrum on the stimulation effects. Another set of experiments is described in chapter 6, devised to study the interaction between the prestimulus activity and the stimulation intensity in the generation of the poststimulus activity. However, no such interaction could be identified, shedding strong doubt over the feasibility of the adaptive stimulation approach in patients. The results and their implications for closed-loop systems and other future stimulation paradigms for patients are discussed in chapter 7. In the appendix, the details of the patients (appendix A) participating in the studies are summarized and a detailed description of the procedures in the main experiments (appendix B) are given.

2 Fundamentals

2.1. Interfacing with the brain

In order to realize closed-loop stimulation as a novel rehabilitation method, the most basic prerequisite needed is a bidirectional interface with the brain of the patient: First, one needs to record and analyze the brain signals, for example to determine whether a patient wants to move the paralyzed limb or not, thus a technology is needed to record the brain activity. Secondly, methods are needed to stimulate the neurons. And thirdly, these methods need to be compatible such that stimulation and recording is possible simultaneously. Thus, in the first section, methods are reviewed to record neural signals and to apply brain stimulation.

2.1.1. Recording

There are a multitude of possibilities to record brain activity, ranging from the blood-oxygen-level dependent (BOLD) response measured by functional magnetic resonance imaging (fMRI) and near-infrared spectroscopy (NIRS) to magnetoencephalography (MEG) which measures the magnetic fields caused by neural activity. In this work, however, electrophysiological methods to record the electrical activity of neurons are used. The most important types, electroencephalography (EEG), electrocorticography (ECoG) and recording via microelectrodes, are introduced in this section.

Electroencephalography (EEG)

The EEG is a fairly easily applicable, noninvasive technique to record brain activity with high temporal resolution. After work in the late 19th century, especially in Eastern Europe, on the electrical brain activity in animals [127], the first human EEG was obtained by Hans Berger in 1924 [12]. He discovered that oscillations of the measured signal in the frequency range around 10 Hz are much stronger present if the subject has the eyes closed than for open eyes - the so-called alpha blocking response. Over the following decades, the EEG gained credence as a tool for the diagnosis of a variety of neurological diseases, in particular epilepsy.
The EEG is recorded by electrodes fixed to the scalp, positioned according to a

standardized system such as the 10-20 system [5]. The signal recorded from these electrodes is generated by extracellular field potentials [127] of a cortico-thalamic network and is typically analyzed in terms of *oscillations* in the spectral domain or *event-related potentials* in the time domain. The EEG oscillations are grouped into frequency bands: δ (below 3.5 Hz), θ (4-7.5 Hz), α (8-13 Hz), β (14-30 Hz) and γ (above 30 Hz), although several subdivisions and additional rhythms have been proposed [127]. Event-related potentials are detected in the time domain as summed activity of neural populations time-locked to a stimulus. According to Nunez and Srinivasan [130], several tens of millions of neurons have to be consistently active to produce measurable potentials at the scalp.

Electrocorticography (ECoG)

The very first human EEG recordings by Berger [12] were actually performed with dural electrodes in patients with skull defects, thus he also pioneered the cortical EEG, or *electrocorticogram* (ECoG) [127]. The basic difference to EEG recordings is that it requires an invasive procedure, where electrodes are placed between the brain and the skull instead of being fixed on the scalp. Obviously, this requires a surgery, thus the technique is limited to works with patients and animals. The implantation of ECoG electrodes has evolved into common clinical practice, especially for the localization of seizures in epilepsy patients, but there exists an infrequent risk of complications [58]. In particular, if the electrodes are connected to an external amplifier, infections can be problematic. Thus, such external connections are rarely used for more than 2-4 weeks, before either the electrodes are removed or all cables and devices are internalized.
However, these risks for the patient have to be weighed against the better signal-to-noise ratio that can be obtained by ECoG in comparison to EEG, due to the smaller distance to the brain and the removal of the influence of the skull. An important effect of this is that the usable bandwidth in BCI experiments is higher for ECoG than EEG, allowing the use of frequencies in the higher γ band. These high frequency components have been very useful to decode information from the brain signal which is inaccessible from EEG, for example the discrimination between movements of individual fingers [120]. However, the ECoG signal is not superior to the EEG in all regards. Nunez and Srinivasan [130] described the difference between ECoG and EEG recordings as the first one seeing only the trees, the second one only the forest. The use of ECoG offers a small window into the brain to observe local activity with high spatial resolution and bandwidth. However, it is usually only possible to implant the electrodes in a small portion of the cortex, whereas the EEG, can measure global neural activity across the whole head.
A second advantage of implanted electrodes over scalp electrodes is that they can also be used to deliver electrical stimulation (see below). Thus, these electrodes offer a way to realize a bidirectional interface with the brain. ECoG electrodes can

be placed either sub- or epidural with epidural placement considered to be the less invasive alternative, because the dura mater is not opened and the electrodes are not in direct contact with the brain. Modeling studies suggest, that there is little or no loss of signal quality from subdural to epidural placement [154].

Microelectrodes

Microelectrodes can be discriminated from macroelectrodes, such as those used for EEG and ECoG, unsurprisingly by their size and their position relative to the brain. According to Cogan [40], microelectrodes typically have a surface area less than 10,000 μm^2 and penetrate the brain tissue, while macroelectrodes have a surface area of more than 100,000 μm^2 and are located on the surface of the brain or the scalp. The first microelectrode studies were undertaken in the 1950s with microwire arrays and have evolved since then to multielectrode arrays (MEAs) containing up to 100 electrodes. The electrodes are inserted into the brain tissue, thus this technique has to be considered to be more invasive than the ECoG electrodes because brain tissue damage is more likely. Because of this, their use for human patients is limited to a handful of cases, but when used to acquire signals from tetraplegic patients to control a computer cursor [77] and a robotic arm [42, 76], intended movements were decoded with high accuracy and up to 7 degrees of freedom without explicit training of the participant. In comparison to the methods above, microelectrodes offer the unique possibility to record action potentials from single neurons, while millions of neurons have to be simultaneously active to be measured by macroelectrodes.

2.1.2. Stimulation

While the recording of brain activity can be used to construct an efferent pathway from the brain to peripheral devices, brain stimulation allows the direct transmission of information into the brain (afferent pathway) without the need to transmit the information through sensory channels. A short overview of brain stimulation methods is given here, distinguished by the criterion whether the stimulation is applied non-invasively (transcranial) or invasively (intracranial).

Transcranial stimulation

To stimulate the brain transcranially, two methods are used: Electrical stimulation via large surface electrodes in the form of transcranial direct or alternating current stimulation (tDCS/tACS) or transcranial magnetic stimulation (TMS) [137, 170]. Because this work is concerned with pulsed stimulation, not with continuous stimulation, only TMS is described here. TMS was introduced in 1985 by Barker et al. [8] and has since then become one of the most important tools for the study, diagnosis and therapy of the nervous system via non-invasive stimulation [88]. To apply

TMS, a coil is placed on the scalp above the target point of stimulation. A rapid, time-varying magnetic field is generated by the coil, inducing a current in the brain which activates cortical neurons, especially at fiber terminations and axon bends [51]. Such an induced activation can then indirectly modulate the activity of distant neurons.
Several different stimulation paradigms exist for TMS, depending on the application: Single pulse TMS can be used to probe cortical excitability of a specific area at precise time points which is useful for the study of brain function and organization. The first and still most popular single pulse paradigm is to stimulate the motor cortex. This can elicit twitches in the muscles associated with the stimulated area, given a suitably high intensity, which helps to identify properties of the cortico-muscular connections. Repetitive TMS (rTMS), where a large number of stimulation pulses are given with a fixed inter-stimulus interval, on the other hand is investigated for therapy in a variety of conditions, from depression [44] to stroke rehabilitation [129] and amyotrophic lateral sclerosis (ALS) [47], because of its effect of modulating the excitability of the stimulated region [56].

Intracranial stimulation

There are three basic ways to deliver intracranial electrical stimulation: Epidural/subdural electrodes, depth electrodes and cortical microelectrodes. Using the first type of electrodes, the pioneering work of Penfield and Jasper resulted in the discovery of the somatotopic organization of the somatosenory areas [134]. Today, cortical stimulation via epidural or subdural electrodes is not only used for such cortical mapping applications [104, 117, 118], but also for therapy, for example in the case of chronic pain [162] and epilepsy [156]. Typically, short ($\leq$ 1 msec) mono- or biphasic pulses are used, either as single pulses or as pulse trains with frequencies of 20 Hz and above [20, 104]. Intensities for cortical mapping are chosen to be high enough to evoke cortical and peripheral potentials (see next section, suprathreshold, $>$ 1 mA [104]) from one or just a few pulses. For therapeutic stimulation the intensities are set much lower (subthreshold), but the stimulation is delivered in pulse trains lasting for minutes, hours or even longer [20, 79].
For deep brain stimulation (DBS), depth electrodes are implanted, for example to treat Parkinson's disease [10, 178] or Tourette's syndrome [148]. Its purpose is to target deeper brain structures which can not be reached by surface electrodes. Some cortical areas, for example the insular cortex [132], also lie too far from the surface, thus stimulation is applied via depth electrodes.
Unlike most DBS applications, multielectrode arrays as the third subtype of intracranial stimulation again target cortical neurons. Their implantation requires a penetration of the brain tissue, thus they are rarely an option for human patients. With the exception of a case study where microelectrodes were used to stimulate the visual cortex of a blind woman [151], intracortical microstimulation (ICMS) via

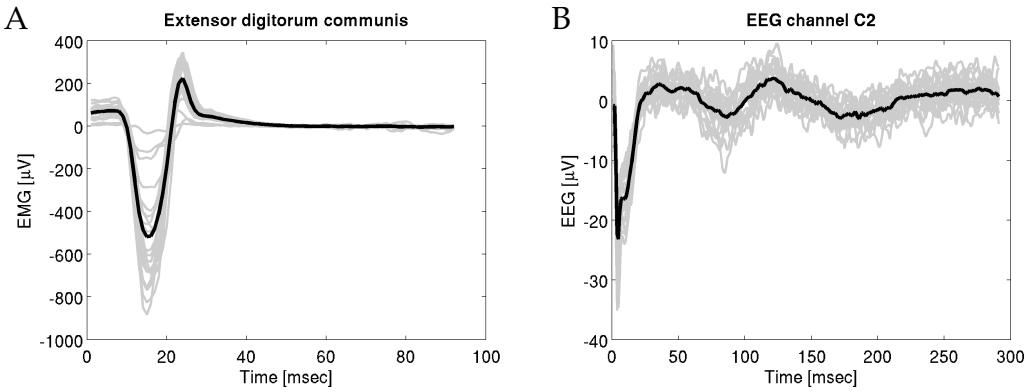

Figure 2.1.: 19 evoked responses of a healthy participant after TMS. Each individual response is shown as a grey line and the mean as a black line. **(A)**: MEPs on the finger extensor muscle EDC. **(B)**: Responses on EEG channel C2, close to the location of stimulation near EEG channel C4.

these electrodes has so far been only applied to animals. The much smaller scale of stimulation compared to epidural/subdural electrodes allows very specific stimulation. This makes these electrodes good candidates to study closed-loop stimulation paradigms such as those described in section 2.3.2.

2.2. Stimulation-evoked neural activity

Valuable information about the way stimulation interacts with active neural networks can be extracted on brain signal (EEG, ECoG) and muscle signal recordings (electromyography, EMG) from the analysis of stimulation-evoked activity. These signals contain not only electrophysiological correlates of the stimulation effects, but allow insights into the functional connectivity of neural populations [71, 117]. Two forms of evoked potentials can be distinguished:

- **Motor-evoked potentials (MEPs)**: If stimulation with a sufficient intensity is applied over the motor cortex, neurons of the pyramidal tract can be excited and a volley of activation travels via the cortico-spinal tract to the motor unit, resulting in a muscle contraction. This muscle twitch can be measured using EMG, where a MEP is found typically with a latency between 10 and 30 msec after the pulse. This finding can be used to perform a cortical mapping procedure, where systematically points on the cortex are stimulated with different intensities and MEPs are measured. With this, a *hotspot* can be defined for each muscle as the point on the cortex which has the lowest intensity threshold to evoke an MEP. MEPs are usually recorded with a bipolar setup (the signals from two close EMG electrodes on the same muscle are subtracted), and parametrized in terms of latency, peak-to-peak amplitude or total area. For a

resting muscle and stimulation close to the threshold, the amplitude and the area correlate well with the force of the twitch [91].

- **Cortico-cortical evoked potentials (CCEPs)**: Similar to the MEP generation, the stimulation also leads to the activation of cortico-cortical and cortico-thalamic fibers and thus activity at distant cortical sites. In figure 2.1, a comparison is shown between the MEPs (A) of a healthy person and the CCEPs (B) evoked by the same stimuli. While the MEP is typically a simple, biphasic response lasting only a few milliseconds, CCEPs can consist of several longer lasting subcomponents which vary widely in shape, reflecting the complex dynamics evoked by the stimulus in the brain. Their amplitudes and latencies can help to identify effective (i.e. anatomical) connections within the brain.

Instead of an evoked potential, Rosanova et al. [145] interpreted the effects of a TMS pulse on the EEG as evoked oscillations and analyzed it in terms of event-related spectral perturbation (ERSP). For this thesis, however, CCEPs and MEPs are used, not the ERSP.
While MEP studies have been common since the introduction of TMS, simultaneous TMS-EEG recordings became possible following improvements in recording hardware in recent years [83]. This has spurred a multitude of studies that attempt to characterize the evoked activity measured with EEG after TMS pulses and the influence of different stimulation parameters (coil location, coil angle, stimulus intensity,...) [32, 55, 71, 97, 98, 145]. It became clear that the effects of stimulation depend strongly on the stimulation parameters, especially location, polarity and intensity but that they are fairly reproducible if the parameters are constant [32]. However, the reaction of the brain to stimulation is not stereotypical, but influenced by its own activity. This is the focus of chapter 5 and reviewed there in more detail.

2.3. Open-loop and closed-loop stimulation systems

So far, the basic tools to measure electrophysiological brain activity and to stimulate the brain have been described, along with the way how the reaction of the brain to stimulation can be recorded. These methods are important because they provide the basis to introduce the concept of closed-loop stimulation in this section where recording and stimulation take place simultaneously.

2.3.1. Open-loop systems

The devices used for chronic stimulation in clinical practice today are typically of an open-loop design (figure 2.2 A): Stimulation parameters are independent from the activity of the stimulated system and the stimulator is controlled by external trigger signals. Stimulation parameters are programmed externally by a clinician

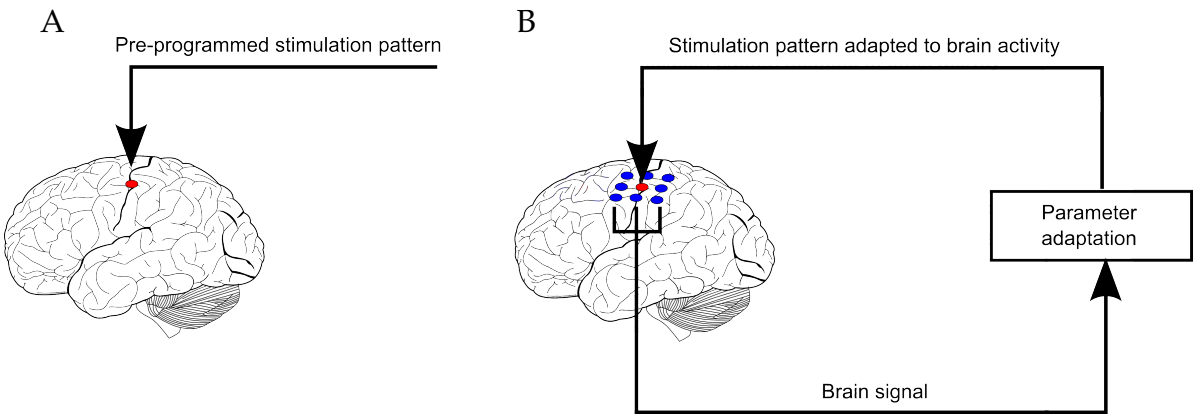

Figure 2.2.: Conceptual difference between an open-loop **(A)** and a closed-loop **(B)** system: For an open-loop system the stimulation parameters are pre-determined, while for a closed-loop system, the parameters are adapted to the simultaneously recorded brain activity.

and transmitted wirelessly to the device. In this simple form, stimulation can be a therapeutic tool with fixed parameters that can be switched on and off, without any measurement of the response of the brain. It has been used in this way for chronic pain [109, 126, 162], epilepsy [156], depression [44], Parkinson's disease [10] and first studies have been conducted for rehabilitation after stroke [21, 79, 106]. Although such a design has the benefit of being simple and well-established, it ignores that the brain is a dynamic, changing system and treats it just as a static recipient of stimulation. It does not allow for any kind of feedback between the ongoing brain activity, the effects of the stimulation and the device. For example, in the case of epilepsy therapy, a stimulation system which has an in-built seizure detection module could trigger stimulation exactly at the right moment to disrupt a developing seizure [59, 156], whereas conventional stimulation devices either need to stimulate continuously or wait for the implanted person to detect the seizure and trigger the stimulator. In the case of stroke rehabilitation with cortical stimulation, it has been suggested [136] that closed-loop systems might provide better results than open-loop systems as well.

The electrophysiological recording of the neural activity evoked by stimulation could be helpful not only by increasing the effectiveness of stimulation systems, but also as a source of information to understand brain processes. When recording the evoked potentials in an open-loop paradigm, stimulation may be used for example to probe the excitability and response of the brain for different patient groups in comparison to healthy participants (perturb-and-measure [101]). This allows one to gather information about the effects of the pathology on the reaction of the brain to stimuli and to investigate the use of brain stimulation as a diagnostic tool. Example applications for this are epilepsy [92, 93, 163], aging [31], hyperactivity in children [22] and brain injury [146].
For within-subject analysis, changes in the neural responses depending on the task

can be of interest. In the example of movement-related processes, the timing of the stimulation is adapted to the structure of the experiment to assess for example how the evoked potentials before and during a cued movement differ from each other [74, 128].

2.3.2. Closed-loop systems

The basic idea for closed-loop systems is that the ongoing brain activity is used as a source of information to adapt stimulation parameters online (figure 2.2 B), i.e. in almost real-time during the experiment. Hence, in addition to the parameters used for conventional open-loop stimulation systems (for example the placement of electrodes and the identification of an approximate set of stimulation parameters), one has to determine which characteristics of the brain signal are important and how they are translated into stimulation parameters such as the timing, the intensity and the location of stimulation. When applied to patients, this depends heavily on the condition which is to be treated and possibly also on the individual characteristics of the implanted patients. For example, the presence of cortical lesions which can perturb the currents induced by stimulation [169] can pose a problem. Again, in the example of closed-loop stimulation for epilepsy, important characteristics of the signal are those which can be used to predict seizures. The detection of a seizure in real time triggers the stimulator, hence the timing of stimulation is adapted to the brain activity.

From a technical point of view, several features are needed to upgrade current open-loop stimulation systems to closed-loop systems:

- A *sensing interface* to record brain activity, possibly also requiring additional electrodes
- *Feature extraction* modules to extract important signal characteristics in real time
- A *classifier* or another *translation algorithm* to determine stimulation parameters based on the recorded brain activity
- A *stimulation interface* allowing the triggering and on-the-fly programming of parameters of the stimulator

This makes a closed-loop stimulation system a special case of a brain-computer interface (BCI) [179]. In the following sections, an overview of studies on closed-loop stimulation systems is given:

Closed-loop stimulation for patients

Extracting information from the measured neural activity online during the experiment to optimize stimulation parameters opens up possibilities for novel research questions and therapies which should be more effective than open-loop therapy [143]. However, the literature regarding practical implementations of therapeutic closed-loop cortical stimulation with human patients is very scarce. For the treatment of epilepsy, the Responsive Neurostimulator System (RNS) (NeuroPace Inc., Mountain View, CA) [59] was recently evaluated in a clinical study with 191 patients with intractable partial epilepsy. Using electrocorticography (ECoG), the brain activity was continuously monitored and pre-programmed electrical stimulation was triggered when abnormal neural activity was detected. Such activity patterns had to be defined by a physician individually per patient. A significant reduction in seizures for patients with this device implanted in comparison to patients that did not receive stimulation was found [124]. Even more sophisticated approaches for seizure control are in early stages of development. The goal is to continuously analyze the response to the stimulation and adjust the stimulation if it does not have the desired effect, i.e. if the seizure is not disrupted by it [156].

Closed-loop stimulation with animal models

Apart from this clinical approach, research on closed-loop stimulation of neural tissue in vivo is focused on animal models. Stimulation is in this case usually applied with microelectrodes which are also used for recording of local field potentials (LFP) and action potentials (spikes). The advantages of microelectrodes over surface electrodes are a better control over the environment of the stimulation and smaller area of activation around the electrode, thus possibly leading to more specific stimulation [40]. Two directions of the research can be distinguished: (1) Stimulation as a means to directly transmit information about the external environment to the brain and (2) stimulation to manipulate and reorganize the neural connections in the vicinity of the electrodes.

In the first case, intra-cortical microstimulation (ICMS) can act as a device providing the animal with feedback on its task performance [115] or to transmit commands and cues, which task to execute [57, 131]. This approach is also at the core of many developments in the field of sensory neuroprosthetics, where Dobelle and Mladejovsky [49] demonstrated the possibility of directly stimulating primary sensory areas, in this case the visual cortex, with the goal of eliciting sensations similar to those a healthy person would have in the same environment. They proved the feasibility of this approach with a visual prosthesis in a blind person [48]. It has been hypothesized, that a closed-loop control of the applied stimuli which takes the

ongoing neural activity and the effects of the stimulation into account in order to reduce the variance of the evoked activity by adapting stimulation parameters [25] could improve the stability and selectivity of such neuroprosthetics [110]. This application provides the basis for the paradigm investigated in chapters 5 and 6 and is discussed in more detail there. Campbell et al. [29] applied prediction and control of neural activity to cochlear implants which are to date the best established form of a sensory prosthesis. Apart from these neuroprostheses, closed-loop stimulation in the hippocampus [70] and prefrontal cortex [69] has been shown to improve memory function and cognitive performance in monkeys.

In contrast to the assistive nature of a neuroprosthesis, another research target is to repair injuries of the brain directly by using stimulation to "rewire" the neurons. Hence, this direction is more of a restorative nature and very interesting in the context of stroke rehabilitation. The hope is that the formation of neural connections between affected brain areas can be facilitated by stimulation. This field is in a very early phase, especially regarding the question on how to achieve lasting and specific changes in neural connections. Jackson et al. [84] concentrated on two neurons in the motor cortex of monkeys and demonstrated that the activity of a target neuron can be conditioned if ICMS pulses are applied to it with a fixed time interval after a different trigger neuron produced an action potential. This is inspired by the hypothesis of Hebb [75] that the strength of a connection between neurons is modulated by the relative timing of their activity, paraphrased often concisely as "Neurons that fire together, wire together". They also found that such conditioning can lead to long-lasting changes in the evoked motor response to ICMS when stimulating the conditioned neuron. These changes in stimulation-evoked responses by a Hebbian pairing of pre- and postsynaptic activity can have direct implications on behavior, such as a modification of the intensity threshold at which the animal perceives that an ICMS pulse has been applied [141]. Improvements in understanding how to effectively induce and detect changes in the organization of larger neural populations [142] are crucial considering that restorative stimulation probably will have to act on much larger scales than just a few neurons to be effective for stroke patients. A second problem is that the stimulation-induced changes in the neural connectivity are often short-lasting. While the changes in motor output in the study of Jackson et al. [84] lasted for at least 10 days after the period of stimulation had ended, the effects found in Rebesco et al. [142] and Rebesco and Miller [141] receded to baseline within a day after the end of the stimulation. Thus, a lot of research is needed before such highly specific approaches to induce neuronal reorganization can be practically applied to human patients.

To summarize, while most clinical applications of cortical stimulation employ open-loop stimulation systems, closed-loop systems are a research target right now,

because an increase in specificity and effectiveness of stimulation is expected by them. At the moment closed-loop stimulation is closest to reaching clinical practice for epilepsy patients, while most other research is carried out with animal models. One problem of bridging the gap between animal research and the application in human patients is the fact that microelectrodes are the tool of choice for the work with animals. While this is understandable from the point of view of stimulation specificity, implantations of microelectrodes in humans are scarce at the moment due to their invasiveness. Hence, research about closed-loop stimulation with macroelectrodes could be a more viable candidate to create more opportunities to apply closed-loop stimulation for patients.
One problem for this is that the availability of usable devices for closed-loop stimulation in humans is very limited. For closed-loop stimulation, online signal analysis and adaptation of stimulation parameters has to be possible, but using external hardware for this would be very cumbersome for the patients. Therefore, implantable stimulators suitable for long-term therapeutic interventions would be very welcome. Such devices have to be designed with low power usage in mind and certified for the use in human patients, a very costly process. Rouse et al. [147] in cooperation with Medtronic (Fridley, USA) constructed a prototype of an implantable device. It allows online time-domain and frequency domain analysis of ECoG signals on up to 4 channels. A programmable digital signal processor on a microcontroller can be used to realize for example a support-vector machine for signal classification. The stimulation hardware is based on off-the-shelve open-loop stimulators from Medtronic, routinely applied in patients, and extended with an interface for the microprocessor to enable online programming of the stimulator. First implantations had been performed in monkeys with an evaluation of the classification performance when all signal processing is done on the device. In a more recent evaluation of this device after implantation in an ovine model, Afshar et al. [2] demonstrated the use of online adaptation of stimulation parameters to suppress post-stimulus after-discharges. However, while the hardware looks promising, there are no published studies of its application in human patients, yet, and this is the only way to judge its effectiveness for therapy.

2.4. Use of stimulation and brain signal decoding for rehabilitation

Following this introduction into closed-loop stimulation, the next question is how such stimulation systems could be adapted to stroke rehabilitation: On the one hand, stimulation parameters are needed which might be beneficial for rehabilitation, on the other hand one needs to extract information from the brain signals which could be useful to ”close the loop”, i.e. adapt the stimulation parameters to it. Thus, this

section gives an overview over recent attempts to use cortical stimulation or the analysis of brain activity in the form of BCIs to support stroke rehabilitation.

2.4.1. Cortical stimulation for stroke rehabilitation

It has been hypothesized that the stroke leads to a decrease in the activation of the affected hemisphere, such that the motor cortex of the intact hemisphere is increasingly active for movements of the paretic hand [94]. Hence, re-balancing the relationship between healthy and affected hemisphere might be beneficial for rehabilitation. Thus, the two main approaches are to either downregulate the excitability of the healthy side or to upregulate the excitability of the lesioned hemisphere (see Hummel and Cohen [81] and Alonso-Alonso et al. [4] for reviews). Stagg et al. [157] found that stimulation of the affected hemisphere was the more effective option.
The idea to use invasive cortical stimulation for rehabilitation is based on animal studies demonstrating that pulsed electrical stimulation applied to rats after an induced lesion in the sensorimotor cortex can restore motor function [1, 161]. In these studies, electrodes were placed subdural or epidural over the motor cortex of the animals and different stimulation parameters (polarity, pulse frequency) were tested. A stimulation frequency of at least 50 Hz and anodal stimulation was found to lead to the most beneficial effects.

This approach was transfered to human stroke patients by Brown et al. [21], Levy et al. [106] and Huang et al. [79] who applied 50 Hz electrical stimulation with epidural electrodes placed over the affected motor cortex during a standard rehabilitation paradigm in several hospitals. As with the studies on rats, stimulation pulses were given continuously during rehabilitation sessions. However, although the first studies with patients led to significant improvements in upper limb function [79, 106], this could not be replicated in a follow-up study with 146 patients. After that, suggestions were brought forth by Plow et al. [136] who argued that the specificity of the stimulation was maybe not sufficient and could be improved by taking into account the brain activity at the moment of stimulation.
Instead of implanted electrodes, less invasive approaches for stimulation have been suggested as well [4, 81], in particular TMS and tDCS. However, improvements in motor performance have been moderate and often short-lived with these approaches, but the independence from risky surgeries keeps this a viable option for further research.

2.4.2. Brain-computer interfaces for stroke rehabilitation

While stimulation opens an afferent pathway to the brain by directly modulating the brain activity, BCIs provide an efferent pathway. Their three basic components are [179]: *signal acquisition* to digitize the brain signal, *signal processing* to extract features

from the recorded signal which are then translated to *control signals* for external devices. This makes BCIs attractive for patients with neuromuscular disabilities (for example amyotrophic lateral sclerosis (ALS), brainstem stroke, cerebral palsy and many other diseases [179]) in which control over the natural efferent pathways, the muscles, is almost totally lost. They can serve as a communication channel with these patients, allowing them to interact with their environment by operating for example a spelling interface [15] or controlling a robot [76].

In contrast to this, restorative BCIs from the field of neurorehabilitation aim to restore function, not replace it, after an injury destroyed neural connections. For example, a stroke might severe fibers of the pyramidal tract, thus cutting the main communication line between the motor system of the patient and certain muscles, leading to paralysis of the affected muscles. In this case, the aim of brain-computer interfaces for movement restoration is the re-establishment of the sensorimotor loop [65]. In a healthy person, movement commands from the brain are transmitted via the corticospinal tract to the muscles where the movement is executed. This execution is accompanied by kinesthetic, proprioceptive and visual feedback to the brain, thus closing the feedback loop. In a stroke patient with paralysis, the corticospinal tract can be affected resulting in zero or only a very small amount of fibres connecting the brain to the paralyzed muscles. Hence, motor commands, if they can be sent to the muscles, are not strong enough to elicit the intended movement. Without a movement, there is also no sensory feedback from the movement, the sensorimotor loop is severed.
However, if the motor cortex is still able to generate the necessary commands, one can try to restore control by detecting the intended movement from the brain signals and using external devices, for example an orthosis, to execute this movement (figure 1.1). Ang et al. [7] confirmed that "the majority of stroke patients could use EEG-based motor imagery BCI." Buch et al. [27] were the first to realize this approach with stroke patients with a chronic hand plegia, demonstrating that even severely affected stroke patients are still able to learn to control a BCI with imagined movements of their paralyzed hand. The BCI utilized the event-related desynchronization (ERD) of sensorimotor rhythms (SMR) during motor imagery (SMR-BCI, section 4.1). Unfortunately, learning to control the BCI did not lead to significant clinical improvements in hand function, possibly because the hand movement was not controlled continuously by the patients. The first controlled study with a larger number of patients was conducted by Ramos-Murguialday et al. [138], who showed that the motor function of severely affected stroke patients can be improved with the use of a ERD-driven EEG-based BCI which detected the intention of the patient to move the paralyzed hand in real time and closed the sensorimotor loop with an orthosis continuously controlled by the movement intention of the patient. They suggested that by providing such a contingent link between the intention and the

action, neural connections associated with the movement could be strengthened to the point that volitional control of movements through residual cortico-spinal fibers becomes possible again.

2.5. Decision making from brain signals

The general goal of a BCI is to infer information about the intention of the user from the brain signal - informally put: to ”decode” the brain signal - and use it to communicate with external devices. For a closed-loop stimulation system, features of the brain signal have to be translated to stimulation parameters. Thus, given a brain signal X, one has to make a decision. The result of this decision can be either in the form of a category (e.g. ”The patient intends to move the hand / the foot / looks at this part of the computer screen”) or as a real-valued control signal (e.g. ”Set the velocity of the cursor / the wheelchair / the intensity of the stimulation pulse to Y”). The former paradigm is a *classification* problem, the latter a *regression* problem. A large variety of algorithms have been developed by the Machine Learning community to deal with these kinds of problems, from simple linear algorithms to complex nonlinear ”black box” algorithms such as neural networks. However, at least for supervised classification problems for BCIs, Support Vector Machines (SVM) seem to be the most efficient ones [112], due to their robustness against noise, outliers and high dimensionality. For regression problems with neural closed-loop stimulation data, Support Vector Regression (SVR) has been employed successfully [26]. Thus, in this section a short introduction on the fundamentals on SVM-based classification and regression algorithms is given, using the nomenclature and notation of Schölkopf and Smola [152] for the special case of real-valued features.

2.5.1. Regression and classification

In general terms, a *regression* model M provides a way to estimate a dependent variable Y (the ”output”) from independent variables $\mathbf{X}$ (the ”input”), such that $M(\mathbf{X}) \approx Y$. For this work, $Y \in \mathbb{R}$, while $\mathbf{X} \in \mathbb{R}^d$ is a vector containing d features of the recorded brain activity. Thus, the simplest way for a relationship between $\mathbf{X}$ and Y would be to assume that it is linear: $Y = \mathbf{w}^T\mathbf{X} + b$ with $\mathbf{w} \in \mathbb{R}^d$ as the *weight* vector and $b \in \mathbb{R}$ as a *bias* term. Using for example the method of least-squares, $\mathbf{w}$ and b can be easily calculated from a set of n training instances $(\mathbf{x}_i, y_i)_{i=1}^n$ with $(\mathbf{x}_i, y_i) \in \mathbb{R}^d \times \mathbb{R}$. The $\mathbf{x}_i$ are called *patterns*, while the y_i are *labels*.
In classification, the dependent variable is discrete: The goal is to assign each pattern to a class y_i. This can be achieved by learning a *decision function* on the training data, for example by finding the parameters $\mathbf{w} \in \mathbb{R}^d$ and $b \in \mathbb{R}$ of a hyperplane $\mathbf{w}^T\mathbf{x} + b = 0$. This is useful in particular for binary classification problems ($y_i \in \{\pm 1\}$), although a discrimination between multiple classes can be achieved by combining several

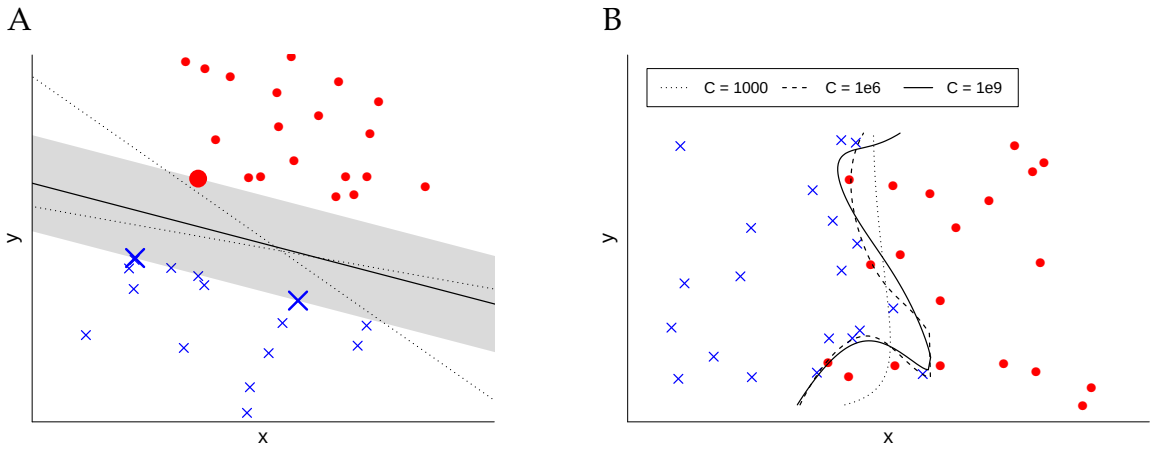

Figure 2.3.: Toy examples to illustrate the SVM: **(A)**: In a separable problem to distinguish between circles and crosses, the optimal hyperplane (solid line) is the one with the largest margin. The 3 support vectors are marked by larger symbols and the margin is indicated by the grey shaded area. Dotted lines show examples of other hyperplanes that are not optimal, although they separate the training data perfectly, because their margin is smaller. **(B)**: To solve a non-separable problem, SVMs with RBF kernel are trained. Their hyperplanes are shown for three different settings of the regularization parameter C.

hyperplanes. From this follows the binary decision function $f(\mathbf{x}) = \text{sign}(\mathbf{w}^T\mathbf{x} + b)$ [152]. Of particular interest is the *margin*, i.e. the smallest distance of a point to the hyperplane. For a separable problem, an infinite number of hyperplanes can be found that separate the patterns perfectly, but they are not equally suited (figure 2.3). Intuitively, the optimal hyperplane can be defined as the one with the maximum margin because it keeps the greatest distance from the training samples, thus leaving the most room for unknown test data. This hyperplane can be found by solving the optimization problem [152]

$$\max_{\mathbf{w},b} \min \left\{ \|\mathbf{x} - \mathbf{x}_i\|, \mathbf{x} \in \mathbb{R}^d, \mathbf{w}^T\mathbf{x} + b = 0, i = 1, \ldots, m \right\}.$$

These rather simplistic approaches to classification and regressions are limited in several ways. First of all, they assume a linear relationship between $\mathbf{x}_i$ and y_i. This is rarely the case in reality, therefore non-linear approaches can lead to improved results. Secondly, the problems of outliers and non-separable classification problems have not been considered. Soft-margin SVMs can deal with these kinds of problems and are introduced in the next section.

2.5.2. Support Vector Machines (SVM) for classification

Today's commonly used form of soft margin SVMs was introduced by Cortes and Vapnik [43]. It has several desirable characteristics:

- **Sparseness**: The only training patterns which influence the position of the hyperplane are those lying on the margin, the so-called *Support Vectors* (figure 2.3 A). These gain their name from the idea that they "hold the hyperplane in place". If patterns outside of the margin are added or removed this does not change the solution. Thus, for a trained SVM model, only the support vectors need to be stored and the impact of outliers is reduced.

- **Flexibility**: Prior knowledge about the problem can be introduced into the SVM with the use of *kernels* (section 2.5.4) without the need to change the training algorithm. While an SVM at its core is always performing a linear separation with a hyperplane, the use of non-linear kernels has the effect that this separation is done after - conceptually - projecting the training patterns to another space more suited to the problem. Thus, kernels allow a nonlinear classification.

- **Robustness**: One problem with the use of kernels is that the decision boundary can become very complex when attempting to achieve a perfect separation of the training data. This can be undesirable, because zero error on the training data does not ensure that unknown test patterns are classified correctly, which, ultimately, is the goal of training such an algorithm. A too complex boundary can result from the algorithm simply "remembering" the training data, a problem called *overfitting*. The insight that simpler solutions can achieve better results, a concept also known as Occams Razor, is incorporated into SVM training with the use of *regularization*. A parameter C controls the trade-off between the smoothness of the decision boundary and the number of classification errors (figure 2.3 B). A larger C penalizes errors stronger, leading to a more complex, less smooth decision boundary. To allow such misclassifications, slack variables ξ_i are introduced which represent the error for training pattern $\mathbf{x}_i$ if $\xi_i > 0$. This property also makes SVMs effective for high-dimensional data.

For linear classification, this results in the primal optimization problem [152]

$$\min_{\mathbf{w},\boldsymbol{\xi},b} \frac{1}{2}\|\mathbf{w}\|^2 + C\sum_{i=1}^{m}\xi_i$$

subject to $\xi_i \geq 0 \; \forall \; i = 1,\ldots,m$ and $y_i(\mathbf{w}^T\mathbf{x} + b) \geq 1 - \xi_i \; \forall \; i = 1,\ldots,m$. For nonlinear classification, the optimization problem is [35]

$$\min_{f\in\mathcal{H}} \|f\|_{\mathcal{H}}^2 + \sum_{i=1}^{n}\max(0, 1 - y_i f(\mathbf{x}_i))$$

where $\text{sign}(f(\mathbf{x}_i))$ with $f(\mathbf{x}) = \sum_{i=1}^{n}\beta_i k(\mathbf{x}_i, \mathbf{x})$ is the decision function. The β_i are the coefficients of the solution and k is the kernel function with its associated reproducing kernel Hilbert space (RKHS) $\mathcal{H}$ (section 2.5.4). Although in practice these

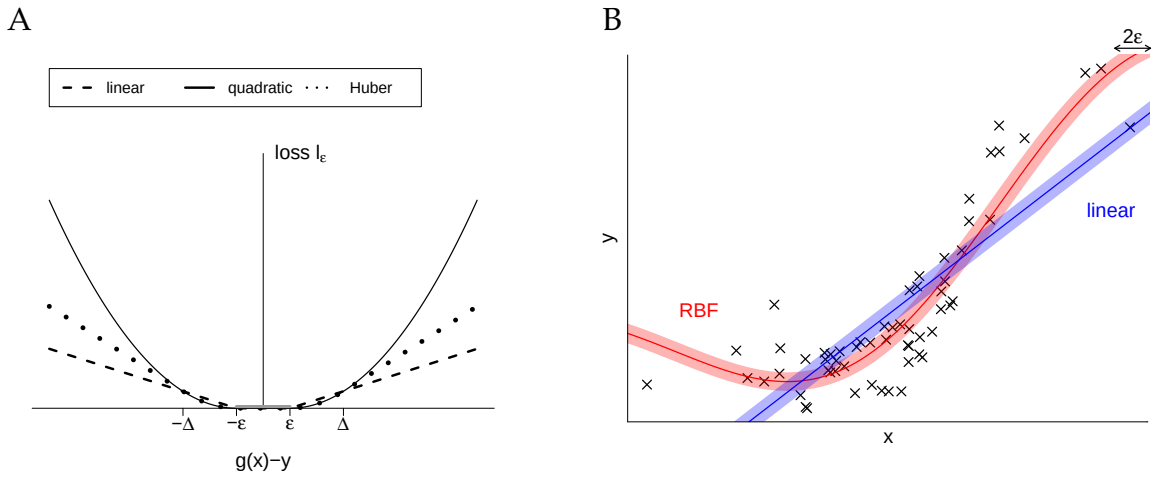

Figure 2.4.: Toy examples to illustrate the SVR: **(A)**: Comparison of the linear, the quadratic and the Huber loss function. **(B)**: Results for a SVR with linear (blue) and RBF kernel (red). The estimated function is shown as a solid line, the shaded area around the function indicates an ϵ-tube.

problems are often solved in the dual form instead of the primal one because it simplifies the optimization constraints, the basic concepts of SVMs are easier to explain with the primal form which is why it is presented here. Furthermore, one advantage of primal optimization over the dual one is that hyperparameters of the SVM can be tuned more easily [35] (see section 2.5.5).

2.5.3. Support Vector Regression (SVR)

The SVM above can be extended to regression problems such that $y_i \in \mathbb{R}$ instead of $\{\pm 1\}$. In this case, the class loss function $\max(0, 1 - y_i f(\mathbf{x}_i))$ is not applicable. Typically, an ϵ-insensitive loss function l_ϵ is used, which penalizes patterns only if $|y_i - f(\mathbf{x}_i)| > \epsilon$. Typical penalties can be linear (l_1- or *hinge loss*) or quadratic (l_2-*loss*). The l_1-loss is not differentiable, hence the *Huber loss* was introduced by Bo et al. [16]. It is a differentiable approximation that contains linear and quadratic parts (figure 2.4 A).
Instead of finding the optimal hyperplane, SVR fits a tube with width ϵ to the data points (figure 2.4 B) such that only patterns with $l_\epsilon(f(\mathbf{x}_i - y_i) > 0$ play a role for the solution. Following Brugger et al. [26], the regression model $g(\mathbf{x}) = \sum_{i=1}^{m} \beta_i k(\mathbf{x}, \mathbf{x}_i) + b$ is found by

$$\min_{\boldsymbol{\beta}, b} \left(L_\epsilon(\boldsymbol{\beta}, b) = \frac{1}{2} \sum_{i=1}^{n} l_\epsilon(\mathbf{K}_i \boldsymbol{\beta} + b - y_i) + \frac{\lambda}{2} \boldsymbol{\beta}^T \mathbf{K} \boldsymbol{\beta} \right)$$

where $\mathbf{K}_i$ the i-th row of the kernel matrix $\mathbf{K}$, $\boldsymbol{\beta}$ are the coefficients in the solution, b is the bias term and $\lambda = \frac{1}{C}$ is the regularization parameter. This algorithm re-

tains the advantages of SVMs for classification in terms of sparseness, flexibility and robustness.

2.5.4. Kernel

One important aspect of classification and regression is the notion of the *similarity* between patterns. Intuitively, if a test pattern with unknown label is more similar to all the patterns known to belong to class y_i than to those of other classes, then it might be sensible to classify it as also belonging to class y_i. The question is how to define similarity between patterns for a particular problem. In its simplest form, one can do this by comparing the test pattern $\mathbf{x}_i$ with another pattern $\mathbf{x}_j$ feature-wise via the computation of the dot product: $\langle \mathbf{x}_i, \mathbf{x}_j \rangle = \mathbf{x}_i^T \mathbf{x}_j$. This is a simple linear operation, but it does not allow any dependencies between features or other nonlinearities. If one expects such nonlinear influences for the problem to be solved, one can deal with this issue by first projecting the input feature vector to some appropriate space $\mathcal{H}$, using a nonlinear function $\Phi(\mathbf{x}_i) : \mathbb{R}^d \to \mathcal{H}$ and then computing the dot product in $\mathcal{H}$: $\langle \Phi(\mathbf{x}_i), \Phi(\mathbf{x}_j) \rangle_{\mathcal{H}}$. If the function Φ is suitably chosen such that the nonlinearities vanish in $\mathcal{H}$ then the linear operation of the dot product is sufficient to capture the similarity between patterns. However, especially if the space $\mathcal{X}$ is of high dimension, this operation can be very costly. This is where the so-called *kernel trick* opens up a shortcut:
A *kernel* $k(., \mathbf{x}_i) : \mathbb{R}^d \mapsto \mathbb{R}, \ \mathbf{x} \mapsto k(\mathbf{x}, \mathbf{x}_i)$ is a function which performs the two steps of (i) projection from the input space $\mathbb{R}^d$ to the feature space $\mathcal{X}$ and (ii) computation of the dot product in $\mathcal{H}$ implicitly, thus avoiding the problem of the dimensionality of $\mathcal{H}$. The prerequisite for k to be considered as a kernel is that it has to be positive definite. Only then can it be thought of as an implicit dot product in the associated RKHS [152]. Examples of popular kernel functions are:

- **Linear kernel**: $k(\mathbf{x}_i, \mathbf{x}_j) = \mathbf{x}_i^T \mathbf{x}_j$
- **Polynomial kernel**: $k(\mathbf{x}_i, \mathbf{x}_j) = \langle \mathbf{x}_i, \mathbf{x}_j \rangle^o$
- **Gaussian radial basis function (RBF) kernel**: $k(\mathbf{x}_i, \mathbf{x}_j) = \exp\left(-\frac{\|\mathbf{x}_i - \mathbf{x}_j\|^2}{2\sigma^2} \right)$

The linear kernel simply realizes the computation of the dot product in the input space. The polynomial and the Gaussian RBF kernel allow nonlinear interactions between features, but each one has an additional parameter, either the order o of the polynomial kernel, or the width σ of the RBF kernel. The next section discusses, how appropriate settings for these hyperparameters and the other parameters of an SVM or SVR can be found automatically.

2.5.5. Model Selection

In the training procedure of SVMs for classification or regression, hyperparameters need to be selected. These are parameters needed by the learning algorithm for example to adjust its internal cost function. Of particular importance is the parameter C which controls the trade-off between the maximization of the margin and, thus, the smoothness of the decision function, and the minimization of the training error [152]. With the exception of the linear kernel, there are usually also hyperparameter associated with the kernel functions. For example, in the case of an RBF kernel, the width σ of the kernel needs to be selected. Specific for SVR is the parameter ϵ, which controls the width of the loss function. In order to optimize these parameters for the particular problem at hand, one can use a regular search grid where all combinations of a discrete set of possible values for the hyperparameters are tested on the training data [33]. The parameter setting which performs best on the training data is then used for the actual classification or regression procedure. This method can find good parameter settings given a suitable spacing of the grid points (a logarithmic spacing is very common), but it can be very time consuming, especially if there are more than two hyperparameters to optimize [37].
The aim of the model selection step is to find settings for the hyperparameters which minimize the error on unknown test data for optimal generalization. This measure is obviously unknown, but one can find upper bounds for the leave-one-out error (LOOE) of the SVM which provides an unbiased estimate for the probability of the test error [166]. The LOOE is the error rate obtained by training the SVM on all instances except one and classifying the remaining instance, repeated for all instances. From this, one can derive a heuristic for the model selection, by finding hyperparameters such that the upper bound for the LOOE is minimized. The span bound [36, 166] in particular gives the best results to automatically tune the hyperparameters of an SVM [37]. This bound can be used for SVR model selection as well [34] with the small change that the LOOE in the regression case is not the classification error rate, but the average error of the estimation. As the optimization is a gradient-based procedure, solvable for example via Quasi-Newton methods, the number of runs of the classification/regression procedure is much smaller than for the grid search explained above if there are more than two parameters to be optimized [34].

2.5.6. Feature Selection

Each training pattern $\mathbf{x}_i \in \mathbb{R}^d$ consists of a vector of d features: $\mathbf{x}_i = (x_{i1}, \ldots, x_{id})$. Let the set of all values for a particular feature j in the set of training patterns $\mathbf{X}$ be denoted by $\mathbf{X}_j$. Starting from a large number of features which may contain noise and redundancies, it is often advisable to reduce the input dimension by selecting a subset of features $S \subset \{1, \ldots, d\}$ which still contains all relevant information for the problem $M(\mathbf{X}) \approx Y$. This dimensionality reduction can improve the quality of the

classification or regression substantially, because it reduces the risk of overfitting. In the field of Support Vector-based methods, overfitting is to some extend under control thanks to the use of regularization which enforces a smoothness constraint on the decision function. However, these methods can still benefit from a reduction of the dimensionality of the feature space [68]. Feature selection methods can be grouped in two regimes: *filter* and *wrapper* methods [67, 95]. Filter methods compute criteria for feature relevance independently from the employed regression or classification method. Examples for filter methods are [67]:

- r^2 **value**: The square of Pearson's r for the linear correlation between $\mathbf{X}_j$ denotes the fraction of the variance of the labels explained by a linear relationship between the feature and the labels. With Pearson's r, only linear relationships can be captured. However, this can be extended to nonlinear relationships either by computing r between $f(\mathbf{X}_j)$ and Y, where f is a nonlinear function such as the square or a logarithm, or for a monotonous relationship by using Spearman's correlation coefficient instead of Pearson's.

- **AUC value**: The Receiver Operating Characteristic (ROC) is especially helpful for feature selection for two-class classification problems $Y \in \{\pm 1\}$. The value of a threshold t is varied over all values of $\mathbf{X}_j$. For each threshold, all training instances are assigned to a class depending on whether their value x_{ij} for feature j is smaller or larger than t. Each threshold gives a true positive and false positive rate (TPR/FPR) in comparison with the original labeling of the training instances. The area under the curve (AUC) when plotting TPR versus FPR is a measure, how well the training instances can be separated into the two classes using only the value of x_{ij} as a predictor [53, 67]. Similar to the r^2 value above, only a linear relationship between $\mathbf{X}_j$ and Y is evaluated with this.

- **Mutual information**: The mutual information is an information theoretic measure for the dependency between the probability density of $\mathbf{X}_j$ and the probability of Y. It is not restricted to linear relationships but hard to estimate, because the true densities are unknown.

A general problem of filter methods is that they judge each feature independently from all others, thus they cannot account for interactions between features. A particular feature $\mathbf{X}_j$ which is uncorrelated with Y might still be useful for solving the problem, because its interaction with another feature k could provide otherwise unobtainable information (see Guyon and Elisseeff [67] for examples). Therefore, it can be useful to evaluate feature subsets, thus covering the interactions within the subset, instead of individual features in order to select the most appropriate feature set.

Wrapper methods use the regression or classification algorithm as a black box to get a measure for the suitability of the input feature set. For a particular feature

subset, one evaluates its suitability by computing a performance measure for the black box algorithm trained on this feature subset, for example by cross-validation. Performance measures might be the classification accuracy or the prediction error. In principle, one could perform this performance evaluation for all possible feature subsets, but this brute force approach is only feasible if the number of features is very small, because the number of subsets increases exponentially with the number of features. Greedy search strategies such as forward selection and backward elimination can serve as heuristics in order to find a good feature subset [67]. In comparison to the filter methods, where only a pre-processing step has to be performed on the features, the wrapper methods are computationally more expensive, because for the evaluation of each subset, a full training and testing procedure of the classification or regression algorithm has to be performed. However, the wrapper method allows one to judge features directly in the realm of interest: their suitability for the algorithm to be used in practice. One popular wrapper method for feature selection in the case of Support Vector methods, usable only with a linear kernel, is Recursive Feature Elimination (RFE) [68]. RFE works with backwards elimination, starting from a full set of features and gradually removing more and more. The weight of each feature is used as the removal criterion: If the absolute weight of the feature is large, it is probably more important than features with small weights. However, this means that all features have to be scaled to the same range (e.g. by using the z-score to normalize the raw feature values to zero mean and unit variance, or by doing a linear scaling to an appropriate range of values), otherwise the weights are not comparable.

3 Overview over the research framework and the research questions

This work took place within the ERC-funded project "BCCI - a bidirectional cortical communication interface" (grant # 227632) aiming to investigate the utility of the combination of brain-computer interfaces and cortical stimulation for the communication with locked-in ALS patients as well as for stroke rehabilitation. It was a joint project of the Department of Computer Engineering at the University of Tübingen together with the Department of Neurosurgery and the Institute of Medical Psychology and Behavioural Neurophysiology of the University Hospital in Tübingen. For this thesis, only the stroke rehabilitation part is important.

In contrast to all earlier studies on stroke rehabilitation with human patients, this idea of a bidirectional interface with the brain makes it necessary to be able to record the brain activity and stimulate the brain at the same time. As outlined in section 2.1, there are several possibilities to realize this prerequisite, ranging from noninvasive means as in combined TMS-EEG up to very invasive methods such as implanted multi-electrode arrays. For the BCCI project, epidural implantation of electrodes was chosen as a compromise between invasiveness and signal quality: Their intracranial placement means that they are closer to the brain than EEG electrodes, that there is no influence of the skull on the recorded signals and that they can be used to deliver electrical stimulation. While a surgery is necessary to implant these electrodes, they are not in direct contact with the brain but sutured to the dura mater, while microelectrodes would penetrate the brain tissue.

In total, 5 patients were implanted with epidural electrodes during the BCCI project: The first one was an amputee suffering from chronic phantom limb pain, the second one a stroke patient also suffering from chronic pain and paralysis of the left hand. These patients are described in more detail in Walter et al. [173]. Combined brain stimulation and brain signal recording was not attempted with the first patient and experiments on this with the second patient did not lead to satisfying results because almost no neural reaction to the stimulation could be recorded, likely

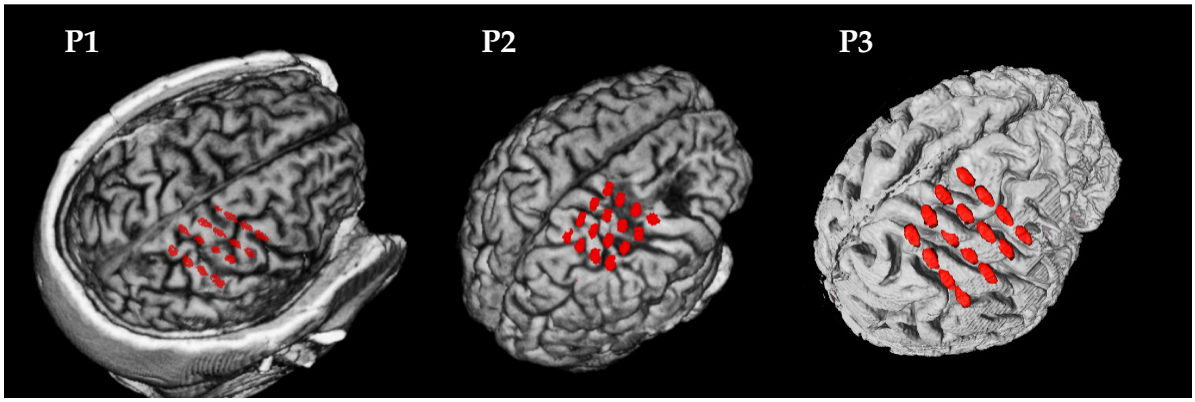

Figure 3.1.: ECoG electrode positions from overlay of MRI and post-surgical CT for the three patients. From left to right: P1-P3. From Walter et al. [172]

due to problems with the implanted electrodes. Thus, data from these patients is not included in this thesis. Three more chronic stroke patients suffering from a paralysis were implanted with epidural electrodes and for these, recording of stimulation effects was successful. The data from these patients thus forms the core of this thesis. A general overview over the patients, the research questions and challenges as well as the experiments is given in the next sections.

3.1. Patients

Data was recorded from three chronic stroke patients (table A.1) suffering from paralysis of the left hand induced by the stroke. None of the patients was able to produce voluntary finger movements with the left hand and conventional physiotherapy did not lead to improvements of hand functions. The patients were implanted in a *compassionate use* protocol using cortical stimulation and BCI for stroke rehabilitation conducted at the University of Tübingen. All procedures were approved by the local ethics committee of the medical faculty of the university hospital in Tübingen and the patients gave written informed consent. After extensive tests to assess motor function and ensuring that the patients had no history of psychological exclusion criteria such as depression or physiological conditions such as epilepsy, they trained for 4 weeks with a noninvasive version of the BCI system without concurrent cortical stimulation. This noninvasive phase was performed to test whether improvements can be attributed only to the BCI training, or whether there is a further beneficial effect of an invasive BCI training coupled with stimulation.

After the conclusion of the noninvasive phase, each stroke patient was implanted with 16 epidural platinum iridium disk electrodes (Resume II, Medtronic, Fridley, USA) with a contact diameter of 4 mm placed over the ipsilesional S1, M1 and premotor cortex on 4 strips with 4 electrodes each and an inter-electrode center-to-center

distance of 10 mm. They were arranged in a 4x4 grid-like pattern (figure 3.1) centered on the hotspot for eliciting MEPs on the extensor digitorum communis (EDC). The EDC muscle is responsible for opening the fingers of the hand, hence it was chosen as the main target for rehabilitation of the hand function. This hotspot was identified by TMS mapping [177] before the surgery. Following the implantation, the BCI and stimulation experiments were conducted during a period of 4 weeks where the ECoG electrodes were accessible from the outside by cables through the skull and scalp. After this invasive phase with 4 weeks of externalized cables, these were internalized in a second surgery and connected to an implanted programmable pulse generator (Medtronic, Fridley, USA). After that, the patients received cortical stimulation through this stimulator. As all connections to the electrodes were internalized and the implanted pulse generator had not the ability to measure the brain signals, no further closed-loop stimulation experiments were possible following the second surgery.

3.2. Research questions and experiments

In the first chapter, two approaches for closed-loop stimulation were introduced: brain-state-dependent stimulation and adaptive stimulation to control the shape of the evoked brain activity. In practice, there are a number of challenges to be solved to realize these ideas:

3.2.1. Brain-state-dependent stimulation

The basic idea of brain-state-dependent stimulation for stroke rehabilitation is to apply stimulation pulses only if the patient intends to move the paralyzed hand. This makes it necessary to be able to decode the movement intention of the patient from the brain signal continuously even while stimulation is applied. The challenge is that stimulation induces artifacts which distort the brain signal. Thus, inferring the brain state from such distorted brain signals would be unreliable and it would be preferable to either clean the signal from these artifacts before further analysis or at least to correct for their presence. Chapter 4 is dedicated to this topic:
After a discussion of the detection of the movement intention from the brain signal and the influence that stimulation after-effects have on this detection process, algorithms are proposed to minimize the effects of the stimulation on the decoding process, in particular on the estimation of spectral power. The basic idea of these algorithms that is introduced here is to identify the period of time in which the stimulation after-effects occur, to remove this segment of the signal leaving a gap and then to use different strategies to deal with this gap to allow spectral estimation. The algorithms are applied on EEG and ECoG data recorded from movement experiments with the three stroke patients. In these experiments, the task of the patients

was always the same: After an acoustic cue, the patients had to attempt to open the paralyzed hand for 6 seconds and then to relax for 8 seconds. The details on these experiments are given in appendix B.1 and B.2. For the evaluation and comparison of these algorithms, the following steps are taken:

- **Spectral power estimation on data without stimulation:** Starting with data from experiments where the patients performed cued attempted movements but were not stimulated, one can simulate stimulation artifacts in these data sets. Then, the proposed algorithms are applied to the data and it is tested, how strongly the estimated spectral power with simulated artifacts differs from the correct spectral power estimated on the original data sets. If the stimulation artifact is removed perfectly by the algorithm, there should be no difference. Such a performance is unlikely, but finding an algorithm that introduces no systematic error (*bias*) into the spectrum would be very welcome because it ensures that at least on average the features used for brain signal decoding are not influenced by the presence of stimulation after-effects.

- **Movement intention decoding on data without stimulation:** Having a largely unbiased estimate of the spectrum might not be enough. For the application, the output of the classifier of detecting either the presence or the absence of an intention to move is the crucial part because this controls the feedback to the patient. Thus, one has to test on the same data sets as for the spectral power estimation, whether the classification between a *movement* state and a relaxed state (*rest*) would be biased when after-effects of stimulation are corrected with one of the proposed algorithms. As different classifiers might produce slightly varying results, a general measure of the discriminability between data from two classes is used as a measure for this, the area under the ROC curve (AUC).

- **Open-loop vs. closed-loop stimulation:** If there is a bias in the movement intention decoding when stimulation artifacts are present, it might be more or less pronounced depending on the stimulation paradigm. In an open-loop paradigm, stimulation occurs during the *movement* and during the *rest* phase, so the output in both phases would be biased. In the closed-loop paradigm, stimulation is only applied if the classifier detects an intention to move within the *movement* phase. Thus, if the bias occurs only during the movement it might even artificially "improve" the decoding performance. To quantify this, stimulation artifacts are simulated for open-loop and closed-loop paradigms and the AUC scores are analyzed and compared to the correct scores without simulated artifacts.

- **Real stimulation data:** While simulations allow the exploration of different parameters and properties of the algorithms, they have to be tested in a realistic environment as well, i.e. on data sets with actual cortical stimulation. For

this, data sets were used from experiments where the patients performed the same task but with concurrent stimulation, either in an open-loop or closed-loop paradigm. The bias of the algorithms can not be computed for this data because there is no correct, undistorted output one could compare the results with: The stimulation after-effects and their distortions are part of the raw data. However, in comparison to each other, the algorithms should behave similarly as in the simulation. For example, if an algorithm had a positive spectral bias by leading to a consistent overestimation of the spectral power in the simulations, the spectral power after its application on stimulation data should be higher than for an algorithm that had a negative spectral bias.

Only with an algorithm in place that allows the estimation of the spectrum and, in turn, the decoding of the movement intention of patients even if cortical stimulation is applied concurrently, were other experiments possible that make use of online brain signal analysis and cortical stimulation. This includes the BCI rehabilitation paradigm with stimulation for the chronic stroke patients B.1 as well as the experiments introduced in the next section to study the effects of stimulation in different movement-related brain states B.2.

3.2.2. Adaptive stimulation to control the evoked activity

A stimulation paradigm where stimulation parameters are adapted to the ongoing neural activity in order to compensate for the effects that fluctuations in the prestimulus activity have on the shape of the poststimulus activity requires that there is a detectable influence of the pre- on the poststimulus activity. Otherwise, such a paradigm does not make sense. To test for such a relationship, the patients performed the movement task described in section 3.2.1 while stimulation pulses were applied in a regular interval independent of the brain activity of the patient (open-loop). This data was analyzed to answer several questions:

- **Brain state dependency:** Does attempting to move the paralyzed hand change the shape of the evoked activity compared to stimuli while the patient is relaxed? If yes, then the intention of the patient should be taken into account when selecting stimulation parameters. A statistical analysis using permutation tests was performed to find time points in the poststimulus activity for which the amplitudes differed significantly between *movement* and *rest*.

- **Brain activity dependency:** Is there a direct correlation between the spectral power of the prestimulus activity and the amplitudes of the poststimulus activity? If this is confirmed, then it would be worthwhile to analyze the brain activity online to decide on stimulation parameters, for example by predicting the shape of the evoked activity from the spectrum and stimulating only if this prediction is close to a predefined target. The most relevant frequency

bands for movement-related brain processes are the μ- and the β-band. Thus, it was tested for which time points of the poststimulus activity there is a significant correlation between their amplitude and the prestimulus μ- or β-power. This analysis was repeated with just the stimuli applied during the movement phase, because this is the relevant subset for closed-loop stimulation.

So far, the stimulation parameters were kept constant while the patient was encouraged by the task to modulate his brain activity. Such a design is sensible to investigate the (postulated) pre- to poststimulus relationship in the brain activity, but in order to compensate for fluctuations in the prestimulus activity by adapting the intensity to it, one needs to study the effects of different intensities on the evoked activity. To this end, experiments were performed with the patients in which they were instructed to lie on the bed with open eyes in a relaxed state in order to discourage activity-related changes in the brain activity. During that time, the patients were stimulated with pulses of varying intensities and a fixed inter-stimulus interval, applied on different brain areas. Research questions for this experiment were:

- **Intensity dependence of evoked activity:** How well is the intensity "encoded" in the shape of the evoked activity? How does this vary for different positions of the stimulation and recording electrode? If the applied intensity is easily recoverable from the evoked activity with a regression analysis, there is no good incentive to use adaptive stimulation. If one wants to evoke a specific target waveform in the evoked activity, one could simply use the regression model to compute the appropriate intensity for the target waveform.

- **Influence of prestimulus activity:** Adaptive stimulation would take the ongoing brain activity into account to select the optimal intensity to elicit the target waveform. With this experiment it can be tested whether this is promising by testing if regression models that take both pre- and poststimulus activity as input to infer the applied intensity are superior to models using only the poststimulus activity. If not, adaptive stimulation is not a promising approach as it would not bring a benefit.

The results of the movement task with open-loop stimulation are reported in chapter 5, while the results of the experiments on intensity-dependency of the evoked activity are covered in chapter 6.

3.2.3. Longitudinal analysis of stimulation-evoked potentials

With these patients and their implanted electrodes, being able to stimulate the brain and record the brain activity for several weeks during a rehabilitation process is a unique opportunity. Functional improvements of the patients during rehabilitation

training could be due to plastic changes in their brains. As stimulation-evoked potentials have been used as markers for neural connectivity [117, 118], it is sensible to look for coherent changes in the potentials during the 4 weeks of rehabilitation, especially for patients where clear functional improvements are found over time. As this is the first time that such an analysis is possible and no prior research exists on the question, which changes in stimulation-evoked brain activity occur during functional recovery, this is an exploratory analysis.
The experiments mentioned so far, both the attempted movement tasks with open-loop stimulation paradigms as well as the experiment with varying stimulation intensities in relaxed patients have been repeated 2-4 times per patient, usually with 1 week between repetitions, thus covering the full or at least a large portion of the 4 weeks of rehabilitation training. The most promising experiment for this is the movement task with open-loop stimulation for patient P1, because patient P1 showed clear functional improvements, the experiment was repeated 4 times and the stimulation parameters were kept constant between repetitions. The findings of this analysis are found in chapter 5.

4 Brain-state-dependent stimulation

The clinical tests of cortical stimulation via implanted electrodes for movement restoration in human stroke patients used open-loop stimulation in conjunction with physiotherapy [21, 79, 106, 136]: While patients performed physiotherapy sessions, stimulation pulses with a fixed frequency were applied to the damaged motor cortex. In this open-loop design, the stimulation is independent from the actions and the brain activity of the patient during physiotherapy. Its general purpose is to increase the excitability of the ipsilesional cortex or decrease the excitability of contralesional areas [81, 136]. This might facilitate brain plasticity during concurrent physiotherapy, but one has no control over whether the reorganisation happens in the desired fashion, to achieve recovery of lost motor function. If the stimulation could be applied specifically while the patient is actively trying to move the paralyzed limb, then there is a direct association between the stimulation and its activating effect on neurons, the movement of the limb (by a physiotherapist or an orthosis) and the brain activity patterns responsible for movement planning and execution. This is an extension of the hypothesis of Ramos-Murguialday et al. [138], that the association between movement intention and the contingent BCI-controlled movement of the orthosis strengthens residual cortico-muscular neural connections, possibly leading to improved recovery of motor function. Hence, instead of an unspecific modulation of cortical excitability, stimulation would serve to form a link between the brain activity and the peripheral activity of a movement of the affected limb. In this way, one might reinforce brain reorganisation specifically of areas associated with control of the paralyzed limb.

In general, this approach can be seen as a form of *brain-state-dependent stimulation* (BSDS) [85]. The concept of BSDS is to monitor the brain activity online and to present stimuli only if specific patterns of brain activity are found. For example, Bergmann et al. [13] monitored participant's EEG during sleep and applied TMS pulses if either an *up*- or *down*-state in non-REM sleep was found. The stimuli in a BSDS paradigm do not have to be TMS or other forms of direct cortical stimulation, they could be as simple as a visual or auditory stimulus. For this work, however, cortical stimulation is used and the brain state in question is whether or not the

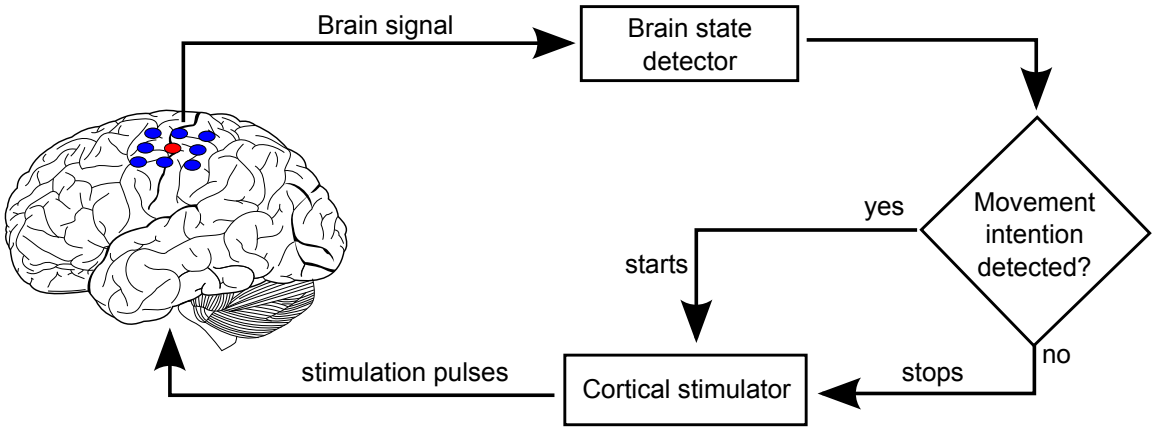

Figure 4.1.: General idea of brain-state-dependent stimulation for stroke rehabilitation: The delivery of stimulation pulses is started and stopped depending on whether an intention to move the paralyzed limb can be decoded from the brain signal.

patient is trying to move the paralyzed limb. The basic process is given in figure 4.1: A state detection algorithm determines, whether the patient tries to perform a movement and starts and stops the stimulator accordingly. While one could use muscle signals as input for the state detector to detect whether a healthy participant is actively performing a movement, this approach is problematic for paralyzed patients. Ramos-Murguialday et al. [139] found that although some patients still show faint modulations of electromyographic (EMG) activity when attempting to move the limb, this might not be strong enough to allow reliable decoding of movements from EMG, especially considering that muscle spasticity which impairs voluntary muscle activity is very common in stroke patients. Hence, brain signals are used as input in the BSDS paradigm and the state detection algorithm has to detect the intention of the patient to move the paralyzed hand from the recorded signals.
In the next section, the state of the art for movement intention decoding from brain activity is described.

4.1. Detection of movement-related brain states from brain activity

The term ”brain state” is based on the idea that the execution of a specific task is associated with a specific configuration of the neural activity of the brain. The state can refer to ”levels of wakefulness etc; or to contrasts between particular tasks; or even to different conditions within a cognitive task” [50]. As the main focus of this work is on movement restoration for stroke survivors, brain states related to movement are the most interesting ones, especially the discrimination between the

movement and the *rest* state. One has to differentiate here between three different types of movements:

- **Active movements**: The participant either actually moves the muscles or at least attempts to move them. This is usually accompanied by the generation of muscle activity detectable via EMG, to some extent even in patients attempting to move the paralyzed limb.
- **Imagined movements**: The participant visualizes to conduct the movement, but no visible movement is performed and the EMG activity is similar to the activity during rest. The limb whose movement was visualized may or may not be moved externally during the imagined movements.
- **Passive movements**: Another person or an external device, for example a robot or an orthosis, moves the limb while the participant stays relaxed. EMG activity should not be detectable.

The brain activity patterns of all these different types of movements can be discriminated from rest and differences between the individual movement types are found as well [140]. To perform this discrimination, meaningful characteristics of the measured brain signal have to be identified. Apart from the (discrete) brain state identifying the type of movement, other parameters of movements, in particular the direction of movement, have been shown to be detectable from the neural activity [18, 149]. Two domains are discussed as a source of signal features to decode movement states and parameters: the *time domain* and the *frequency domain*.

4.1.1. Time domain features

Neurons in the primary motor cortex (M1) can be tuned to abstract features of movements such as movement direction in extrinsic [62, 63] or muscle space [87]. Such neurons typically have a preferred movement direction which leads to the strongest increase in the rate of action potentials (spikes) before and during the movement compared to rest. Spike rates can increase more than 100 msec before movement onset [62]. Thus, if one can measure action potentials of single cells using implantable multi-electrode arrays (MEAs), one can discriminate movements from rest quite easily by counting the number of action potentials over an ensemble of neurons in M1 in a small time window, a procedure known as *binning*. The movement direction can be inferred from the population vector [63]. As the increase in neural firing rate starts before movement onset, one can even predict the start and direction of movement before it is visible. These characteristics of single neuron time domain activity have been used to construct neural prostheses which translate the spike rates into movements of a robotic arm or a computer cursor. Using MEAs, this has been tested mainly in animals [30, 38, 60, 61, 64] and in a few studies with tetraplegic humans

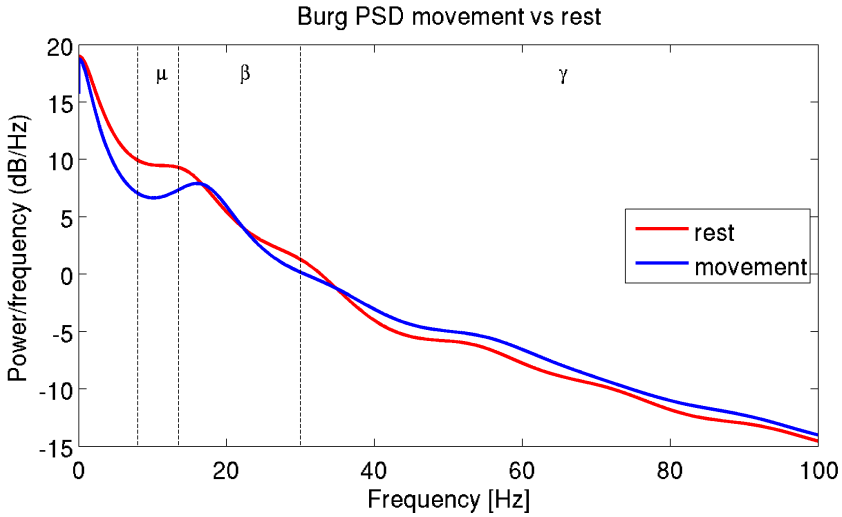

Figure 4.2.: Spectral power computed from a screening session with P1 during intended movement (blue) and rest (red) as an example of event-related synchronization (ERS) and desynchronization (ERD). ECoG data was acquired from a channel close to the motor cortex. The standard definition of the μ, β and γ band [127] are shown as dashed vertical lines.

as well [42, 76, 77].
As the use of MEAs is uncommon in humans, ECoG or EEG are alternatives but do not allow the measurement of action potentials of single cells. Still, time domain features of these signals can yield useful information about the ongoing movement [61, 99, 149]. Schalk et al. [149] termed a low frequency component the *local motor potential*, because its time domain evolution was highly correlated with the movement direction, and used it for the offline decoding of movement direction from the ECoG signal.

4.1.2. Frequency domain features

Especially for recording methods such as EEG or ECoG, where neural spikes can not be obtained, the power spectrum of channels near sensorimotor cortex (in particular primary motor cortex (M1), premotor cortex (PMC) and primary somatosensory cortex (S1)) has been shown to yield very useful information about movements. The main effect is described by event-related synchronization (ERS) or desynchronization (ERD) [135]: Modulations in the power spectrum of certain frequency bands before, during and after movements in comparison with rest (figure 4.2). An ERD is characterized by a reduced spectral power in comparison to rest, while ERS indicates the opposite. Pfurtscheller and Lopes da Silva [135] identified three frequency bands which are important in this regard:

- **μ or sensorimotor rhythm (SMR)** (8-13 Hz): Starting about 2 s before movement onset, the power in the μ band decreases on channels over the sensori-

motor cortex contralateral to the movement (contralateral ERD). This becomes a bilateral ERD at the moment of movement execution.

- **β rhythm** (14-30 Hz): The temporal evolution of the ERD is similar to the μ rhythm. After a voluntary movement is finished, ERS in the β-band is found, the so-called β-rebound.

- **γ rhythm** ($>$ 30 Hz): In the γ band, ERS is found during movements.

In the example of figure 4.2, while μ ERD and γ ERS are clearly seen, the β ERD is less clear and centered around 30 Hz. Thus, these features are subject-specific and should be individually adjusted. Typically, the spatial extent of these spectral modulations becomes smaller and more focal, the higher the frequency. Due to the somatotopic organization of the somatosensory and motor cortex, this means that a spatiotemporal analysis of the spectral modulations of high frequencies could allow a discrimination of different movement types. Unfortunately, the signal to noise ratio decreases for higher frequencies, making these rhythms difficult to measure. With EEG for example, γ band modulations usually can not be analyzed on a single trial level, hence movements are more commonly decoded from the μ and β band. However, for ECoG, γ band activity yields useful information for the detection of movement intention even for single trials [173, 181].
The fact that these rhythms are modulated both by active as well as by imagined movements forms the basis for the SMR-BCIs which have been developed for a multitude of studies since the 1980s [14, 179].

4.1.3. Online detection of movement-related brain states from spectral power (SMR-BCI)

In this work, spectral information is used because it is the most reliable tool for EEG and ECoG as input signals. In an actual experiment with BSDS, one has to ensure that the movement state can be decoded online during the experiment in order to provide fast and accurate feedback to the patient. The ability to detect brain states almost in real time is one of the core principles of BCIs, and movement-related brain states, especially from imagined movements, have been in use as a control signal for a long time. The lateralization of ERD and ERS can be utilized by discriminating between left and right hand movements, or the somatotopic organization by discriminating tongue from foot movements [179]. Another slightly simpler possibility is to decide between movement and rest (e.g. [140, 173]).
In any case, the system has to work online, hence the decision about the brain state has to be made within a short time. For a SMR-BCI [100], this involves the following steps:

1. **Data acquisition**, using EEG or ECoG.

2. **Signal processing**:
   a) **Spectral filtering**, for example to remove power line noise (optional).
   b) **Spatial filtering**, for example to improve focality with a spatial Laplacian [130] (optional).
   c) **Buffering** of the data by keeping the last several hundred milliseconds of the signal in a FIFO buffer.
   d) **Spectral estimation** of the data in the buffer (feature extraction).
   e) **Classification** of the brain state using the spectral power as input. The classifier is usually trained to discriminate between brain states using data from a screening session.
3. **Feedback** to the user, where the output of the classifier is used to generate a control signal for the feedback device.

When using a feedback device such as an orthosis, which opens and closes the hand of the patient depending on the output of the classifier [27, 138], the patient can learn to control the movement of the device and thus also of his hand. In the next section, it is discussed how cortical stimulation can be included into this setup to deliver brain-state-dependent stimulation.

4.2. Spectral estimation during cortical stimulation

Starting from the online BCI for the detection of movement intention, the question is now how this can be combined with cortical stimulation to apply stimulation only while an intention to move is detected (figure 4.1). The crucial point is that one has to ensure that the brain state is decoded properly even if stimulation is applied. The approach taken in other studies [13] is to alternate between a *decoding* and a *stimulation* mode in order to avoid having to deal with stimulation artifacts and other after-effects (figure 4.3). If the decoder detects the appropriate state, a stimulus is given. Then, the system waits until the stimulation effects have ceased, starts to collect data and begins the decoding process anew. In the example of Bergmann et al. [13] who used time domain features for the detection of the brain state, the latency until state decoding was restarted after a stimulus was greater than 3 seconds. If the decoding is performed on spectral features, a data buffer needs to be refilled from the start, before the first features after a stimulus can be calculated. In the case of the discrete Fourier transform, the length of such a data buffer should be at least 2 times the period length of the lowest frequency of interest. In practice a greater buffer length is preferred to reduce the variance of the spectral estimator, although one has to consider the trade-off between the variance, the responsiveness of the system and the expected non-stationarities within the brain signal: The longer the data buffer,

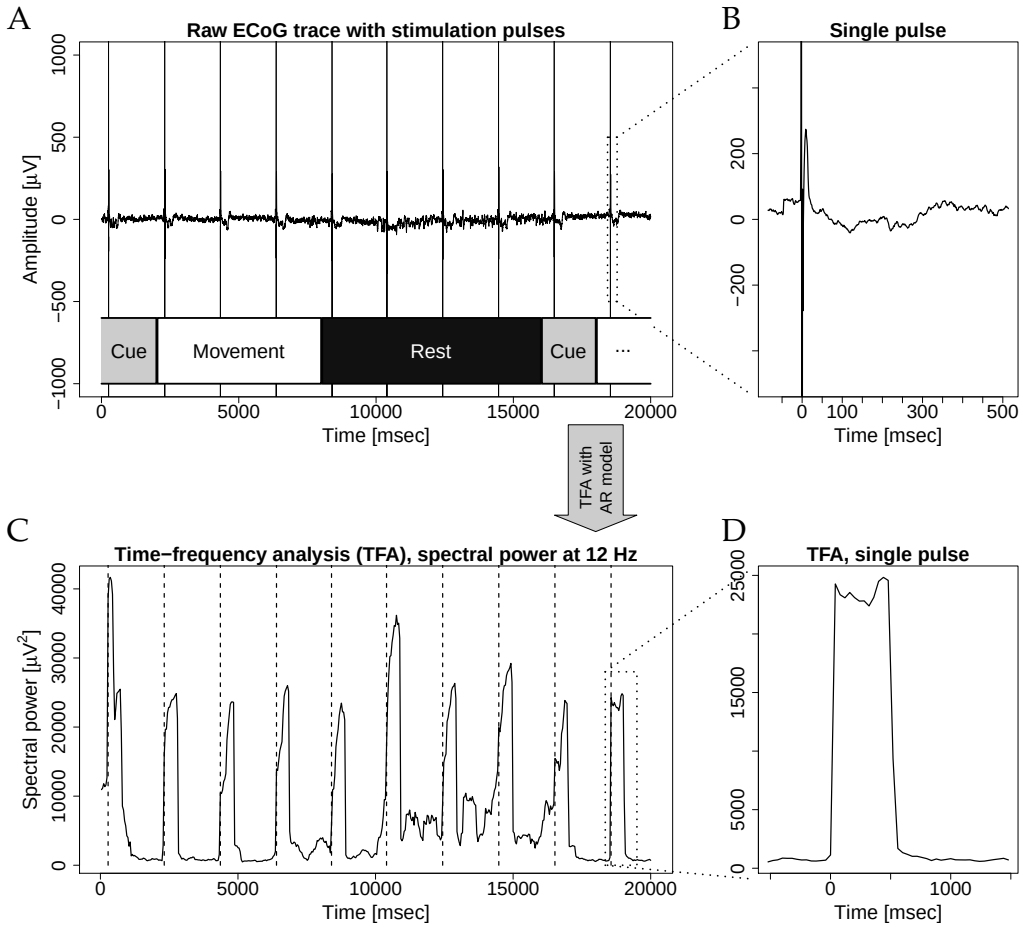

Figure 4.3.: **(A)**: 20 seconds of ECoG with several stimulation pulses, marked by stimulation artifacts. The task of the patient was to switch on cue between attempting to move the paralyzed hand (*movement*) and relaxation (*rest*). **(B)**: Zoom on one stimulation pulse. **(C)**: Time course of the spectral power at 12 Hz. Stimuli are marked by dashed lines. **(D)**: Zoom on one stimulation pulse. Adapted from Walter et al. [172].

the less variance there is in the spectral estimation. However, if the data buffer is too long, short-term changes in the signal spectrum might be missed and a BCI which uses these features as input would not be able to respond to such fast changes in the brain state. One might even lose the contingency between the intention of the user and the response of the BCI.
Consequently, the first response of the brain state decoder can be given $e + b$ msec after the stimulus, where e is the expected length of the stimulation artifact and the part of the waveform of the evoked activity which are considered too different from the normal, ongoing data on which the decoder is trained and b is the length of the FIFO buffer (figure 4.4). This leads to two issues: First, the system can not give a response for several hundred milliseconds or even longer after the stimulus, thus violating any claims for continuous decoding. If other devices are coupled to the decoder, not only the stimulator, the patient might become confused if the behavior of these devices does not match his brain state, because they have to be on "automatic" mode as long as there is no input from the decoder. For example, if a patient operates a wheelchair or a rehabilitation device with the command signals from the decoder, these devices either need some intelligent control to cover these silent periods, continue to execute the last command from before the stimulus or simply stop during that period which is very disruptive for concentration. It is very likely to make it harder for the patient to learn to control the movements of his hand via the rehabilitation device.
A second issue with this alternating scheme is that it enforces an upper limit on the minimum inter-stimulus interval (ISI). As at least one output of the decoder is needed to start the next stimulus, the ISI has to be at least $e + b$ msec. Depending on the application, this might not be sufficient. In TMS for example, stimulation frequencies of 2 Hz and above are associated with facilitation of cortical excitability, while lower frequencies seem to reduce MEP size [56]. So, if one wants to apply excitatory stimulation with a frequency of at least 2 Hz on average, $e + b$ has to be smaller than 500 msec, prohibiting the use of very low frequencies for decoding of the brain signal because the data buffer might be too short for their reliable estimation. One could remedy this issue by eliciting a pulse train with the desired frequency instead of a single pulse if the decoder reports the desired brain state, but then one has no guarantee that the participant remains in this state throughout the stimulation train. Also, as discussed in the previous paragraph, external devices coupled to the decoder output would have to cover silent periods of length $t + e + b$ msec autonomously, where t is the length of the pulse train.

A better solution is therefore to enable spectral estimation in the presence of stimulation pulses. This allows continuous decoding of the brain state, but one has to ensure that the spectrum is not disturbed by the stimulation, otherwise the application of the decoder will not lead to meaningful results. Obviously, as shown in

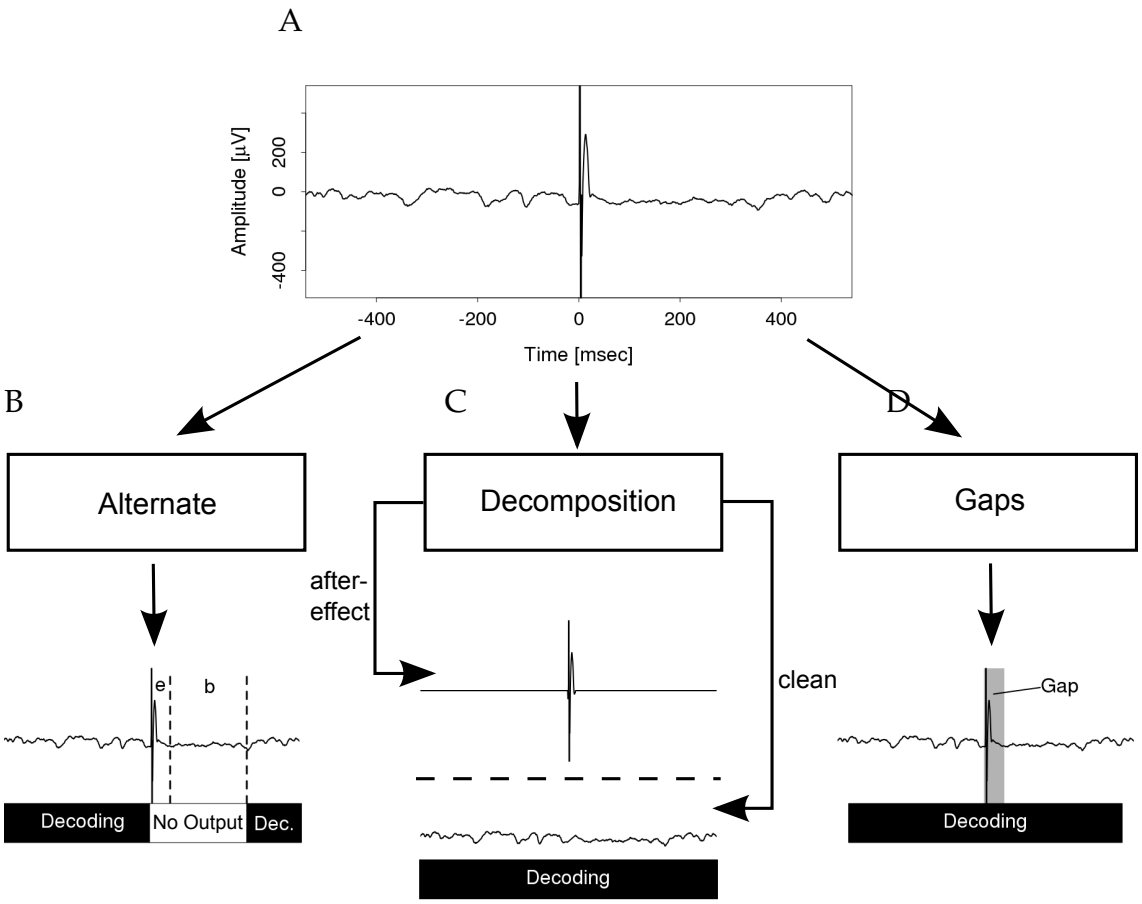

Figure 4.4.: Approaches to decode brain activity in the presence of stimulation: **(A)**: ECoG signal with a stimulation pulse at time point 0. A clear stimulation artifact and evoked activity is visible. Bottom: Three possibilities to decode brain activity in the presence of stimulation after-effects. **(B)**: Decoding is stopped after each stimulation pulse and resumed only if $e + b$ msec have passed. For a short period of time, there is no output from the decoder. **(C)**: The signal is decomposed and only the "clean" part is used for decoding. **(D)**: A gap is introduced to mask the stimulation after-effects such that they are ignored in the decoding process. In contrast to (B), decoding continues uninterrupted but the decoding system has to account for the gap in the data. See also section 4.2.2.

figure 4.3, simply using the raw input signal is out of the question, as the presence of the stimulation artifacts alone has a massive effect on the spectrum. Depending on the position of the recording electrode, neural activity evoked by the stimulation can reach amplitudes of several hundred microvolts [117, 118] and is in its shape vastly different from the background brain activity. Thus, having either of these effects in the data buffer from which the spectrum is calculated invalidates the assumption that the signal in the buffer has to have a stationary spectrum. In practice, if one computes the spectrum of such a time window, for example by using autoregressive models (see below), then the resulting spectral power is vastly greater than for time windows without stimulation after-effects (figure 4.3 C and D), making it clear that the results are simply dominated by the stimulation effect, not by the underlying neural signal one is actually interested in.
The best course of action to deal with this problem is to attempt to remove the after-effects of stimulation from the data buffer before spectral estimation. There are two approaches for this (figure 4.4): One can either attempt to decompose the recorded signal into a clean part and an "after-effect" part and compute the spectrum only on the clean part. Alternatively, one could remove all segments of the buffer that contain any after-effects of the stimulus.

4.2.1. Signal decomposition for artifact removal

The idea of signal decomposition rests on several assumptions:

1. There must be "clean" neural data obtainable at every time point. Otherwise, there will be gaps in the decomposed signal.

2. The stimulation after-effect is additive, or, stated in different words, once the after-effect is removed, the statistics of the clean neural data have to match the ongoing neural activity without stimulation. Otherwise, results of the analysis of the cleaned signal are not directly comparable with results without stimulation.

3. The characteristics of the stimulation after-effects are constant over time. Otherwise, the decomposition would need to adapt over time.

4. The decomposition must be doable in real time in a BCI setting.

These assumptions may be problematic in practice:

1. This condition puts strict constraints on the recording setup, as one has to make sure that the full extent of the stimulation artifact can be recorded without any amplifier saturation. This is a common problem in concurrent EEG recording and stimulation. For example, Veniero et al. [167] attempted to characterize the stimulation artifact in TMS-EEG for different stimulation parameters and

stimulated tissue but the limited dynamic range of their amplifier of $\pm$ 3.2 mV prevented them from recording the full extent of the artifact. If a very distant electrode is used for decoding such that the stimulation artifact is small, this might be feasible, but for electrodes close to the stimulation site, artifact amplitudes in the range of several hundred millivolts or even several Volts are possible. Ideally, an amplifier should be used with a dynamic range large enough to cover all artifacts.

2. The brain signal recorded at an electrode consists of the population activity of a large number of neurons. A stimulation pulse might activate some of these neurons, either directly or by an incoming stimulation-evoked volley of action potentials, resulting in an evoked potential (CCEP). Thus, if the evoked potential is removed by a decomposition, the residual signal before and after the stimulus differs because the contributions of the stimulated neurons are missing. Still, due to the inherent nonstationarities within the brain signal, this effect might be fairly small. Exactly these nonstationarities on the other hand prevent a measurement of the strength of this effect because a true reference signal can not be obtained.

3. It is well known that electrode characteristics can change over time. This is especially prominent for EEG, where drying of the electrode gel can influence the electrode impedance and change the size and shape of the recorded signal and thus, in turn, the stimulation artifact and the evoked activity. This might induce a drift in the recorded after-effects over time. Furthermore, there has to be a precise synchronization between the stimulator and the amplifier to ensure that the time of the pulse is aligned with the sampling time or, as a second option, one has to use a sampling rate high enough to accurately sample the artifact. Otherwise, if this is not done precisely, the artifact can differ from stimulus to stimulus. As the stimulation pulses are typically shorter than a millisecond and can have complex shapes, a sampling rate in the area of at least 5-10 kHz would be preferable.

4. The progress in computational speed makes it possible to operate even very complex algorithms in real time, thus CPU cycles are less of an issue. More difficult might be that one has to ensure that the algorithms work on a single-stimulus level and that a representative training set of artifact shapes can be obtained to train these algorithms. However, it prohibits the use of purely offline artifact removal methods such as the use of Kalman filters proposed in Morbidi et al. [122].

Although none of the challenges above is prohibitive, one assembles many constraints when trying to implement a decomposition scheme for online use. For example, the high sampling rates as a possible solution for problem 3 are excessive

if one is interested in decoding brain rhythms as low as the sensorimotor rhythms, placing unnecessary stress on the data transfer and online signal processing setup, especially if the recording is done from many channels. The questions about the stability of the evoked effects make it debatable, whether simple decomposition methods such as template subtraction could work reliably. Even more importantly, if one plans to use different stimulation parameter sets in an experiment, one would have to construct templates for each individual parameter sets as the responses to individual stimulation pulses, both artifacts [167] and evoked neural activity [32], strongly depend on the applied parameters. This quickly becomes unfeasible as soon as one considers stimulation paradigms where a stimulation parameter such as the intensity is adapted to the ongoing brain activity (see chapter 6). In this case, the stimulation parameter set is not predetermined and constructing a template for each set is not possible. Thus, for any but the simplest stimulation paradigms, signal decomposition is not a promising approach.

4.2.2. Introducing gaps for artifact removal

A different approach to the problem of spectral estimation in the presence of stimulation artifacts has been proposed in Walter et al. [172]. Instead of a signal decomposition, the segments of data with strong after-effects are removed from the data buffer, thus one is independent of any of the assumptions necessary for e.g. template subtraction. On the other hand, this approach brings a different set of challenges: In particular, if we remove a segment of data from the buffer, how can we calculate the spectrum for this buffer? Most spectral estimation methods require a data buffer with regularly sampled data. There exist methods for non-regularly spaced data, especially from the field of geology where data might be sampled over the course of several years, but not necessarily always at the same date. However, such methods, for example the Lomb-Scargle periodogram [111], are not established for the analysis of brain activity. Common methods to assess changes in sensorimotor rhythms for movement decoding in BCIs are: Fast Fourier Transform-based methods (FFT) such as Welch's algorithm, squaring of the signal after the application of bandpass filters and autoregressive (AR) models [9].
AR models have beneficial characteristics for BCI research, as they allow spectral estimation on relatively short data buffers, where an FFT would have to rely on averaging of several sub-buffers such as in Welch's method to keep the variance of the estimator at bay, sacrificing frequency resolution. AR models are a parametric method and although they allow continuous evaluation of the spectrum as opposed to the discrete results of the FFT, one has to specify a model order that is appropriate for the data [119]. Otherwise, the model might misrepresent the data. The ability of getting a good spectral estimate on short buffers of data make the AR model a good approach for BCIs, as it allows an online system with a short response time.

4.2.3. Autoregressive (AR) models

Given a data buffer holding N values $x(t_k)$, $0 \leq k < N$ which have been sampled at regular intervals, the first step to estimate the spectrum of this buffer with AR models is to fit an appropriate AR model to the data. The basic equation of an AR model is given as:

$$x(t_k) = -\sum_{i=1}^{p} c_i x(t_{k-i}) + e(t_k), \tag{4.1}$$

where p is the model order, x are the measured samples and $e(t_p)$ is a sample from a white noise sequence. For a perfect autoregressive process this means, that each sample within the buffer can be reconstructed as a weighted sum of its predecessors (or successors, because the model is time-invariant) except for a random deviation. The goodness of fit of an AR model can be quantified by computing the forward and backward prediction errors f and b for each sample $x(t_k)$:

$$f_{p,k} = x(t_k) + \sum_{i=1}^{p} c_i\, x(t_{k-i}) \qquad \text{with } k = p, \ldots, N-1$$

$$b_{p,k} = x(t_{k-p}) + \sum_{i=1}^{p} c_i\, x(t_{k-p+i}) \qquad \text{with } k = p, \ldots, N-1$$

These errors capture the deviations between the actual measured value and what value the AR model would have predicted for the sample. As a parametric method, the model order p has to be chosen beforehand. If it is chosen too high or too low, it might produce an insufficient representation of the data. A naive criterion for model selection would be to minimize the prediction errors b and f, but adding more variables to the model by increasing the order will always lead to lower f and b. Therefore, to prevent overfitting, one can evaluate criteria such as the Akaike Information Criterion (AIC) [3] which weighs the goodness of fit of the model against the number of variables (the model order) to find a good trade-off between model complexity and modeling error.
An AR model, once it has been fitted to the data, can be interpreted in two ways that are important for this work. First of all, one can see it as a linear predictor to extrapolate a new sample $\hat{x}(t_k)$ from known samples $x(t_{k-i})$, $i = 1, \ldots, p$ by evaluating the weighted sum on the known samples. Secondly, an AR model can be interpreted as an all-pole infinite-impulse-response (IIR) filter which operates on the white noise samples e and produces the measured samples $x(t_k)$ as output [133]. The coefficients of the filter are equivalent to the AR coefficients c_i.

Estimation of AR coefficients

For a certain model order, the AR coefficients c_i have to be fitted to the data buffer. Methods to achieve this are least-squares estimation, the Yule-Walker algorithm or

the Burg algorithm [28]. The latter algorithm has the advantage over the other two methods that the resulting coefficients are guaranteed to lead to a stable model, hence it is the one most commonly used for AR estimation [90]. The Burg algorithm, also called the Maximum Entropy Method (MEM), needs p steps and in each step j, the coefficients $c_{j,l}$ for an autoregressive model of order j are computed. Hence, if the Burg algorithm is applied to fit an autoregressive model of order p, the coefficients for all model orders smaller than p are computed as well. The algorithm works as follows [90, 172]:

An initial estimation of the power of the white noise component e in the AR model is obtained as the power of the signal:

$$P_0 = \frac{1}{N} \sum_{k=0}^{N-1} |x(t_k)|^2.$$

Then, step by step starting with an AR model of order 1, the AR coefficients for each order are computed. If the coefficients $c_{i-1,l}$, $1 \leq l < i$ for order $i-1$ have been found, a new coefficient $c_{i,i}$ is computed by minimizing the forward and backward prediction errors $f_{p,k}$ and $b_{p,k}$ with the formula

$$c_{i,i} = \frac{-2 \sum_{k \in I_i} f_{i-1,k} \cdot b_{i-1,k-2}}{\sum_{k \in I_i} (|f_{i-1,k}|^2 + |b_{i-1,k-1}|^2)}, \quad I_i = \{i+1, \ldots, N-1\}. \tag{4.2}$$

Each previously computed coefficient $c_{i-1,l}$ is then adjusted by

$$c_{i,l} = c_{i-1,l} + c_{i,i} \cdot c_{i-1,i-l}$$

to get the AR coefficients for order i. The white noise power estimation is then updated to

$$P_i = (1 - |c_{i,i}|^2) \cdot P_{i-1}$$

and the forward and backward prediction errors to:

$$\begin{aligned} f_{i,k} &= f_{i-1,k} + c_{i,i} \cdot b_{i-1,k-1} \\ b_{i,k} &= b_{i-1,k-1} + c_{i,i} \cdot f_{i-1,k} \, . \end{aligned}$$

After p steps, this results in the AR coefficients $c_i = c_{i,p}$, $i = 1, \ldots, p$ for the AR model of order p.

Estimating the spectrum from an AR model

In order to get an estimate of the spectrum of the measured signal from the AR model, one can use the interpretation of the AR model as an IIR filter: Following

Pardey et al. [133], it states that the measured signal x has been generated by filtering the white noise sequence $e(t)$ with the IIR filter A with coefficients c_i, leading to the basic AR model of equation (4.1). Hence, in the frequency domain, one arrives at the equation

$$E(z) = A(z)X(z)$$

where

$$A(z) = 1 - \sum_{i=1}^{p} c_i z^i$$

and $E(z)$ and $X(z)$ are the z-transforms of $e(t)$ and $x(t)$, respectively. This means that for a frequency ω, the frequency response $A^{-1}(\omega) = H(\omega)$ of the transfer function of the filter, multiplied by the spectrum $E(\omega)$ of the noise process, gives an estimate of the spectrum $X(\omega)$ of the measured samples x. Because we assume that the noise process is white, its spectrum is flat and $E(\omega)$ is constant. Thus, after finding the p autoregressive coefficients c_i and the power P_p of the white noise process, one can estimate the spectrum by evaluating the transfer function

$$H(z) = \sqrt{P_p} \left(1 - \sum_{i=1}^{p} c_i z^i \right)^{-1}$$

of the filter to find power values

$$P(\omega) = \frac{P_p}{|1 - \sum_{i=1}^{p} c_i e^{-ji\omega}|^2}$$

at (normalized) frequencies ω. In contrast to an FFT where the spectrum is computed only for discrete frequencies, this means, that the spectrum obtained by an AR model can be evaluated for arbitrary frequencies.

4.2.4. Spectral estimation in the presence of gaps

The Burg algorithm described above works on continuous data segments, but is not suited to deal with missing segments. Therefore, the goal has to be to do spectral estimation with AR models on data where segments are missing. For clarity, such missing segments will be called *gaps* from here on. There are three basic possibilities to deal with such data:

1. Fill the gap with artificial data, then apply standard AR estimation (figure 4.5 B and C)

2. Remove the gap and join the segments before and after the gap, then apply standard AR estimation (figure 4.5 D)

3. Modify the AR estimation algorithm such that it can deal with gaps

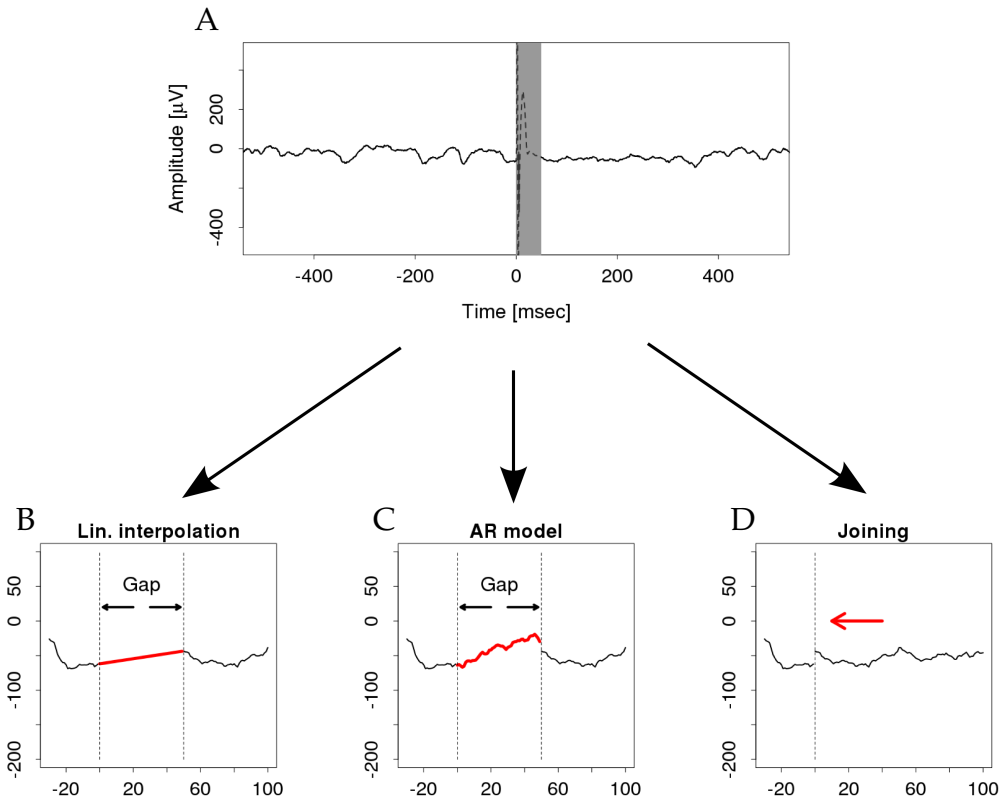

Figure 4.5.: Methods to deal with gaps in the data buffer: **(A)**: ECoG signal with a stimulation pulse at time point 0 and a gap (gray area) covering the first 50 msec after the pulse. Bottom: Three possibilities to produce a seemingly continuous time window. **(B)**: Linear interpolation connects the start and the end of the gap. **(C)**: The signal before the gap is extrapolated with an AR model to fill the gap. **(D)**: The segments before and after the gap are joined together.

Phrase	Defined on	Short description	Tested values
model order	page 51	Order of the AR model.	16, 32, 64
buffer size	page 46	Length of the segment of data on which the AR model is fitted and evaluated.	500 msec
gap size	page 55	Length of the segment of missing data (the gap).	5 - 100 msec
frequency	page 52	Frequency bin for which the AR model is evaluated.	5 - 100 Hz
packet size	page 55	Number of samples in each data packet arriving from the amplifier.	40
sampling rate	page 55	Number of samples recorded per second on one channel.	1000 Hz

Table 4.1.: Nomenclature for the important parameters of the AR model and the BCI system which are being used throughout this chapter. For parameters that are varied in the simulations, the tested values are given in the rightmost column.

In the following sections, the algorithms to test these three approaches are described as in Walter et al. [172]. The important terms for this section are summarized in table 4.1. One important consideration for these algorithms is that they have to be usable in an actual experiment where the spectrum of a data buffer holding the signal is computed each time that the buffer has been updated with newly recorded samples. These samples typically arrive in packets holding a fixed number of samples (*packet size*). Therefore, they have to be on the one hand fast enough that the constraint, that processing of the signal buffer should be finished before new data points are acquired, is not violated and secondly, the algorithms need to be able to deal with gaps at the end of the signal buffer where clean samples after the gap have not yet been measured.

Linear interpolation

Gaps in the data can be bridged by linear interpolation between the last sample before and the first sample after the gap (figure 4.5 B):

$$\hat{x}(t_{g+k}) = x(t_{g-1}) + \frac{k+1}{l+1} \cdot \left(x(t_{g+l}) - x(t_{g-1})\right),\ 0 \leq k \leq l-1 \tag{4.3}$$

where x are the signal samples recorded at times t_i, l is the length of the gap in samples and t_{g-1} is the index of the last sample before the gap.

While this might work for offline analysis of a data set, in the case of online analysis during a BCI experiment, in which data is received in a sample- or packet-wise system, one might have not yet received the first clean sample after the gap when

trying to produce an estimate for $x(t_{g+k})$ within the gap. A simple approach to solve this problem consists of filling the gap with the value of the last sample before the gap ($\hat{x}(t_{g+k}) = x(t_{g-1})$) as long as the packet containing the end of the gap has not been received and using linear interpolation for the rest of the gap otherwise. This approach is termed *online compatible linear interpolation*.

AR modeling

As a somewhat more sophisticated technique compared to linear interpolation, data can be generated from an AR model to fill the gap (figure 4.5 C). This uses the interpretation of an AR model as a linear predictor which has been introduced above: Values $\hat{x}$ for time points covered by the gap are extrapolated from samples recorded before the gap, using the coefficients c_i of the AR model estimated for the data buffer directly before the gap:

$$\hat{x}(t_{g+k}) = -\sum_{i=1}^{p} c_i x'(t_{g+k-i}) + \sigma \cdot e(t_{g+k}),\ 0 \leq k \leq l-1, \tag{4.4}$$

$$x'(t_{g+j}) = \begin{cases} x(t_{g+j}) & \text{if } j < 0 \\ \hat{x}(t_{g+j}) & \text{otherwise} \end{cases}$$

x' can refer to either actually recorded samples before the gap or estimated samples by the AR procedure. σ is the standard deviation of the white noise component in the estimated AR model and $e(t)$ one value of a white noise process.
While this approach has the property to generate data for the gap consistent with the previously measured data, one might prefer to use a mixture of AR modeling and linear interpolation for the online case. This would avoid jumps in the data when merging generated data within the gap with new samples acquired after the gap. This combination has been implemented here by performing AR extrapolation when information about the first sample after the gap was not available and using linear interpolation otherwise. In the recording setup of this study, the signal was received in packets with a length of 40 msec. If a packet contained the start and the end of a gap, then linear interpolation was used to fill the gap. If it contained only the start or if the whole packet was part of the gap, then the AR model was used as a linear predictor to fill the gap. If it contained only the end of the gap, then the last sample of the last packet and the first sample after the gap were connected by linear interpolation.

Joining two segments

If one chooses to ignore the information of the gap altogether when estimating the model, one might consider simply joining the two segments around the gap, therefore sacrificing information about the timing in the vicinity of the gap (figure 4.5 D).

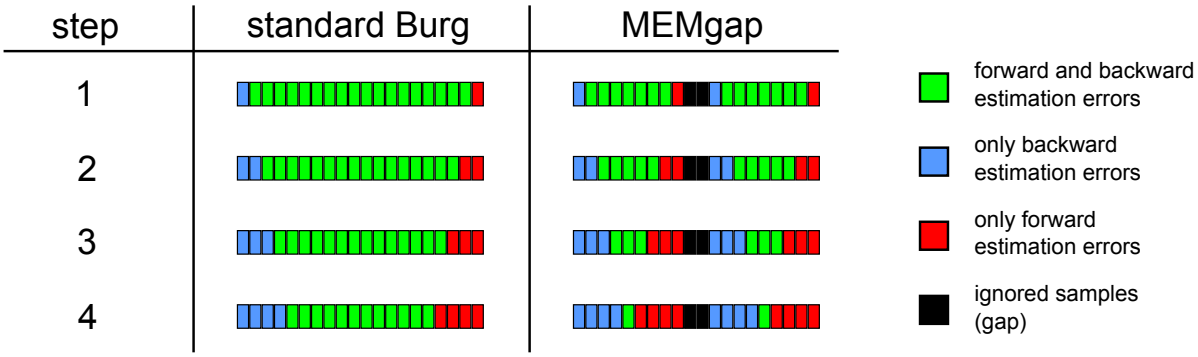

Figure 4.6.: Comparison of the standard Burg and the MEMgap algorithm. An AR model of order 4 is estimated on a buffer of 20 samples. For each step i, the colors indicate, for which samples forward and backward estimation errors are used in the computation of the AR coefficient $c_{i,i}$. For MEMgap, a gap is placed in the center of the buffer. Around the gap, an increasing number of samples contribute only either forward or backward prediction errors, not both.

In practice, this means that the data buffer is updated only with those samples from a newly acquired data packet that do not belong to a gap. In order to keep the buffer size for spectral estimation constant, this has the consequence that older samples are used to compute the spectrum with this method compared to the other algorithms.

Burg algorithm for segments (MEMgap)

For standard algorithms that compute the AR coefficients (Burg, Yule-Walker, least-squares), the samples within the data buffer need to be continuous. The least-squares estimation of the AR coefficients can be made compatible with data containing gaps by eliminating all equations from equation (4.1) that contain samples from within a gap and then solving the rest of the equations for the coefficients c_i. As the Burg algorithm (see section 4.2.3) yields more stable AR models than the least-squares estimation, it was modified to work with gaps based on the Burg algorithm for segmented data proposed in [46]. This was achieved by limiting the computation of forward and backward prediction errors in each step of the algorithm to those samples that are far enough away from a gap. In the remainder of this thesis, this algorithm is called *MEMgap* (Maximum Entropy Method for data with gaps) for brevity.

If one assumes that a sequence g of length N exists and that $g(n) = 1$ only if the corresponding sample $x(t_n)$ is part of a gap in the data and 0 otherwise then one just has to make sure that none of the samples $x(t_n)$ with $g(n) = 1$ influence the estimation of the model coefficients. The Burg algorithm computes the AR coefficients for order p in p steps, yielding in the i-th step the coefficients of an AR model with order i. If one uses in the i-th step only those samples fully for computation of the

AR coefficients that are at least $i+1$ time steps away from a sample with $g(n) = 1$, one achieves the desired effect.
To be more precise, the coefficients are computed by evaluating forward and backward prediction errors (see section 4.2.3). In the MEMgap algorithm, forward prediction errors are only computed for samples that are at least $i+1$ time steps after a gap, backward prediction errors only for those at least $i+1$ time steps before a gap. Formally, this is done by modifying I_i in equation (4.2) to the set

$$\begin{aligned} I_i = &\{k \mid g(k) = 0 \ \wedge \ i < k < N \ \wedge \\ &(k-n < 0 \ \vee \ k-n > i) \ \forall n \text{ with } g(n) = 1\}. \end{aligned}$$

This set can also be computed iteratively in each step of the Burg algorithm as $I_i = I_{i-1} \cap I'_{i-1}$, where I'_{i-1} is the set I_{i-1} with each entry incremented by 1 and $I_0 = \{k \mid g(k) = 0 \ \wedge \ 0 < k < N\}$ is the set of all indices corresponding to samples belonging to a gap. This resembles a "forbidden zone" that initially contains only the gaps but grows in each step of the algorithm by one sample. This process is visualized in figure 4.6. The estimation of the white noise power P_0 has to be calculated only with samples outside of gaps: $P_0 = \frac{1}{|I_0|} \sum_{k \in I_0} |x(t_k)|^2$. The rest of the algorithm works in the same way as the standard Burg algorithm described in section 4.2.3.

Obviously, this method can only work if the continuous segments between gaps are long enough. Therefore, there needs to be at least one segment of samples with a length that is at least equal to the model order p in order to make an estimation of the spectrum with this method. In practice, it is preferable if the number of samples in such a segment is several times higher than the model order in order to reduce the bias and variance of the estimator. If there are n_s segments of clean data with a length greater than p and the total number of samples in these segments equals M, then only $M - 2n_s p$ forward and backward prediction errors are available in the p-th step of the MEMgap algorithm, although all M samples are evaluated to compute these errors. This means that even if the total number of samples within gaps might be the same, one can expect that the variance of the spectral estimation will be smaller if there are only a few large gaps in the data compared to having many small gaps because less samples contribute fully in the second case. According to de Waele and Broersen [46], the same holds for the estimation bias which is inversely proportional to the number of available samples.

4.2.5. Evaluation of the algorithms

The reason why algorithms to deal with stimulation after-effects are employed is that one expects a distortion of the spectrum by these external effects. Unfortunately it is possible that the application of a suboptimal algorithm for the correction of these after-effects also distorts the spectrum. While this might be the "lesser evil"

compared with leaving the stimulation after-effects unprocessed, it still raises the question whether the spectral features extracted from data segments with stimulation and the output of further processing on these features can be trusted.
This issue gains even more importance if extracted features and classification results influence the extraction and classification of later time steps. An example where this occurs is an adaptive brain-computer interface, where the classifier is adjusted online during the experiment to correct for nonstationarities in the data. Distortions of the spectrum because of the stimulation or the algorithms applied to deal with its after-effects could influence this adaptation process unfavorably.
Hence, it is crucial that the spectrum after the introduction of a gap is as close to the original spectrum without the gap as possible. This can not be tested with actual stimulation data, because the stimulation after-effects are present in the recording, distorting the spectrum.
Therefore, the tests to assess the influence on the spectrum by the different algorithms are performed on data without stimulation. This data was recorded from patient P1 in a BCI training session with ECoG but without stimulation. The task of the patient is described in section B.1. The data is divided into many small overlapping segments of length 500 msec with an overlap of 460 msec. This overlap value was chosen to mimic the behavior of the recording system which delivered a new data packet every 40 msec. Reference spectra for these segments are obtained via the classical Burg algorithm. Then, gaps are introduced into the segments and the algorithms described above are applied to deal with these gaps, either by filling them with artificial data, joining the segments before and after the gap or by using the MEMgap algorithm. The spectra obtained with gaps are then compared to the gap-free spectra. Three main measures were used to evaluate the difference between gap-free spectra and those from data with gaps:

$$\text{bias}(f) = \frac{\frac{1}{n}\sum_i (P(f,i) - P_0(f,i))}{\overline{P_0(f)}}$$

$$\text{RMSE}(f) = \frac{\sqrt{\frac{1}{n}\sum_i (P(f,i) - P_0(f,i))^2}}{\overline{P_0(f)}}$$

$$\text{var}(f) = \text{Var}\left(\frac{P(f) - P_0(f)}{\overline{P_0(f)}}\right)$$

$P(f,i)$ is the spectral power of data buffer i for frequency bin f, $P_0(f,i)$ is the power of the original data buffer without gaps and $\overline{P_0(f)}$ is the average power of the full original recording without gaps for frequency bin f. n is the number of data buffers that are affected by gaps (i.e. data buffers where $P(f,i) - P_0(f,i)$ is not zero). $\text{var}(f)$ is the variance of the difference between the power values of the original data and the power values of the data with gaps for all data buffers affected by gaps and frequency bin f, divided by the average power for frequency bin f in

the data set without gaps. For example, a normalized bias of -0.1 means that the estimated power after application of the stimulus processing algorithm is on average 10% smaller than the power of the original data set if a gap is present.
The results of the evaluation of the algorithms throughout section 4.2 have been presented in Walter et al. [172] as well.

4.2.6. Algorithm performance on clean data

Several parameters of the spectral estimation are expected to influence the performance of the algorithms:

- **Gap size**: The longer the gap, the more samples are missing for the spectral estimation. Thus, the absolute deviation from the original spectrum without gaps will increase for increasing gap size. Secondly, the longer the gap, the more artificial samples have to be introduced by linear interpolation and AR modeling. If these algorithms introduce distortions, these should become rapidly greater for increasing gap size. Thirdly, it might influence the MEMgap algorithm, because it is the only algorithm where a longer gap means that there are fewer samples from which the AR coefficients can be estimated. As stated in de Waele and Broersen [46], this could lead to an increase in the bias of the estimator.

- **AR model order**: The higher the model order, the less smooth the spectrum. A model where the order is too low might not represent the signal accurately, thus possibly introducing unwanted effects. This could be problematic for AR modeling, where an insufficient model would be used to extrapolate the data, increasing the likelihood of a strong deviation from the actual shape of the signal. For high model orders, more parameters need to be estimated from the data. Thus, MEMgap might run into problems for high model orders and long gaps.

- **Frequency bin**: The frequency bin at which the AR model is evaluated. Low frequencies in relation to the buffer size might pose a problem. These are already difficult to estimate properly such that a considerable bias and variance of the spectral estimator is to be expected. Artifacts introduced by the algorithms or missing samples because of the gap will very likely further intensify this behavior. On the other hand, because linear interpolation removes the high frequency content from the gap, thus reducing the total power of the high frequencies within the data buffer, it should have a smaller impact on low frequencies.

By introducing gaps into a long ECoG recording without stimulation, varying the gap size between 0 and 100 msec in steps of 5 msec, the AR model order between 16,

32 and 64 and the frequency bin between 5 and 99 Hz in steps of 2 Hz, the parameter ranges most interesting for BCI experiments were tested. The buffer size was kept constant at 500 msec.

Influence on the spectrum

Two examples for the analysis on the relationships between the spectral estimation parameters on the differences between gap-free spectra and spectra with gaps are given in figure 4.7 and 4.8. In figure 4.7, the influence of the gap size on the RMSE, bias and variance is displayed for three different frequencies and a model order of 32. Although not shown here, the results for a model order of 16 and 64 are discussed below. In figure 4.8, the normalized bias is shown for the largest tested gap size of 100 msec for three different AR model orders because any effect of the gap on the bias should be most pronounced for the largest gap.
The main findings are [172]: MEMgap is unbiased for all parameters tested. It also achieves the lowest RMSE and variance for gaps greater than 50 msec with the exception of the highest model order.
For shorter gaps, the linear interpolation methods have a lower RMSE and variance. Unfortunately, these methods lead to a substantial negative bias across all tested frequencies. The average decrease in power is close to the quotient of the gap size and the buffer length. For example, for a gap size of 100 msec (out of 500 msec for the length of the entire buffer), there is a reduction in power of about 20 % (figure 4.8). As stated above, this is due to a portion of data being replaced by a straight line, thus removing power in high frequencies. For lower frequencies this decrease is less pronounced but still clearly present.
If the gap is filled by AR modeling, a positive bias is found, especially for a model order of 16. It is likely, that this model order was not sufficiently high. Also, to fill a gap of 50 msec with extrapolated data, an AR model with order 64 will always use actually measured samples as input to generate the samples filling the gap, given the present sampling rate of 1 kHz. For a model order of 16, most of the samples filling the gap will be generated using only samples that had been generated by the model as well, thus potentiating any mistakes. The positive sign of the bias for this method stems most likely from ”jumps” from the last sample within the gap to the first, actually measured, sample after the gap. If there is a large difference, this will manifest as a broadband increase in power. These jumps are significantly smaller for a model order of 64 than for 32, both producing smaller jumps than an order of 16. The average jump height for 100 msec gaps is 20.23 ± 11.94 μV (mean $\pm$ std) for an order of 64. Compared to the average absolute amplitude difference of adjacent samples of 1.68 ± 0.43 μV, this is a difference of one magnitude, implicating that even large model orders will not prevent jumps, making a positive bias very likely for AR modeling. Even if the data extrapolated with an AR model connected perfectly to the data after the gap on this clean test data set (a highly unlikely sit-

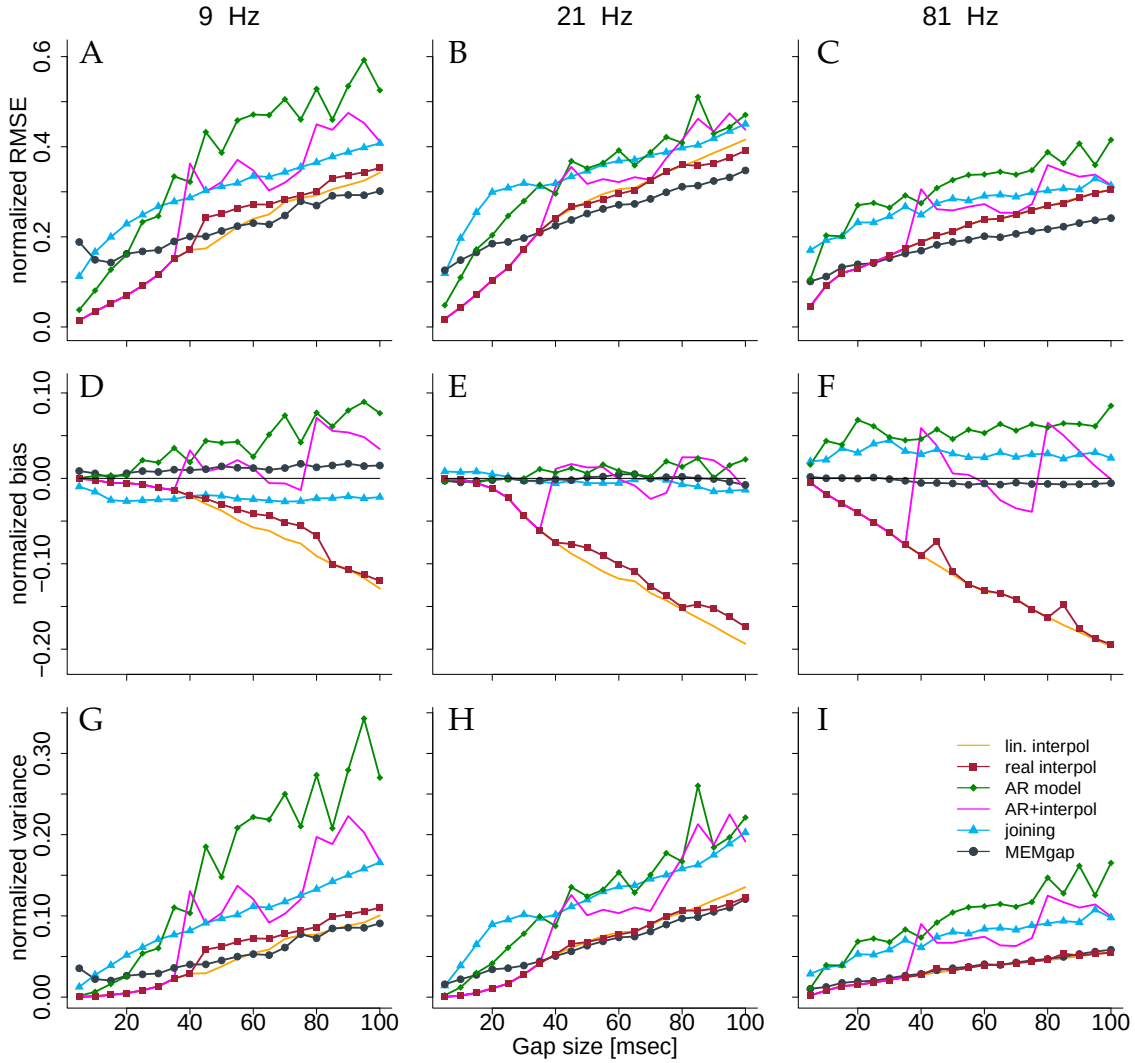

Figure 4.7.: Normalized RMSE, bias and variance of the spectral power estimation for the frequency bin at 9 Hz **(A),(D),(G)**, 21 Hz **(B),(E),(H)** and 81 Hz **(C),(F),(I)** for a model order of 32. The colored lines illustrate the course of the normalized RMSE in (A)-(C), the normalized estimation bias in (D)-(F) and the normalized variance in (G)-(I) relative to the gap size for the different algorithms. The thin black line in (D)-(F) denotes an ideal estimation bias of 0. Adapted from Walter et al. [172].

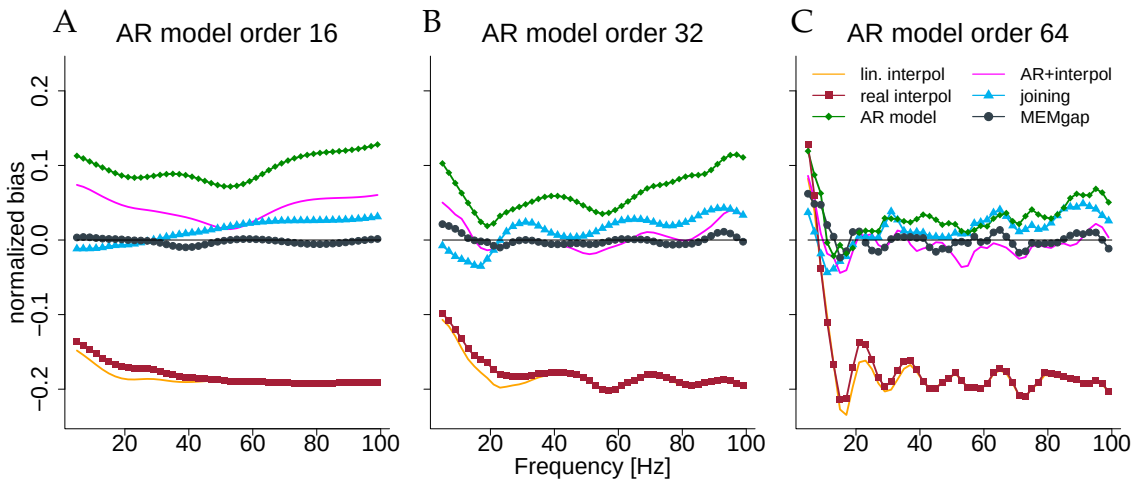

Figure 4.8.: Normalized bias for a gap size of 100 msec and an AR model order of 16 **(A)**, 32 **(B)** and 64 **(C)** as a fraction of the power of the original signal. The thin solid line always indicates a bias of 0. Adapted from Walter et al. [172].

uation due to the random component of the AR model), it is almost impossible for such an algorithm to achieve the same performance with actual stimulation because the recorded neural activity is influenced by the stimulation. If such an influence is present, there will be evoked neural activity in the signal, possibly also a phase resetting of the main oscillations will be observed [164]. These effects are not captured by an AR model fitted to prestimulus data, hence the extrapolated data can not fit to the data measured after the gap. Therefore, AR modeling will always lead to jumps between the gap and the post-gap data for real stimulation. Nevertheless, the drawback of the existence of these jumps might be offset by having data generating the gap which is in its statistics close to the real data.
The mixture of AR modeling and linear interpolation was introduced to remove the problem of jumps at the end of the gap by connecting extrapolated data with real data using linear interpolation. The bias of this method fluctuates between the positive bias of AR modeling and the negative bias of linear interpolation and depends heavily on the relationship between gap size and the update rate of the system / the data packet size. As the gaps are aligned to the data packets in this simulation, a gap size smaller than 40 msec means that the end of the gap is contained in the same packet as the start, thus only linear interpolation is used. For larger gaps, the bias quickly becomes positive, as the deviations produced have to be corrected by interpolation within a few samples, leading to sharp bends in the generated data and thus to a power increase. These bends become less problematic as the gap size approaches two times the packet size (in our case 80 msec), but increase afterward (e.g. figure 4.7). While this method reduces the extreme bias of both AR modeling and linear interpolation, the interaction of the gap size and the packet size makes it difficult to transfer the analysis of the behavior of the algorithm to experimental

	EEG		ECoG		
Patients	**none**	**open-loop**	**none**	**open-loop**	**closed-loop**
P1	1496	44	660	176	264
P2	143	99	682	176	286
P3		99	264	242	
Total	**1639**	**242**	**1606**	**594**	**550**

Table 4.2.: Number of trials of the patients' task to attempt to move the hand used in each paradigm to calculate AUC values for different parameters of the stimulus effect processing algorithms. *None* refers to sessions without stimulation and *open-loop* means that stimuli were applied intermittently throughout the trial. In the trials listed under *closed-loop*, stimulation pulses were given only during the task and if the decoding system reported a detected intention to move.

settings where these parameters are different.
The joining method exhibits only a small bias, compared to the interpolation and extrapolation algorithms. The sign of the bias is negative for frequencies smaller than 20-30 Hz and positive otherwise. Compared to the MEMgap method, this bias is clearly higher and the variance and RMSE of the spectral estimator is also higher. For model order 16, the graphs are very similar to figure 4.7. The main differences are that for order 16, the AR modeling algorithm exhibits a bias which linearly increases with the gap size for all frequencies and that the difference in the RMSE between MEMgap and the other algorithms is even more pronounced. For model order 64, the variance and the RMSE for the frequency bin at 9 Hz is comparatively large, indicating problems when estimating the power of low frequency bins with a large model order. This is also evident from figure 4.8 C where a strong positive bias is found for all methods at frequencies at or below 10 Hz. The linear interpolation methods are the only ones that produce low RMSE, bias and variance for an order of 64 and the 9 Hz frequency bin, but only up to a gap size of 40 msec (the packet size). For 21 and 81 Hz, the graphs are again similar to those in figure 4.7 C,D,F,G,I,J, although the RMSE and variance of MEMgap is now slightly higher than the RMSE and variance of the linear interpolation methods.

Influence on the brain state decoding

The unbiasedness of MEMgap is a very desirable characteristic as it should ensure that there is no systematic distortion introduced into the spectrum and thus the input for the brain state classifier. Therefore, the influence on the actual decoding of brain states should be small. To test this, online BCI experiments were simulated on the data sets described in section B.1 and B.2. The patients had to perform cued attempted hand movements in these experiments, switching between a *movement* and

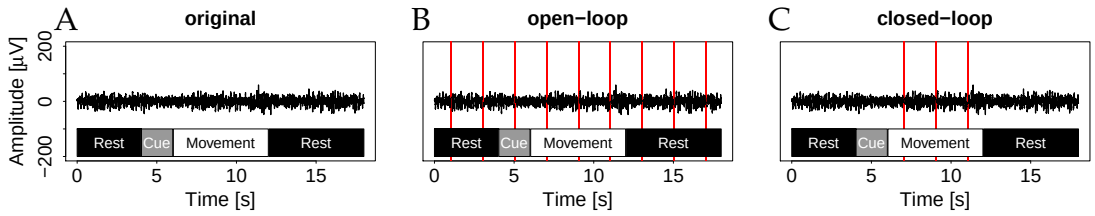

Figure 4.9.: Example for the simulation of open-loop and closed-loop stimulation. **(A)**: Original ECoG signal, source of the reference spectrum. Movement, rest and cue phases of the trial are indicated by white, black and grey boxes, respectively. **(B)**: Gap placement for open-loop simulation. Red lines mark time points where a gap was introduced. **(C)**: Gap placement for closed-loop simulation.

a *rest* state. In comparison to the *rest* state, the *movement* state is associated with event-related desynchronisation, thus a classification of small segments of data to either of the two states should be possible by using the spectral power of sensorimotor rhythms as features. As before, a data buffer of length 500 msec was moved in steps of 40 msec over the EEG and ECoG signal recorded from 3 channels over the left motor cortex.

In the first condition, an *open-loop* or *uncoupled* stimulation paradigm was simulated analogous to the experiment described in appendix B.2: Throughout the whole recording, data samples spaced 2 seconds apart were marked as a stimulation pulse and gaps were placed starting at these samples with varying lengths. In the second paradigm, only data samples within the movement phase were marked as stimulation artifacts, simulating a *closed-loop* or *coupled* stimulation experiment. Again, a spacing of 2 seconds between marked samples was used (figure 4.9).
In both conditions, the spectra were extracted with the different algorithms, the mean of the logarithm of the power between 16 and 22 Hz was taken for each of the three channels, summed over all channels and normalized. The scaling factor and the offset of the normalization step was obtained from a zero mean, unit variance normalization of the data collected in the rest phase. Thus, a negative sign after the normalization indicates a lower power during the movement than during the rest phase, hence ERD. The possibility to discriminate between the two states was measured with the area under the curve (AUC) of the receiver-operating characteristic (ROC, see also section 2.5.6). A value of 0.5 stands for chance level, while values of 0 and 1 indicate optimal separability [53]. Thus, comparing the AUC scores with and without gaps allows to judge whether the stimulation processing algorithms and their possible distortions of the spectrum influence the actual brain state decoding.

Figure 4.10 shows the distributions of differences in AUC scores for open- and closed-loop conditions for EEG and ECoG data, gap sizes of 10, 50 and 100 msec and

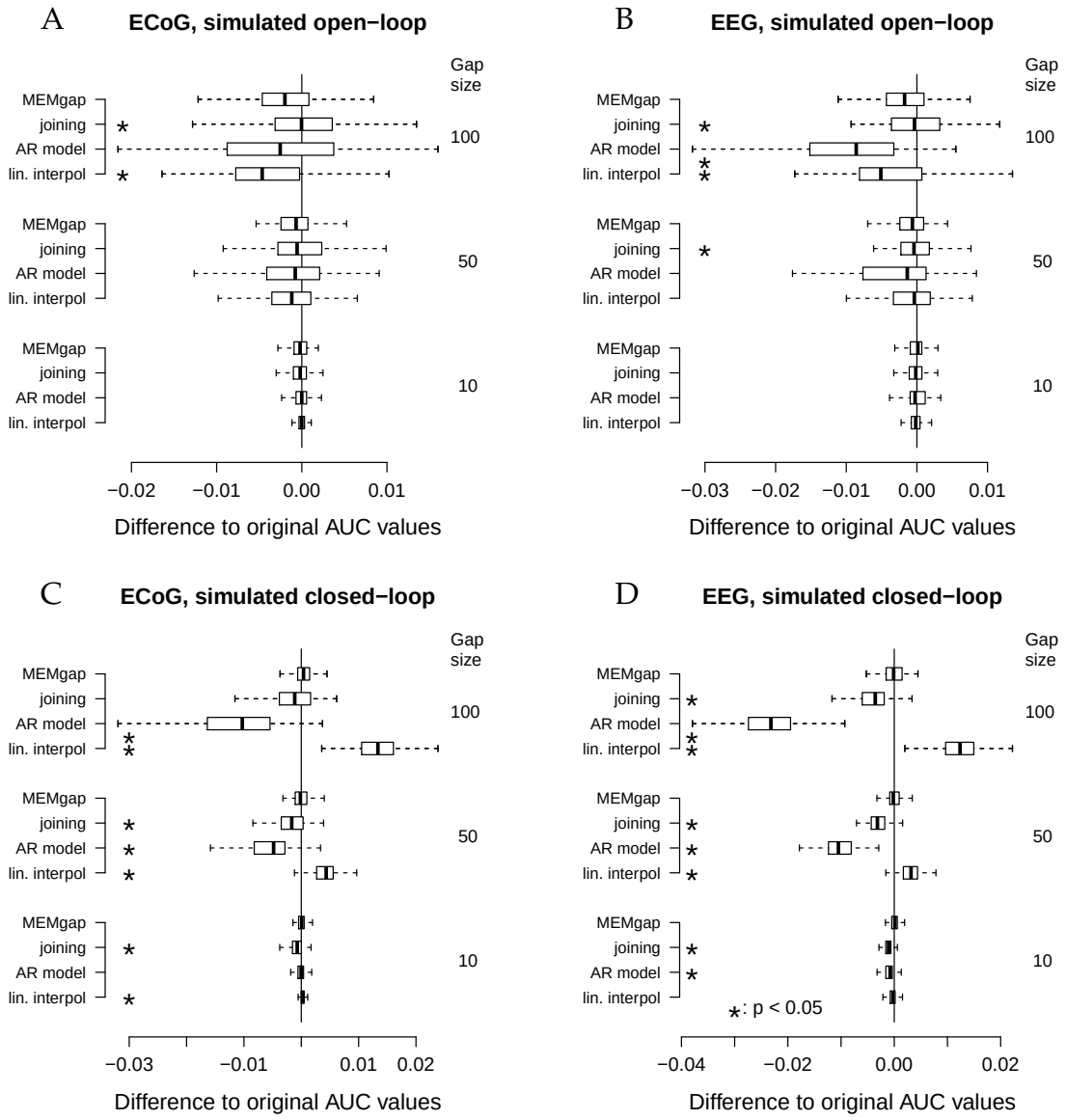

Figure 4.10.: Distributions of the differences between AUC values without gaps and AUC values of gap sizes of 10, 50 and 100 for data sets without stimulation. A deviation from 0 indicates an over- or underestimation of class separability. **(A)** ECoG and **(B)** EEG data with gaps simulated throughout the whole trial (*open-loop* condition, see figure 4.9). **(C)** and **(D)**: Average AUC values computed on the same data sets as in (A) and (B), respectively, but with gaps simulated only within the movement phase (*closed-loop* condition, BSDS). Boxes cover the range between the lower and upper quartile of AUC differences with the median depicted as a black line. The whiskers extend to the most extreme data point which is no more than 1. 5 times the interquartile range away from the box. *: AUC scores differ significantly from MEMgap for this gap size ($p < 0.05$, Friedman test, Bonferroni-corrected). Adapted from Walter et al. [172].

the different algorithms. For each algorithm a, gap size g, a distribution $A(g,a) = \{AUC(i,g,a) - A\bar{U}C(i)\}$ of the deviations and $A'(g,a) = \{|AUC(i,g,a) - A\bar{U}C(i)|\}$ of the absolute differences in the AUC scores was obtained. $A\bar{U}C(i)$ denotes the reference AUC value obtained without gaps for session i. Using non-parametric Kruskal-Wallis tests (Bonferroni-corrected for multiple comparisons) to test the hypothesis that the contents of A' at a particular gap size differ between the algorithms, significantly smaller ($p < 10^{-6}$) absolute deviations from the true AUC values were found for MEMgap and joining than for AR modeling and interpolation in the open-loop case.
Nonparametric Wilcoxon signed rank tests were used to assess, whether there is a significant deviation from 0 in the median of A, which would indicate a systematic bias in the AUC scores and is especially important in the closed-loop condition. Here, MEMgap produces the smallest absolute deviations compared with the other algorithms ($p < 10^{-6}$) and is also the only algorithm where the median difference does not differ from 0 at the $\alpha = 0.05$ significance level in most cases (except the closed-loop ECoG case and a gap size of 100 msec, $p = 0.005$).
Thus, MEMgap is the most promising algorithm as it introduces the smallest changes in the separability. Linear interpolation and AR modeling on the other hand heavily skew the obtained AUC values. The application of linear interpolation to fill the gap for example has the effect that AUC scores increase compared to data without the gap, thus it artificially "improves" the decoding. This supports the hypothesis stated above: A bias in the spectrum is transferred to a bias in the ability of a decoder to separate between the brain states.

Thus, an unbiased method such as MEMgap should guarantee an unbiased and thus reliable decoding of the brain state.

Performance with real stimulation data

Until now, all simulations were performed on data without any stimuli. This was necessary because a baseline spectrum was needed to quantify the spectral perturbations introduced by the stimulation-processing algorithms. Unfortunately, it does not answer the question how the algorithms cope with real stimulation data. Hence, the same evaluations of the AUC score changes on open- and closed-loop data depending on the algorithm and the gap size were repeated, but this time using data with actual cortical stimulation pulses. The patients performed the same task as described above and stimulation was applied either with TMS (in the case of noninvasive recordings, only open-loop) or epidural stimulation (with ECoG, open-loop and closed-loop). TMS pulses were applied with an inter-stimulus interval (ISI) of 3 seconds, epidural pulses with 2 seconds in the open-loop and 0.5 seconds in the closed-loop condition. In the latter condition, stimulation pulses were only applied as long as the online classifier currently reported a *movement* state which meant also that the orthosis was moving at the same time. For each stimulation pulse, the start

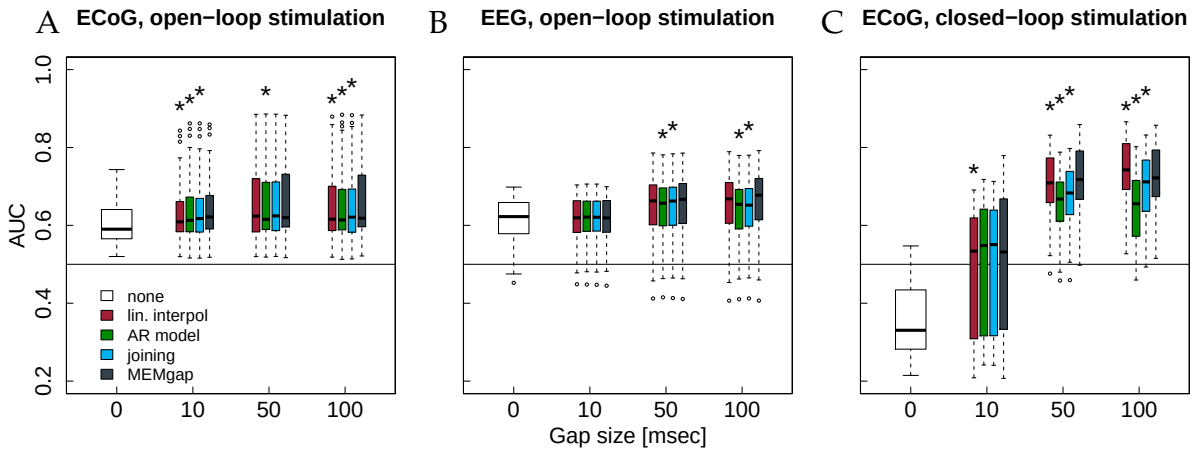

Figure 4.11.: Influence of the stimulation processing algorithm and gap size on the separability between intended movement and rest for experiments with stimulation. No processing of the stimulation after-effects was conducted for a gap size of 0. For gap sizes of 10, 50 and 100 msec, AUC values were calculated after application of the four algorithms (boxes from left to right) *real interpol*, *AR model*, *joining* and *MEMgap*. The chance level AUC value of 0.5 [53] is shown as a solid line. **(A)** Average AUC values for the separation of movement and rest from experiments with epidural stimulation and ECoG recordings. Stimulation pulses were given throughout the whole trial with a fixed ISI of 2 sec and the gap size was varied between 0, 10, 50 and 100 msec. **(B)** Same as (A), but for TMS-EEG data with an ISI of 3 sec. **(C)**: Average AUC values for ECoG data sets where stimulation pulses were triggered only if the BCI system detected an intention to move within the movement phase (BSDS). Boxes are defined as in figure 4.10, open circles depict AUC values outside the range of the boxplot whiskers. *: AUC scores differ significantly from MEMgap for this gap size ($p < 0.05$, Friedman test, Bonferroni-corrected). Adapted from Walter et al. [172].

of the gap was placed 2 msec before the beginning of the stimulation artifact and the gap size was varied between 0, 10, 50 and 100 msec. As in the simulations above, this was followed by the computation of the AUC scores. Further statistical analysis were performed on the raw AUC scores, not on differences, because no reference AUC score existed. Thus, when comparing the results between different algorithms, a correction for row effects (i.e. using the same sessions for all algorithms such that correlations are to be expected) is necessary. Therefore, instead of Kruskal-Wallis tests, Friedman tests are used which are the nonparametric equivalent of a repeated-measures ANOVA.

Figure 4.11 A and B shows the results for the open-loop experiments. While there are no significant differences in the AUC scores between the algorithms, in the case of the ECoG data, AUC scores with a gap size of 0 or 10 are significantly lower than scores for 50 and 100 ($p < 0.01$), independent of the applied algorithm. Thus, introducing sufficiently long gaps such that the extent of the stimulation artifact and the initial evoked activity are covered is beneficial for decoding. The closed-loop data

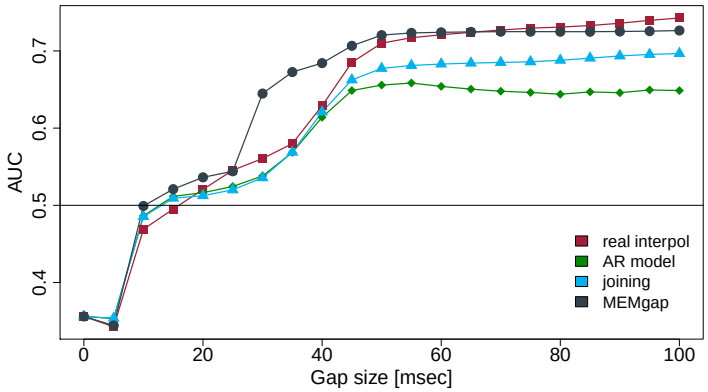

Figure 4.12.: Mean AUC values for different settings of the gap size for ECoG data obtained in the closed-loop condition with real stimulation. The baseline AUC value of 0.5 is shown as a thin solid line.

in figure 4.11 C finally shows the expected pattern in the AUC scores which was expected from figure 4.10 C and D: For a gap size of 100, AUC scores are significantly different between the algorithms ($p < 10^{-6}$): AUC values for AR modeling and linear interpolation are smaller and values for linear interpolation are higher than MEMgap. Thus, the expected spectral bias of AR modeling and interpolation also introduces a decoding bias for real stimulation data and MEMgap as an unbiased method is the best choice for a gap processing method.
Two oddities of figure 4.11 C are that the AUC scores for a gap size of 0 are smaller than 0.5 and that the scores for 10 msec have a large variability. AUC scores lower than 0.5 mean, that the average power during the movement phase is actually higher than during the rest phase, indicating ERS instead of ERD, something which is physiologically very unlikely when working with the β band [135]. Instead, this effect is due to the task-dependent existence of the stimulation after-effects in the closed-loop setting: The large stimulation after-effects that occur only during the movement phase lead to a very high spectral power of this phase. Thus, the spectral power of the movement phase is very well separable from the power of the rest phase for a gap size of 0. The variability at a gap size of 10 is present because for one of the 3 patients, a gap of 10 msec was not sufficient to cover all artifact-related jumps in the recording, resulting in AUC scores lower than 0.5.

If the after-effects are dealt with by using a gap size of 50, the relationship between the power during rest and feedback reverses and resembles the expected ERD/ERS pattern. Comparing the AUC values for a gap size of 10 with longer gaps, it is also clear that a gap size of 10 is not sufficiently long even if it covers in 2 out of 3 patients the direct stimulation artifact. The reason for this is probably that the early

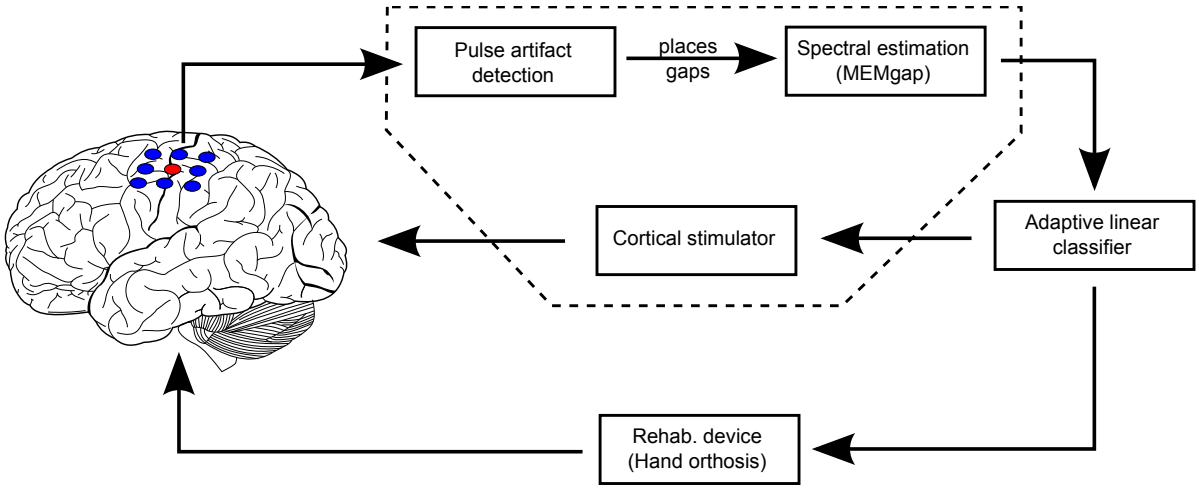

Figure 4.13.: Flow chart of the online setup for brain-state-dependent stimulation. All modules are implemented in the BCI2000 framework. The dashed parts mark modules which are specific for the use in BSDS paradigms.

evoked neural responses which usually peak between the first 20-30 msec after the stimulus can also distort the spectrum and have to be covered by the gap. This can be achieved by choosing a gap size of 50 msec or more, where the mean AUC values (figure 4.12) remains almost constant, at least for MEMgap.

The main conclusion from this study is that MEMgap is the most suitable algorithm for stimulation after-effect processing due to its unbiasedness. Thus, the MEMgap algorithm can be used to design bidirectional BCI systems, as long as spectral features are used for the detection of the user's intention or brain state, because it guarantees that the features are not distorted by stimulation. In contrast to earlier approaches, the decoding process can run continuously even while pulsed stimulation is applied. The specific parameters of the algorithm, in particular the gap size, obviously have to be adapted to each experiment. In the next section, the implementation and useful settings for the parameters of the first realization of such a bidirectional system are described.

4.3. Online brain state decoding and stimulation with a bidirectional BCI

For online decoding of movement-related brain states with concurrent pulsed brain stimulation, the general-purpose framework BCI2000 [149] was used and extended with custom-developed signal processing modules (figure 4.13):

1. **Pulse artifact detection**: An exact localization of the timing of stimulation artifacts to determine the starting point of gap placement. This was necessary

because a direct synchronization between the stimulator and the amplifier is not guaranteed to be present in all experiments and the software modules should not be too dependent on the exact hardware setup do be usable in different settings. The crucial feature of the artifact of a stimulation pulse is the fast very high slope of the first milliseconds, where the measured signal usually fluctuates between several millivolts, positive and negative (see e.g. figure 4.4). Thus, if the sum of absolute amplitude differences within 1 millisecond exceeds a certain threshold, an artifact is detected. While this threshold can be freely chosen in the software, a value of 1 mV has proven to be useful for ECoG data and epidural stimulation. For TMS, smaller values might be needed. 200 μV are suitable here, although the exact value depends on the impedance and the location of the recording channel in relation to the reference and the location of the stimulation. A higher threshold makes false positives less likely. If the stimulation is not triggered manually but by the BCI application (as in the experiments described in appendix B), then a state variable within the BCI2000 software is set to mark whether a stimulation pulse was triggered recently. If this is the case, then the pulse artifact detection is only active if this state variable is set.

2. **Gap placement**: An auxiliary data channel is introduced which contains a 1 for every sample that belongs to a gap, otherwise a 0. If a pulse artifact is detected, then as many samples are marked as the predefined gap size. The start of the gap is set 3 samples before the time point reported by the pulse artifact detection to avoid missing early portions of the artifact that were below the threshold. Following the analysis in the previous section, a gap size of 50-70 msec has been successful in practice.

3. **Spectral estimation with gaps**: This replaces the standard AR spectral estimation with the MEMgap algorithm. As described in section 4.2.4, it evaluates the information on the auxiliary gap channel, masks the unwanted samples and corrects for the missing data.

The resulting spectral power values are sent to an (adaptive) classifier to determine the brain state. In the special case of BSDS for stroke rehabilitation, the classifier discriminates between movement and rest and its binary output is used to control the movement of a hand orthosis capable of opening and closing the paralyzed hand of the patient. The orthosis started to open the hand of the patient as soon as the classifier reported an intended movement 5 times in a row and it was stopped if rest was detected for 5 consecutive times or if the trial had ended. The condition that the classifier output had to be consistent multiple times before the movement state of the orthosis was altered had been included to ensure a smooth behavior.
Furthermore, a control interface for the cortical stimulation systems was included as an application module in the BCI2000. The external control interface of the TMS was

restricted to TTL pulses which triggered the pre-programmed stimulation. Stimulation parameters had to be set by the researcher manually. For the STG4008 stimulator used with the epidural electrodes, a more extensive control over the stimulation parameters were possible. Stimulation waveforms can be freely defined, sent to the stimulator via USB and triggered by an asynchronous call. Hence, an extensible object-oriented framework was implemented and included into the BCI2000 application module which allows the simple definition of single pulse shapes up to whole pulse trains on several channels, where all stimulation parameters can be set online. This enables a system where all stimulation parameters are adjusted during the experiments automatically based on the online analysis of the ongoing brain activity.

The bidirectional BSDS system described here was used in the rehabilitation for the stroke patients, both with combined EEG and TMS as well as with epidural electrodes. Details on the rehabilitation and stimulation paradigm can be found in appendix B.1.

5 Towards a control of stimulation-evoked activity: The relationship between pre- and poststimulus activity

Two approaches for closed-loop stimulation have been introduced in this thesis. The first one, brain-state-dependent stimulation (BSDS), has been covered in chapter 4. In this and the following chapter, the second approach is studied: The feasibility of applying cortical stimulation with the aim of controlling the response of the brain (figure 5.1).
This approach is inspired by the work of Brugger et al. [23, 24, 25], who realized such a system using microstimulation in the Barrel cortex of rats. They were able to show that the variance of the evoked neural activity, at least for a certain range of stimulation intensities, can be reduced if the intensity is adapted to compensate for fluctuations in the ongoing neural activity before the stimulus. The overall aim was to provide the possibility to define a *target* shape of the activity one wants to achieve, for example because it is associated with a specific percept, and then having a closed-loop system which automatically finds the stimulation parameters most likely to evoke exactly this shape. Their work was originally intended for the use in sensory neuroprostheses, for example to restore sight to blind people by direct microstimulation of the visual cortex, where the closed-loop stimulation system could provide more stable visual perceptions than an open-loop system.
However, one could find a use for such a system in the application of cortical stimulation for stroke rehabilitation as well: If one can identify neural correlates of rehabilitation in the stimulation-evoked activity of stroke patients regaining motor function, it could be advisable to stimulate the patients in a way to reinforce these correlates. No study has looked so far longitudinally on rehabilitation-induced changes in the processing of stimulation pulses in stroke patients, hence no such correlates are known. What is known is that some reorganization of the brain takes place during recovery from stroke - the premotor cortex in particular is a likely ”hot spot” for this [89], while the size of the motor representation of the affected limb in the primary motor cortex is expected to increase as well [108]. Whether general correlates for this

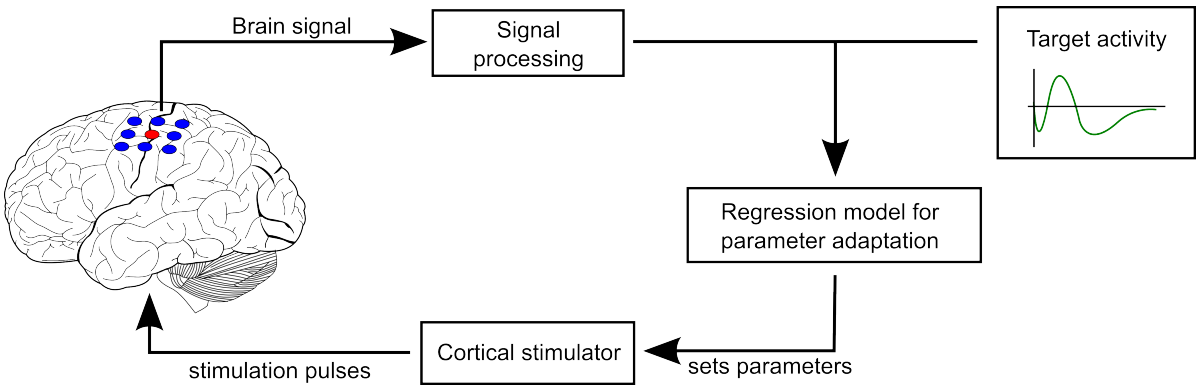

Figure 5.1.: Concept for adaptive stimulation to evoke a target shape of the brain activity.

recovery-associated reorganization exist in the stimulation-evoked brain activity is a question that can not be tackled in this work due to the small number of patients, although the patients at least provide an opportunity to test, whether any coherent changes occur over the time of their participation in the experiment. If this is the case, this would give an indication on where to look in larger groups of patients for "dynamic" features of the evoked activity.
Even if we are unable to draw general conclusions about neural correlates of rehabilitation, it is possible to test, whether a stimulation paradigm is feasible where some features of the poststimulus neural activity are controlled by adaptive stimulation. The work of Brugger et al. [23, 24, 25] provides the starting point for this, but a major conceptual step is necessary to transfer this approach from the animal model to human stroke patients: The implantation of microelectrodes is a very invasive process and they have been implanted only in a handful of human patients so far, with just one case where stimulation was applied via these electrodes (see section 2.1). Less invasive stimulation and recording devices might make such an approach applicable to more human stroke patients, for example by using EEG in combination with TMS or ECoG together with electrical stimulation via implanted electrodes. However, it needs to be tested then, whether the functional relationship between the prestimulus activity, the poststimulus activity, and the stimulation intensity, which was at the core of the work of Brugger et al., can be found as well when using these devices. This step from micro- to macroelectrodes will impact both the spatial resolution of the recording, because the signals of individual neurons are inaccessible with EEG and ECoG, as well as the focality of stimulation: TMS and epidural electrodes require much higher currents than microelectrodes to produce a measurable effect on the brain, thus, presumably, a much larger number of neurons is activated by the stimulus.
A necessary condition for the existence of this postulated functional relationship is, that fluctuations in the prestimulus activity need to have an effect on the evoked activity after the stimulus. If this is not the case, that is, if the reaction of the brain to a

magnetic or electrical stimulus was purely stereotypical, a closed-loop system would not be better than an open-loop system in controlling the evoked activity. However, this is unlikely, not only because of the studies with microelectrodes mentioned so far, but also because of a number of other studies with TMS which investigated the relationship between the brain activity at the moment of stimulation and either the evoked muscle activity in the form of motor-evoked potentials (MEPs) or the evoked brain activity. The following section gives an overview over these studies.

5.1. State of the art

5.1.1. Cortical excitability and stimulation-evoked potentials

One likely candidate process that influences the neural response to cortical stimulation unrelated to the stimulation parameters is the receptiveness of the stimulated area to stimulation, the so-called *cortical* or, when stimulating the motor cortex, *corticospinal excitability*. Corticospinal excitability can be measured easily by applying stimulation pulses strong enough to elicit a muscle twitch. Using electromyography (EMG), this muscle twitch is registered as a motor-evoked potential (MEP) and its amplitude and/or latency serves as the direct measure of the excitability - the greater the amplitude is, the more effective is the relay of the stimulation pulse towards the muscle. One has to control for the strength of the muscle activity at the moment of stimulation, because it also directly influences the amplitude of the MEP: Stronger muscle activity leads to stronger MEPs [114]. Thus, measurements of corticospinal excitability are usually conducted when the muscle is either at rest, or by giving the stimulated person feedback of the EMG activity, thus encouraging a constant level of muscle activity [165].
For cortico-cortical potentials evoked by TMS or electrical stimulation (CCEPs), such measurements are more problematic, as the evoked waveforms can be relatively complex and are not as easily parametrized as the MEP (figure 2.1). Usually, the amplitudes of certain peaks in the evoked activity are used, although the mechanisms of the generation of these waves are not fully understood, especially for late peaks [55, 164]. An interesting component is the N100 response, a negative peak in the EEG which occurs roughly 100 msec after a stimulus over the motor cortex on central channels and is thought to reflect inhibitory activity [11, 17, 22, 128].
An increased level of cortical excitability could indicate that the stimulated brain region is more receptive to incoming information and has been shown to correlate with improved motor function [72]. It can be used as an outcome measure for a clinical intervention where increased cortical excitability could indicate that a brain region becomes more active over time. It is used as a tool to assess the rehabilitation of paralyzed persons [80], where increases in MEP amplitude on the paretic limb are proof that not only there is a corticomuscular connection present but also that the

effectiveness of the connection increased over time.

Brain states

Long term processes, such as the neural reorganization associated with the recovery of motor function in a stroke patient, are of course not the only way to change the excitability of a brain region. By measuring MEP amplitude and latency and/or CCEP subcomponent amplitude, several studies have found that the execution of tasks influences the excitability level of certain brain areas as well. Such short-term modulations can be understood in terms of switching between *brain states*. In its simplest form, an experiment can be designed to investigate the differences in the evoked activity during two states: *task* and *rest*.
In the periphery, the change of MEP amplitudes relative to the brain state has been studied for decades and given insights into the inner workings of the motor system. Major findings have been that not only active movements increase the MEP amplitude compared to rest but that such an increase, although smaller, is also present for imagined movements [52]. In both conditions, this MEP modulation is specific for the muscle: During imagined flexion of the forearm, MEPs on the biceps are increased compared with rest, but no effect is found for forearm extension [52]. Similar results for imagined hand movements lead to the conclusion, that MEPs are only increased if the stimulated muscle is an agonist in the movement [52, 73, 107]. Using MEPs as output measure thus gives information how specific parts of the motor cortex and their connection to the muscles are influenced by the execution of tasks.
The analysis of CCEPs, however, allows the investigation of brain states not related to the motor system. The latency and size of evoked waveforms also highlights functional connectivity within the brain [117, 118, 160], thus one can use the strength of the reaction to the stimulus of different brain areas and its task-related modulation to infer information about how these areas are involved in the cognitive processing of the task. Thus, the study of CCEPs and their task-related modulations might be worthwhile to gain a better understanding of the brain. For example, it was shown that the state of consciousness of the stimulated person is reflected in the shape of the evoked activity: While under anesthesia [54], during deep sleep [116] or in a minimally conscious state [146], the evoked brain potentials strongly differ from CCEPs elicited in awake persons. The waveform in the non-awake state is less complex, has a stronger early response and is constrained to a smaller brain area than evoked activity during wakefulness. This so-called *breakdown of effective connectivity* [116] thus gives insights about the neural correlates of consciousness. This finding is independent from the integrity of the motor system, because cognitively present locked-in patients without muscle control show similarly complex responses as healthy, awake persons [146].
In awake persons, the N100 peak in the EEG has been used as a measure for brain-state-dependent modulations of cortical excitability. Nikulin et al. [128] found that

the N100 amplitude is reduced during and shortly before movements. They attributed this to a reduction of the inhibitory response reflected in the N100 if the stimulated brain region is active at the moment of stimulation, e.g. because a movement has to be planned or executed. Morishima et al. [123] investigated the role of the frontal eye field during a visual feature attention task and noticed differences in the N100 response depending on whether a face or a moving stimulus was shown as long as the TMS pulse was given late enough to ensure that the subjects had time to prepare for the task. Johnson et al. [86] reported an increased N100 during a short-term memory task and increased power in the β and γ range of the stimulation-evoked event-related spectral perturbation (ERSP). Bonnard et al. [17] found an increased N100 while subjects tried to resist an MEP, compared to a state where the subjects did not fight the MEP. This again indicates that an increased N100 might reflect increased inhibition. Häusler et al. [74] as one of the first to investigate movement-related changes in stimulation-evoked brain potentials showed that the slow brain potential near the center of the scalp (EEG position Cz) following a TMS pulse over M1 is larger when the participant is executing a thumb movement compared to the preparation of the movement.
These studies demonstrate that the task and its associated brain state have a profound influence on how stimulation is processed in the brain. It also becomes clear that the analysis of stimulation-evoked effects can highlight changes in functional brain connectivity [71, 117], thus serving as a bio-marker for task-related modulations of excitability and connectivity.

Ongoing neural activity

The idea of a brain state is a very abstract and probably oversimplified concept, because it ignores the relationship to the underlying neural activity, which is never constant during a specific task. If the brain state is a realization of the neural processing, then changes in the brain state should be detectable from changes in the measured brain activity. This is widely used in brain-computer interfaces, where event-related changes in the brain activity (e.g. μ/β ERD) are used to infer the brain state of the user (e.g. movement imagery). Hence, if the brain state influences the effects of stimulation, one might also be able to find a direct relationship between the ongoing activity and the stimulation-evoked potentials. On the other hand, the changes in observable neural activity and modulations of the cortical excitability could be uncorrelated epiphenomena of a switch in the brain state.
Several studies investigated the relationship between MEP amplitudes evoked by TMS and the signal characteristics of EEG and EMG activity at the time of the stimulation, with conflicting results. Mitchell et al. [121] computed the spectral power of EEG and background EMG while healthy participants performed a grip task and were stimulated either with TMS or transcranial electrical stimulation (TES). While they found a significant correlation of the MEP amplitude with EMG, the correla-

tion coefficients with the EEG power after correction for the background EMG were non-significant or around the significance threshold. In order to test for interactions between EEG and EMG activity, they used a greedy bottom-up feature selection method with leave-one-out cross-validation to predict the MEP amplitude based on EEG and EMG. r^2 values remained mostly below 0.3, thus even the combination of EEG and EMG can not explain most of the variance. They argued that there is probably a difference between the level of activity and the level of excitability of a brain region and concluded that EEG alone is not sufficient to explain the variability in the evoked potential.
Van Elswijk et al. [165] hypothesized that β and γ oscillations are correlates of rhythmic inhibitory processes, thus cortical excitability should depend on the phase of these rhythms. Using TMS during isometric muscle contractions, a task known to induce cortico-muscular coherence between EEG and EMG activity, they examined not only EEG and EMG phase, but also spectral power on their suitability to predict the MEP amplitude. Similar to Mitchell et al. [121], they found no significant relationship of the MEP with EEG power. Surprisingly, neither the EEG phase nor the EMG-EEG phase relation were correlated with the MEP amplitude. However, they found that the EMG phase for frequencies between 5 and 45 Hz modulates the MEP significantly. From this it can be concluded, that the spinal β rhythm that manifests itself in the EMG activity, not the cortical one influences the MEP. This is a bit surprising because the existing cortico-muscular coherence during this task shows that there should be a direct relationship between both rhythms.
Both studies investigated the relationship between cortical rhythms and MEP amplitude within a constant brain state. Furthermore, both removed background EMG as a factor, either by analyzing only the residuals after correcting for EMG influence [121] or by using online visual feedback of a target EMG activity [165]. Neither study found a significant correlation between EEG power and the MEP measuring cortical excitability. This sheds doubt on the hypothesis that the brain activity can explain much of the variance of the stimulation-evoked activity, apart from the variance induced by brain state switches.
On the other hand, Schulz et al. [153] found that EEG spectral power in the β range and corticomuscular coherence in the α range predict MEP size. In their study, TMS was applied over the motor cortex during or shortly after a hand movement. However, this means that the brain state was not constant for all stimuli so that this finding might be explained by the difference between the spectral power during movement and rest and not by a direct influence of the prestimulus spectral power on the MEP.
In contrast to the motor system states that were investigated by Mitchell et al. [121], van Elswijk et al. [165] and Schulz et al. [153], Bergmann et al. [13] studied the CCEP and MEP responses to TMS during sleep. In NREM (non-rapid eye movement) sleep, prominent slow oscillations with frequencies smaller than 1 Hz dominate the EEG.

The phase of this slow oscillations reflects changes in the membrane potential: Positive deflections reflect depolarization (up-state), negative waves hyperpolarization (down-state). Thus, neurons should be more receptive to stimulation during the up-state than during the down-state, because they are closer to the firing threshold. As expected, Bergmann et al. [13] found stronger MEPs during the up-state, reflecting the higher cortical excitability in this state. Using EEG-guided TMS where stimuli are only applied if the absolute amplitude of the slow oscillation is above a threshold, they applied pulses only if the brain was clearly in one of the two states. Beyond this simple discrete state-dependent modulation, they found a weak (Pearson's $r < 0.2$) but significant correlation between the EEG and the MEP amplitude on a single-stimulus level, meaning that for example with a more positive slow-wave amplitude there is a tendency for a greater MEP. This indicates that at least during sleep, there might be a weak direct relationship between the measured neural activity and the evoked potential. Romei et al. [144] found a significant relationship between the posterior α rhythm amplitude and whether TMS pulses over the visual cortex elicit phosphenes in healthy participants or not. This shows that spontaneous fluctuations of neural activity might be associated with a functional role, at least in the visual cortex [83].

In conclusion, discrete changes in the brain state can have a profound effect on the response of the brain to stimulation, but at least for EEG combined with TMS of the motor cortex, a direct relationship between measured neural activity and the parameters of the evoked muscle response in awake participants is doubtful. It is unknown whether the increased signal-to-noise ratio of invasive recording methods together with electrical stimulation might be specific enough to reveal significant correlations between prestimulus and poststimulus activity. In particular, it has not yet been reported whether a relationship between the ongoing neural activity and the evoked brain activity, i.e. the CCEPs, exists. Furthermore, one limitation of the studies on this so far is that they have almost exclusively focused on healthy participants, while the work in this thesis is concerned with patients with pathological changes in the brain.

5.2. Research questions towards closed-loop control

As stated above, a direct influence of the prestimulus activity on the shape of the poststimulus activity is a necessary prerequisite for the feasibility of closed-loop control of the stimulation-evoked activity. When looking at changes in the prestimulus brain activity, one has to distinguish between a changing brain state and fluctuations in the measured EEG or ECoG activity. The former usually induces the latter, but the electrophysiological brain activity will fluctuate even within a constant brain state. Therefore, because the focus of this work lies on motor function, the most basic hy-

pothesis here is:

Hypothesis I
When stimulating the motor cortex, movement-related changes in the brain state lead to changes in the stimulation-evoked brain activity.

Based on the many results reporting brain-state-dependent changes in MEP amplitudes and the work of Nikulin et al. [128] on movement-related changes in evoked brain activity, this hypothesis has a good chance of holding up. However, it needs to be tested whether these effects can be found in severely affected stroke patients and also whether it is a TMS-specific effect or if it can be reproduced with electrical stimulation. A positive result for this hypothesis would lead greater credence to the BSDS paradigm developed in chapter 4, but it allows only a small step towards closed-loop control of the evoked activity: One could envision a paradigm where each brain state is associated with a certain stimulation intensity in order to always produce the same shape of the evoked activity. For example, the stimulation intensity while the patient rests could be higher compared to the time when the patient is attempting to move the hand to compensate for the reduced cortical excitability. Hence in comparison to the BSDS paradigm of chapter 4, the variability of the evoked activity would not be reduced as the stimulation intensity within the *movement* brain state would be the same in both paradigms, but the new paradigm would allow the application of pulses also within the *rest* state, therefore the total number of applied pulses can be increased. However, then the association between the intention to move the hand, the hand movement and the stimulation would be lost again which could be considered a loss of specificity in comparison to the BSDS paradigm of chapter 4.
A more desirable stimulation paradigm would be to retain the temporal association between the movement and the stimulation by stimulating only within the *movement* state, but adapting the stimulation intensity to the ongoing brain activity to reduce the variability of the evoked activity. For this to be possible, the following hypothesis has to hold:

Hypothesis II
When stimulating the motor cortex while a movement is intended or performed, changes in the electrophysiological prestimulus brain activity lead to changes in the stimulation-evoked brain activity.

5.3. Experimental setup

In order to test these hypotheses, an experiment was performed with healthy participants and stroke patients, for the former with combined EEG and TMS, for the latter with EEG and TMS and after the surgery several times using the implanted electrodes. In order to disentangle the influence of movement-related brain states and the ongoing brain activity on the stimulation evoked activity, the stimulation parameters were kept constant for each participant, but by using a movement task, the brain state of the participants was modified because they were instructed to switch on cue between *resting* and a *movement* state. For the movement task, three conditions were tested: attempted, imagined and passive movements with the latter as a control condition. If significant changes in the shape of the stimulation-evoked activity during one of the movement tasks and phases in the experiment where the participant is in a relaxed state can be found, this would confirm hypothesis I. If significant correlations between the EEG/ECoG activity before the stimulus and the evoked activity can be found when analyzing only those stimuli applied within the *movement* phase of the task, then the second hypothesis is confirmed.

5.3.1. Participants

7 healthy volunteers (1 female, mean age 26.5) and the three chronic stroke patients (section A) participated in the experiment. For the patients, the experiment was conducted once before implantation of the electrodes and two (P3) to four (P1 and P2) times with the implanted electrodes present. In this invasive phase, all experimental sessions were spaced one week apart, covering almost the whole 4 weeks of the period in which external connections to the implanted electrodes were present.

5.3.2. Procedure

The task, the recording parameters and the stimulation are described in detail in section B.2. In short, the participants performed for 6 seconds a movement task after an auditory cue, then relaxed for 8 seconds. The *movement* condition was to either actively attempt to open the hand (*active* condition), imagine to open it (*imagined* condition), or be relaxed, while the orthosis passively opens the hand (*passive* condition). Independently of the task or the brain signal, the participants were stimulated with single pulses with a fixed interstimulus interval of 2 (epidural stimulation) or 3 (TMS) seconds. The intensity of the pulses was high enough to elicit measurable MEPs on the left hand extensor muscle. In the *active* and *imagined* condition, the hand of the participant was opened by the orthosis which was controlled by an online detection of the intention to move the hand.

5.4. Data analysis

For each individual stimulus pulse, features are extracted from the pre- and poststimulus data. Thus, the data is not segmented into the *trials* of the task, but the single *stimuli*.

5.4.1. Poststimulus data

All recorded EEG and ECoG data were filtered with a 2nd order Butterworth bandpass filter with cutoff frequencies 3 and 300 Hz and a notch filter to remove the power line artifact at 50 Hz. To avoid an influence of the stimulation artifact on poststimulus data, the filters were applied anti-causally, i.e. on time-reversed data. Where necessary, channels with long-lasting stimulation artifacts or noisy signal were removed from further analysis. For each stimulus, 1 second of poststimulus data was extracted. Semi-automatic stimulus-rejection was performed to exclude stimuli considered to be outliers by using the variance of the EEG/ECoG signal as a criterion and visual inspection. Depending on the condition (rest, active movements, imagined movements, passive movements), stimuli were excluded if the muscular activity did not conform to the task: The *waveform length* $WL = \sum |s(t) - s(t+1)|$ was used as a measure of the EMG activity on EDC in a window of 200 msec preceding stimulation, where $s(t)$ is the emplitude of the rectified EMG signal at time point t. It contains information about the EMG amplitude and frequency and has been identified as the best feature for the detection of movements from EMG [159]. Let WL_{rest} be the distribution of all WL values for stimuli in the *rest* phase. For the active movement condition, if the waveform length did not exceed the median WL_{rest} by two standard deviations of WL_{rest} in the *movement* phase, or if it was not within one standard deviation of WL_{rest} of the median WL_{rest} in the *rest* phase, the stimulus was excluded for the healthy participants because there was either too much EMG activity in the *rest* phase or not enough in the *movement* phase. The EDC activity of the patients was not reliable during active movements because of spasticity and the inability of the patients to control their paralyzed muscles. Therefore, stimulus rejection by EMG activity was unfeasible for the active movement condition and not used for the patients. For passive and imagined movement conditions, all stimuli were excluded for which the WL exceeded the median WL_{rest} by more than one standard deviation of WL_{rest}. Then a spatial Laplacian was applied to the EEG data to increase the focality of the extracted measures and to reduce bias introduced by the reference electrode [130].

5.4.2. Prestimulus data

In order to test for correlations between the spectral content of the prestimulus data and the amplitudes of the evoked activity, the spectral power before the stimulus

was extracted. The spectrum has to be computed over a time window before the pulse. In shorter time windows, only samples immediately before the stimulus play a role, but the variance of the spectral estimation will be higher. For longer time windows, the estimate will be more stable, but samples in the "distant past" will have the same influence on the spectrum as samples directly before the stimulus. Hence, in this case, the spectrum captures more the broad changes in brain activity, less the local fluctuations in the oscillations. As it is unclear, which of these factors is more important, the length of the window was varied between 100 msec and 1 second in 100 msec steps. The spectral power was determined with an autoregressive model of order 50 (determined as a model order well suited for the data by use of the ARMASA Matlab® toolbox [19]) and two frequency bands were extracted: α (8-13 Hz) and β (14-30 Hz). For each sample of the poststimulus data, the Spearman correlation coefficient ρ was computed with the α and the β band power, once for all stimuli and then for stimuli in the *movement* and the *rest* phase separately. Spearman's ρ is a non-parametric measure of the relationship between two variables, because it measures a monotonous relationship instead of a linear relationship computed by Pearson's r. For this reason it is also more robust against outliers compared to r.

5.4.3. Statistical evaluation

Brain-state dependency of evoked activity

The significance of the difference between the waveforms of the evoked activity in the *task* (either active, imagined or passive movement) versus the *rest* conditions was tested with the following procedure, inspired by Casarotto et al. [32] and adapted to the problem of discrimination between CCEPs of different conditions:

1. For each time point t_i, channel c_j and participant s_k, divide the data of all repetitions of the stimulus in two distributions: $D_{task}(s_k, c_j, t_i)$ and $D_{rest}(s_k, c_j, t_i)$ that contain the samples from the *task* and the *rest* period, respectively.

2. Compute the normalized distance of these distributions using Cohen's d for unequal sample sizes. This captures the effect size of the influence of the *task* on the evoked activity compared to *rest* as it takes into account not only the difference in the median but also the variances of the distributions.

3. For a single participant, it was determined if a specific value for d was significant at the 0.05 level with a Monte-Carlo permutation procedure. The condition label of all repetitions (*task* or *rest*) was permuted randomly $n = 3000$ times and d was recomputed for each time point and each channel. This resulted in a distribution $M(c_j, s_k)$ containing the maximum value of d obtained for each permutation and all time points of channel c_j of participant s_k. The significance

threshold for d of channel c_j was set as the value of $M(c_j, s_k)$ corresponding to the one-tailed $(1 - \frac{\alpha}{C})100^{th}$ percentile of $M(c_j, s_k)$ with $\alpha = 0.05$ and C being the total number of channels. Using this procedure, the test result is corrected for multiple comparisons incurred by the number of time points and channels investigated.

4. Because of the variability of the patients, a group analysis was only conducted for the healthy participants. To assess whether the median of d over all healthy participants was significant at the group level, the permutation procedure from (3) was performed for all healthy participants, $\bar{d}$ was computed as the median of d per permutation for each time point and channel over all healthy participants and a distribution M' containing the maximum value of $\bar{d}$ over all channels and time points was extracted. The significance threshold for $\bar{d}$ was then set as the value of M' corresponding to the one-tailed $(1 - \alpha)100^{th}$ percentile of M'. This procedure therefore also corrected for the number of time points and channels.

Spectral dependency of evoked activity

Similar to the brain-state-dependency analysis, significance testing of the correlation between the prestimulus spectrum and the amplitudes of the poststimulus activity has to take into account the large number of tests conducted and the fact that results for neighboring samples of the poststimulus activity are likely to be highly correlated, due to the high autocorrelation of EEG and ECoG signals. For these reasons, significance testing was again conducted using a permutation procedure, but instead of permuting the class labels, the mapping between pre- and poststimulus data was permuted (e.g. in one permutation, prestimulus spectral power from stimuli {1,2,3,4} was correlated with the poststimulus amplitude of stimuli {3,4,2,1}. As above, the α-level of 0.05 was Bonferroni-corrected by the number of channels, the number of repetitions was set to 3000 and three different stimulus sets were tested:

- All stimuli
- Only stimuli within the *movement* phase
- Only stimuli within the *rest* phase

As in the previous section, the significance threshold for a single participant and single channel was computed by extracting the maximum absolute value for ρ per permutation and finding the value at the target α-level, i.e. the $(1 - \alpha) \cdot 3000$-th value when the maximum ρ values were sorted in ascending order. All samples of the poststimulus data where $|\rho|$ exceeded the significance threshold were marked as significant.

5.4.4. Classification of the brain state from evoked responses

For each participant and movement condition, a support vector machine (SVM, libSVM [33]) with linear kernel was trained to classify the preprocessed CCEP waveforms into the *task* class (active, imagined or passive movement) and *rest*. Using the data after offline processing for the statistical evaluation, it was downsampled to 250 Hz and a window was used with a length of 300 msec, starting 5 msec after the stimulus to exclude the initial stimulation artifact, resulting in $75 \cdot n_{channels}$ features. These parameters were found during a first offline evaluation of several settings for the downsampling factor (1,2,4 or 10) and the window length (100 or 300 msec). Different spatial filters (none, common average reference, spatial Laplacian, canonical correlation analysis) were compared for this data set, but no difference was found between them [155]. Thus, the results reported here use the same spatial filtering as in the statistical analysis: spatial Laplacian for EEG and no filter for ECoG.
The accuracy, sensitivity and specificity of the classification was estimated with a 4-fold cross-validation (CV) procedure: In each fold, 75 % of the stimuli were used as training data, the rest for testing. The training data was rescaled to the range from 0 to 1. The scaling factor and offset from this procedure was also applied to the test data. Model and feature selection was performed exclusively on the training data: With recursive feature elimination [68], sizes of the feature set between 5 % and 100 % of the total number of features in steps of 5 % were tested to find an optimized feature subset. In order to also test very small feature sets, sets with 40, 30, 20, 10 and 8 features were included as well. For each set of features, the regularization parameter C was optimized using 10-fold cross-validation in the range of $2^i,\ i \in \{-5,\ldots,5\}$. By permuting the training data and applying another 10-fold CV to it with the best C, the accuracy for each feature subset was computed. The feature subset with the highest CV accuracy was chosen and a SVM was trained on the whole training data using this feature set. This SVM was applied to the test data, predicting either *task* or *rest* for the test stimuli. This procedure was repeated for all 4 folds, resulting in estimates for the classification performance measures.

5.5. Results

In the first part of the results section, it is shown that there are significant differences in the evoked activity between the *movement* and the *rest* state and that at least for the *active* condition, a classifier can be trained to discriminate between *movement* and *rest* from the shape of the evoked activity on a single pulse basis. In the second part of the analysis of this experiment, the question whether there is a significant relationship between the prestimulus EEG/ECoG activity and the evoked activity is addressed.

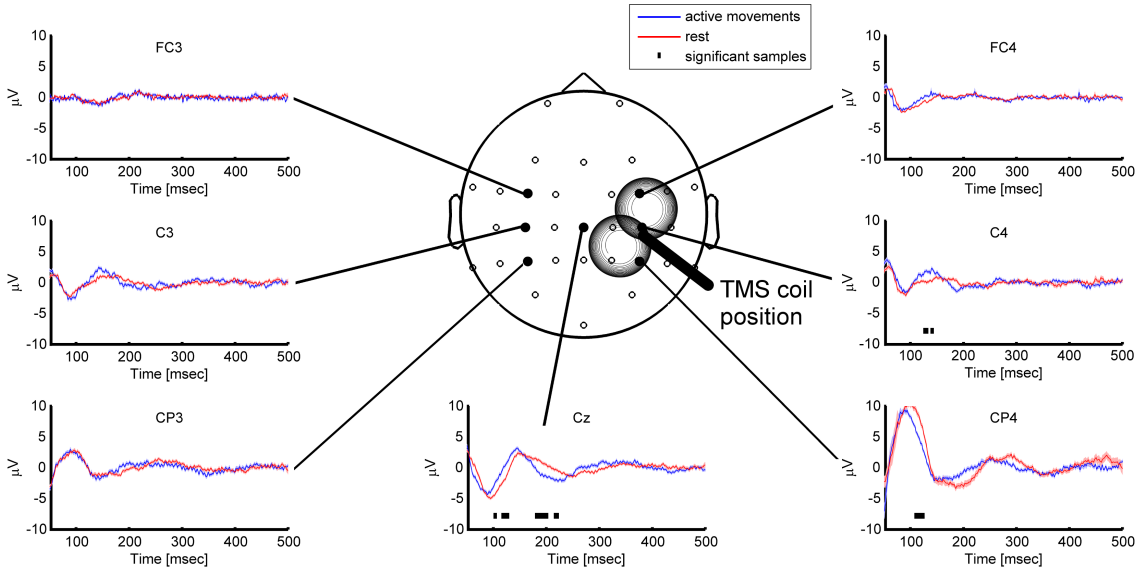

Figure 5.2.: Median CCEP for one representative participant (S4) on different EEG channels. Blue: Activity during active movements, red: activity during rest. Light red and light blue areas cover the median ± the standard error (SE). Black bars below the waveforms mark samples with a significant difference ($p < 0.05$, corrected for the number of channels and samples).

5.5.1. Significant task-dependent differences in the evoked activity

Healthy participants

The effect size d from TMS stimulation and EEG for all three conditions (active, imagined and passive movements) was extracted individually per participant (an example for this is shown in figure 5.2) followed by a group analysis on the healthy participants to test whether an effect can be found across participants (figure 5.3). The stroke patients were not included in the group analysis as the physiological changes associated with the stroke might limit the comparability of their evoked activity with those of healthy participants.

In figure 5.3, the topographical distribution of the maximum effect size within 4 time windows is shown for the active, imagined and passive conditions. Significant differences between the evoked effects during the *movement* phase versus the *rest* phase are found most prominently for active movements, covering ipsi- and contralateral sensorimotor cortex (SMC) in the time window of 100-160 msec after the stimulus and the ipsilateral SMC between 180 and 240 msec. For the other conditions and time windows, only few electrodes display significant effects, mostly those located on ipsilateral parietal SMC. Significant task-dependent changes of the CCEPs in the earliest time window (10-45 msec) are only found for the active movement

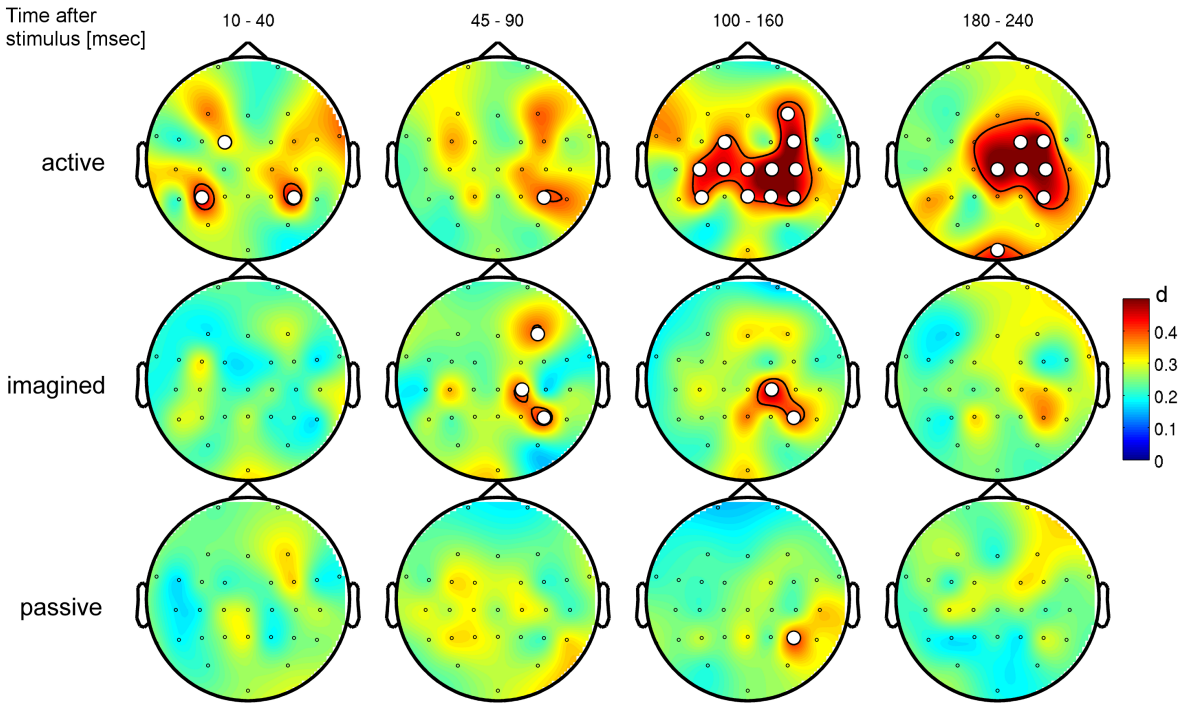

Figure 5.3.: Topographical distribution of the median effect size for all 3 conditions (top row: active movements, second row: imagined movements, third row: passive movements) and 4 time windows (column 1-4: 10-40, 45-90, 100-160 and 180-240 milliseconds after the stimulus) for healthy participants. The thin black line denotes the d value at the significance threshold of $\alpha = 0.05$. Electrodes for which the d value exceeds this threshold for at least one time bin within the given time window are marked by white circles.

condition. No significant differences were found outside these time windows.

The significant modulations 100-250 msec after the pulse over central channels for active movements in healthy participants are in good agreement with Nikulin et al. [128], who also identified the N100 as a component of the evoked activity mainly found on central channels as the component which is most consistently modulated during movement tasks compared to rest. Imagined and passive movements are movement conditions which have not been investigated regarding their effect on modulating the evoked activity so far. Thus, it is interesting to see that imagined movements also lead to significant differences in the evoked activity, although much less pronounced across subjects and that the spatial distribution of these effects in the first 200 msec after the pulse is very similar to the distribution for active movements, but that the pronounced late modulation found for active movements more than 200 msec after the pulse is absent for imagined movements. For passive movements, a significant modulation is only found for a channel over the somatosensory cortex, maybe because of the sensory feedback received during passive movements which might alter the excitability of this cortex area.

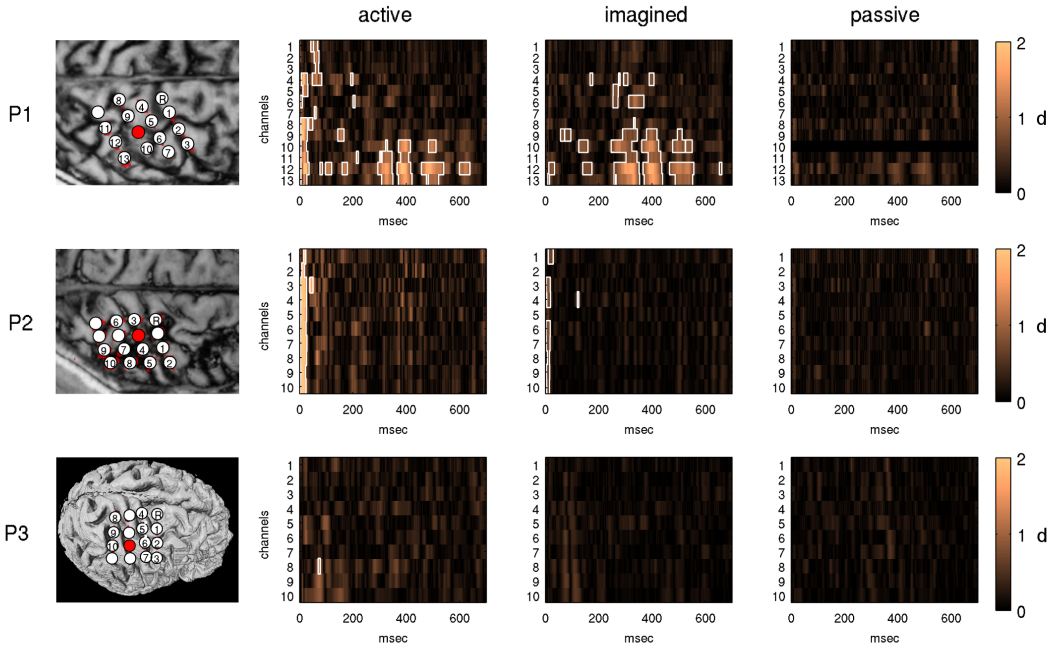

Figure 5.4.: Effect sizes on ECoG data of the first session for all conditions, patients and channels. Segments exceeding the $\alpha = 0.05$ significance threshold (corrected for the number of samples and channels) are framed in white. In the first column, the location of the electrodes is shown for each patient with the channel numbers used in the rest of the figures. Low channel numbers correspond to frontal, high channel numbers to parietal electrodes. The stimulation electrode is marked as a red circle, the reference electrode with *R*. Channels without a number have been removed from the analysis due to strong artifacts or noise.

Patients

For the first invasive session of all patients, the d value is shown for all conditions, patients and channels up to 700 msec after the stimulation pulse in figure 5.4. Later than 700 msec after the pulse, no significant differences were found. The effect size in terms of strength, timing and location varies between patients, but the within-patient effect is consistent with the effect found for non-invasive data: passive movements lead only to minor, non-significant effects, but much higher, significant effect sizes are found for active and imagined movements. Within the first 50 msec, d values are higher for active than imagined movements in P1 and P2. For P1, significant task-dependent changes in the evoked activity between 300 and 600 msec after the pulse are found most strongly on parietal channels in the active and the imagined condition. For P3, only channel 8 in the active movement condition contains a short segment of samples (71-73 msec) that exceed the significance threshold of d. No significant effects were found for passive movements.
In figure 5.5, the same analysis is shown for the last session (fourth for P1 and P2, second for P3). The strongest differences are still found for active movements, with

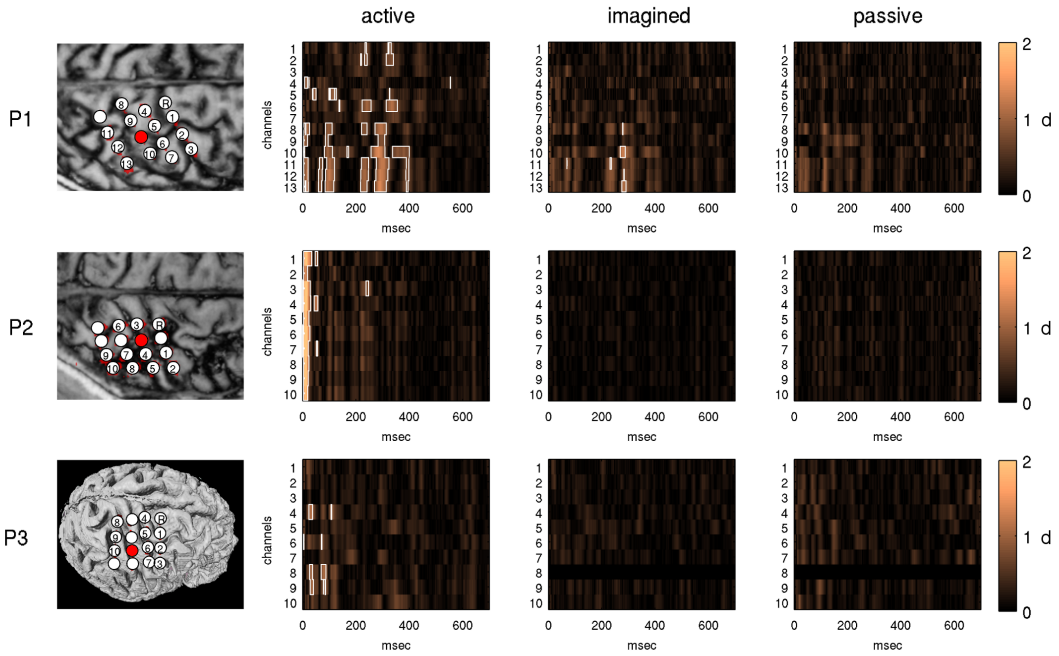

Figure 5.5.: Same as in figure 5.4, but for the last session of the experiment instead of the first.

more samples over the significance threshold in P3. For P1, the large region of significant differences between 300 and 600 msec has shifted to the time range of 200 to 400 msec, a gradual process which is observable in session 2 and 3 as well. The significant region for P2 is still almost exclusively confined to the first 50 msec and observable on all channels. Only P1 displays significant differences for imagined movements, although much less pronounced than for the first session. No patient has significant samples for passive movements.
The shift in the latency of the significant differences for the late evoked activity of P1 warrants a closer look. The average waveforms for *movement* and *rest* are displayed in figure 5.6, with a focus on channel 8 in figure 5.6 C where the late component is the most pronounced.

It is apparent that the significant differences are due to a latency difference in an evoked component which occurs for the displayed session 3 between 100 and 500 msec after the stimulation. During movement, the component occurs roughly 30-50 msec earlier than during rest. This can be quantified by using Woody's method [180] for latency estimation of event-related potentials (ERPs). With this method, a template of the ERP waveform is constructed and cross-correlated with each individual stimulus. The latency of the best match provides an estimate of the latency of the component. In figure 5.7, these latency values are displayed for all active movement sessions of P1. In Walter et al. [176], it was shown that there is a coherent reduction in the latency of this component over the course of the rehabilitation training and a

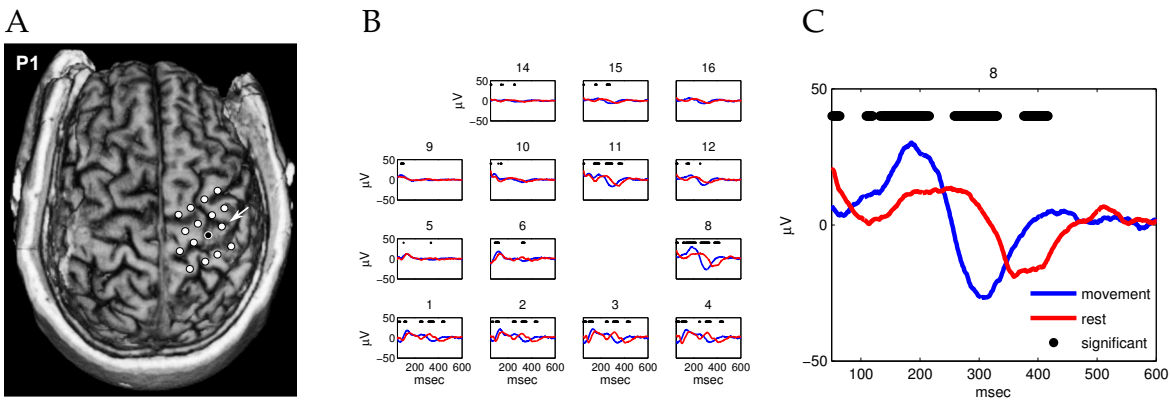

Figure 5.6.: Average evoked activity in the third session for P1. **(A)** ECoG electrode positions overlayed on the MRI of P1. White circles denote recording electrodes, the black circle the stimulation electrode. The white arrow points to channel 8. **(B)** Mean evoked activity on all channels for the *active* condition (blue) compared to *rest* (red). Black dots denote time points with a significant difference between the conditions. **(C)** Zoom on the average evoked activity on channel 8. Reproduced from Walter et al. [176].

significant difference in the latency between movement and rest in each repetition of the experiment (one-sided t-tests, all $p < 0.001$). A two-way analysis of variance (ANOVA) on the latencies of all 4 sessions of P1 reveals a significant reduction over the course of the four *sessions* ($p < 0.001$, $F(1, 1218) = 518.5$) and a significant effect of the *condition* (i.e. movement vs rest) ($p < 0.001$, $F(1, 1218) = 2244.6$) with latencies during *rest* being higher than latencies during movement. The interaction between *session* and *condition* is significant as well ($p < 0.001$, $F(1, 1218) = 41.5$). The latency difference between *movement* and *rest* for all sessions indicates, that the latency of the component might be influenced by movement-related processes in the brain. Other parameters of the evoked activity, such as the area under the waveform or the peak amplitude, exhibit significant changes over time and between conditions as well, but the effect size is far higher for the latency than for the other parameters [176].

5.5.2. Classification results

The results in the previous sections showed that there are significant differences in the evoked activity between stimuli in the *movement* phase of the trial compared to the *rest* phase. This was especially prominent for the active movement condition. This raised the question, whether these differences are observable even on a single-stimulus level. To investigate this, classifiers were trained to discriminate between the CCEPs in the *movement* and the *rest* phase.

The general tendencies of the classification results with EEG and ECoG recordings are in good agreement with each other. For EEG data, classification results for healthy participants and patients are also similar. We obtained on average an accuracy of about 75-84 % for active movements, 66-71 % for imagined and 55-60 % for passive movements (table 5.1). This corresponds to the results of the statistical anal-

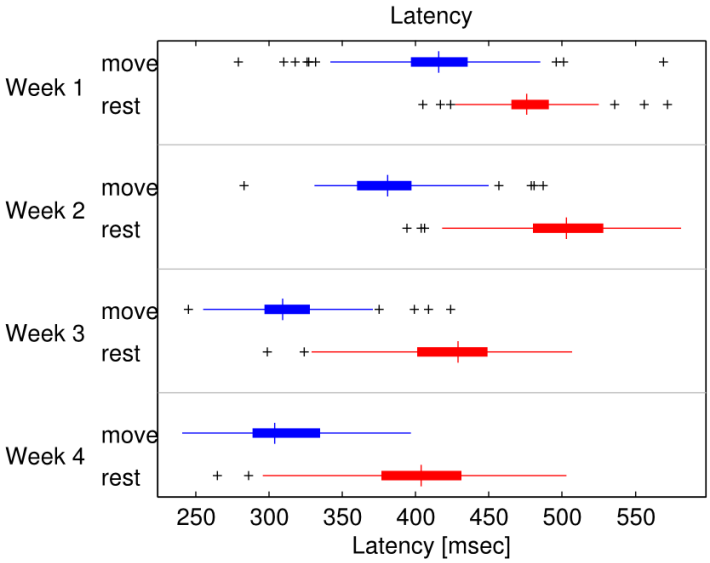

Figure 5.7.: Distributions of the late evoked component latency on channel 8 of P1 for all sessions, analyzed individually for stimuli during the active *movement* (blue) and the *rest* phase (red). Black plus signs denote outliers. In each week, the differences between the latency distributions of movement and rest are significant. Reproduced from Walter et al. [176].

ysis of the waveforms, where active movements resulted in the strongest differences, but significant differences were also found for imagined movements. Passive movements on the other hand elicited the smallest differences compared to *rest* which is resembled by the low classification accuracy. For ECoG data (table 5.2), the classification accuracy reached 85 % on average for P1 and P2, reproducible over 4 sessions, but the classification was much worse for P3 with 64 and 70 %. This is consistent with the presence (and almost absence in the case of P3) of significant differences in the ECoG activity. For imagined movements, there were also differences between the patients: While the waveforms were well classifiable for P1 (81.36 % on average), the results for P2 (55.70 %) and P3 (58.80 %) were close to chance level. A similar relationship between the patients on imagined movements was found for the EEG data, where only P1 had classification accuracies above 80 % (table 5.2). Passive movements lead for all patients to bad classification accuracies, typically smaller than 60 % (table 5.2).
Because the number of stimuli per class are not equal, the chance level for the classification is not exactly at 50 %, but depends on the actual ratio of *movement* to *rest* stimuli per session. On average, after stimulus rejection, 60.76 $\pm$ 6.9 % of the stimuli belonged to the *rest* condition, therefore this number should be regarded as the chance level for the accuracy. The specificity and sensitivity are the fraction of correctly classified *rest* and *movement* stimuli, respectively. Hence, the sensitivity captures, how often a change into the active state is detected. For EEG, this is the case on average for 70 % of the active movement stimuli, 50-60 % for imagined

Participant	Active			Imagined			Passive		
	Acc in %	Spec	Sens	Acc in %	Spec	Sens	Acc in %	Spec	Sens
P1	83.06	0.85	0.80	88.71	0.98	0.72	55.42	0.67	0.39
P2	63.50	0.70	0.56	59.57	0.70	0.45	68.52	0.86	0.33
P3	80.28	0.84	0.75	64.96	0.69	0.60	61.63	0.69	0.53
mean	**75.61**	**0.80**	**0.70**	**71.08**	**0.79**	**0.59**	**61.86**	**0.74**	**0.42**
std	10.58	0.09	0.13	15.50	0.16	0.14	6.55	0.10	0.10
S1	84.58	0.88	0.81	63.35	0.69	0.56	67.72	0.74	0.60
S2	80.92	0.88	0.67	72.14	0.81	0.53	66.13	0.76	0.52
S3	95.10	0.96	0.94	67.87	0.77	0.52	55.94	0.56	0.56
S4	81.64	0.84	0.77	62.50	0.70	0.51	49.68	0.53	0.46
S5	81.31	0.91	0.68	60.62	0.71	0.43	46.08	0.49	0.42
S6	82.97	0.95	0.31	57.74	0.74	0.24	56.00	0.61	0.49
S7	81.48	0.87	0.68	79.26	0.89	0.48	49.11	0.52	0.44
mean	**84.00**	**0.90**	**0.69**	**66.21**	**0.76**	**0.47**	**55.81**	**0.60**	**0.50**
std	5.05	0.04	0.19	7.45	0.07	0.11	8.42	0.11	0.06

Table 5.1.: EEG-TMS classification results, showing accuracy (Acc), specificity (Spec) and sensitivity (Sens) for each movement condition. P: patients, S: healthy participants.

movements and 40-50 % for passive movements The sensitivity is higher for active movements and ECoG data with 77 % and smaller for imagined (52 %) and passive (38 %) movements, but due to standard deviations of 10-15 %, these differences between EEG and ECoG data might be not meaningful.

The fact that a classification of the brain state is possible from the shape of the evoked waveform demonstrates that the modulatory effect of a switch in the brain state is strong enough to have a clear impact on the stimulation processing even of single pulses. Although this classification study was only conducted offline, it seems to be in principle possible, at least for active movements, to determine the brain state by analyzing the evoked response. Hence, one could use the evoked waveform as an alternative input feature for sensorimotor BCIs, in which movement-related changes in brain rhythms [135] are used for communication and control [14, 179]. Of course, the necessary additional effort to include the stimulation setup into the BCI system might be prohibitive in most cases, but the brain-state-dependent changes in the evoked activity might be helpful to achieve communication with so-called ”BCI illiterate” people, i.e. people where no satisfactory modulation of the brain rhythms can be found. According to Vidaurre and Blankertz [168], this could affect between

Patient	#	Active			Imagined			Passive		
		Acc in %	Spec	Sens	Acc in %	Spec	Sens	Acc in %	Spec	Sens
P1	1	83.06	0.85	0.80	78.54	0.85	0.64	64.66	0.70	0.57
	2	90.24	0.92	0.88	89.17	0.94	0.47	58.78	0.69	0.40
	3	89.17	0.91	0.86	75.91	0.82	0.67	61.79	0.70	0.50
	4	84.10	0.87	0.80	81.82	0.91	0.53	59.49	0.77	0.32
P2	1	86.27	0.90	0.81	63.51	0.66	0.60	54.69	0.62	0.43
	2	86.80	0.88	0.85	57.14	0.67	0.44	53.04	0.60	0.44
	3	82.61	0.81	0.84	51.63	0.57	0.44	48.31	0.57	0.34
	4	81.13	0.84	0.77	50.52	0.62	0.36	57.76	0.49	0.00
P3	1	63.95	0.65	0.62	59.91	0.66	0.52	52.53	0.60	0.42
	2	69.85	0.76	0.61	57.69	0.61	0.52	55.93	0.67	0.37
mean		**81.06**	**0.84**	**0.77**	**66.58**	**0.73**	**0.52**	**56.70**	**0.64**	**0.38**
std		8.56	0.08	0.10	13.65	0.13	0.10	4.81	0.08	0.15

Table 5.2.: ECoG classification results, showing accuracy (Acc), specificity (Spec) and sensitivity (Sens) for each movement condition. #: Session number.

15-30 % of all participants. As shown in the next section, there might not be a direct relationship between modulations in spectral power and modulations of the evoked activity, hence the brain-state-dependent changes in the evoked waveforms might be found as well in people without the ability to control their sensorimotor rhythms and thus offer a promising new communication source. If one wants to pursue this direction, it needs to be shown that the online classification of the evoked activity is feasible and that the postulated modulation of the evoked activity can be found in BCI illiterates. These questions are, however, outside the scope of this thesis.

The analysis so far shows that the first hypothesis in this chapter regarding the question whether there is a brain-state-related dependency of the stimulation effect is confirmed. This result goes beyond what has been reported in the literature so far by showing that the effect is present also for severely affected stroke patients during intended movements of the paralyzed hand and for electrical stimulation via implanted electrodes. In addition, it was shown that this effect is detectable on a single-stimulus level for active and attempted movements.

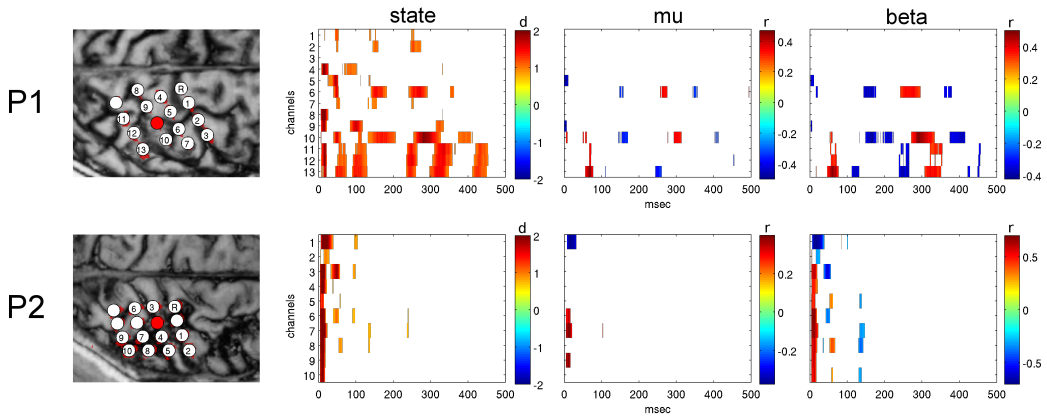

Figure 5.8.: Comparison between brain-state-dependent modulations and correlations with μ and β power. Data is shown from the active movement condition in the third session of the *Stimulation Screening* experiment with P1 (upper row) and P2 (lower row). First column: position of recording and stimulation electrodes. Second column: d-value of significant brain-state-dependent modulations after the stimulus. Third column: Significant correlations of prestimulus μ band power with poststimulus amplitudes. Fourth column: same as third column, only for β band power.

5.5.3. Relationship between spectral power and poststimulus activity

Changes in the brain state between *rest* and *movement* lead to event-related desynchronization in μ and β frequency bands [135]. Hence, it is to be expected that significant correlations between prestimulus spectral power in these frequency bands and the poststimulus data are found roughly in the same spatiotemporal areas as the significant brain-state-dependent changes. This is indeed the case and illustrated in figure 5.8 for one session of active movements with P1 and P2. In this figure, the prestimulus spectrum has been determined over 500 msec of data before the stimulus. For each recording channel, the poststimulus samples which are either significantly modulated by the movement task, or significantly correlated with the prestimulus spectral power are marked. Their color indicates the strength or direction of the influence of the prestimulus activity.

Due to the known covariance of the brain state and the spectral power for movement tasks, the result that the brain-state-dependent and the spectral-power-dependent modulations are quite similar is not surprising. It is more interesting to see, whether the correlation with the spectral power is preserved when only stimuli within the same brain state / trial phase are analyzed. However, both for the *movement* and the *rest* phase, practically no samples with a significant influence of prestimulus spectral power are found. Table 5.3 shows the percentage of samples in the first half second after the stimulus which are significantly modulated by the brain

Method	Participant	BS	All		Movement		Rest	
			μ	β	μ	β	μ	β
TMS-EEG	P1	2.39	0.24	0.30	0.00	0.01	0.00	0.01
	P2	1.44	1.24	1.20	0.16	0.02	0.83	0.39
	P3	0.79	0.35	0.81	0.00	0.03	0.03	0.15
	S1	0.98	0.00	0.05	0.00	0.00	0.00	0.00
	S2	0.01	0.02	0.32	0.00	0.01	0.01	0.03
	S3	4.12	1.20	1.81	0.02	0.06	0.12	0.20
	S4	0.50	0.01	0.32	0.00	0.00	0.00	0.00
	S5	0.29	0.18	0.33	0.03	0.06	0.06	0.11
	S6	0.06	0.01	0.12	0.00	0.01	0.00	0.03
	S7	0.03	0.00	0.01	0.00	0.00	0.00	0.00
ECoG	P1	8.69	2.55	4.48	0.14	0.03	0.00	0.00
		28.00	23.49	27.82	0.00	1.72	0.00	0.00
		17.95	8.48	12.92	0.00	0.00	0.26	0.15
		13.11	4.52	10.92	0.05	0.29	0.00	0.00
	P2	1.92	0.22	0.42	0.00	0.00	0.14	0.12
		4.80	1.18	5.32	0.00	0.00	0.00	2.78
		5.44	1.86	6.20	0.00	0.00	0.16	1.50
		4.58	1.74	5.48	0.00	0.00	0.00	0.04
	P3	0.00	2.96	0.76	0.00	0.00	1.36	0.26
		1.02	2.52	1.40	0.00	0.00	0.74	0.00

Table 5.3.: Percentage of samples of the poststimulus activity which are significantly modulated by the brain state (BS) or significantly correlated with the μ or β spectral power. The spectral correlations are either computed for all stimuli or using only those in the *movement* or the *rest* phase.

state and the spectral power, averaged over the patients and broken down for all stimuli and stimuli during either only the *movement* or the *rest* phase.
The results shown here are for the spectrum computed over a time window with length 1 s before the stimulus. As argued before, the noticeably smaller values for the three patients in their first ECoG sessions compared with the other invasive sessions could be explained by the short time difference of less than five days between the surgery and the experiment. The patients might not yet have become accustomed to controlling the orthosis via ECoG, thus the movement-related spectral changes between *movement* and *rest* are less pronounced than in later sessions. A direct comparison between the EEG and ECoG results is not fair, because the ECoG channels are concentrated close to the location of stimulation, while the EEG channels cover the whole scalp. Thus, many EEG channels might be too distant from

the stimulation site that no stimulation-evoked activity is found there. This would clearly lower the fraction of significant samples. A comparison between the patients in the invasive phase is also difficult, because the electrode locations are not comparable. Thus, an analysis is only sensible on a within-subject basis.
In table 5.3, while a comparably large fraction of poststimulus samples are modulated by the brain state and also by the spectral power if all stimuli are taken into account, almost none are significantly correlated with the spectral power if only stimuli within the *movement* phase are used. This is especially evident for the invasive data, where for P2 and P3 no significantly correlated samples are found in the *movement* phase. Although the percentages are slightly higher for the *rest* phase compared to the *movement* phase for μ power ($p = 0.02$, paired Wilcoxon signed rank tests), no such effect is found for β ($p = 0.07$). The percentages during *rest* and *movement* are much smaller than the values for all stimuli (μ, β: $p < 0.001$). The main result is, however, that there are almost no samples in the poststimulus recording for which the amplitude is significantly correlated with either μ or β power within a constant brain state.
In figure 5.9, the percentage values are shown for all tested time windows between 100 and 1000 msec before the stimulus for patient P1. The spectrum of a short window provides information about the activity occurring immediately prior to the moment of stimulation, but the variance of the spectral estimate might be high. The estimated spectrum for a long window would be more stable but its computation takes information from a comparably long period of time into account, thus it reflects more general, less immediate changes in the brain activity. The results in figure 5.9 demonstrate that the length of the prestimulus time window does not influence whether significant correlations between the spectral power and the poststimulus amplitude modulations in the *movement* phase are found. These are almost absent. Using all stimuli, the steady increase in the fraction of samples of the poststimulus activity found to be significantly correlated with prestimulus spectral power with increasing length of the prestimulus time window shows that short-term fluctuations in the power of brain signal oscillations do not modulate the poststimulus amplitude. Instead, the general power level of the oscillations as a correlate of the brain state is the most important factor.

The absence of a significant relationship does not prove that there is absolutely no relationship (the result is simply "inconclusive") [41]. However, it becomes clear that at least within the *movement* phase, if there is a direct influence of the prestimulus spectrum on the evoked activity, the size of this effect is very small.
Amplitude modulations are not the only way that an influence of prestimulus activity might be observable. For P1, one sub-component of the evoked activity could be identified which displays a dependency of its latency on the brain state (figure 5.6 and 5.7). Similar as for the amplitude modulations, one can test whether there

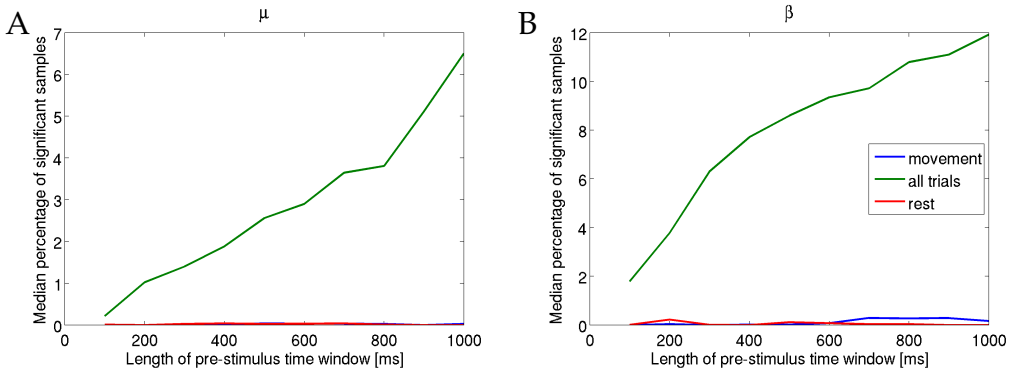

Figure 5.9.: Median of the percentage of samples in the poststimulus ECoG activity of P1 with significant correlations with the prestimulus μ **(A)** and β **(B)** power, in relation to the length of the prestimulus time window used to compute the spectrum. The median is taken over all sessions with active movements in the invasive phase. The correlation between prestimulus power and poststimulus amplitude is computed either for all stimuli (green), only the stimuli in the *movement* phase (blue) or only the stimuli in the *rest* phase (red).

is a significant correlation of the latency with the prestimulus spectral power for all stimuli, *rest* stimuli and *movement* stimuli. Using the Spearman correlation coefficient and permutation tests as before in this section ($\alpha = 0.05$), significant correlations between the prestimulus spectral power and the latency of this component were found (figure 5.10) [176]. These significant correlations exist not only if one takes all stimuli into account (figure 5.10 A), but also if only the *movement* stimuli are used (figure 5.10 B). With the exception of the third session, this frequency range encompasses the frequencies between 5 and 40 Hz across all sessions. Thus, this shows that in principle there might be components of the evoked activity which are modulated by the prestimulus spectral power independently of the brain state. Hence, it might be possible to optimize the stimulation parameters, especially the timing, to control the latency of this component within the *movement* state [176].

Unfortunately, no comparable sub-component was found for the other patients and the external connection with the implanted electrodes of P1 had been removed before it could be tested experimentally, whether the latency of this evoked component can be controlled by a closed-loop system. This stimulation system would have used a regression model trained to predict the latency from the spectral power to monitor the measured ECoG activity and to stimulate within the *movement* phase only, if the predicted latency is below a predefined threshold.

To summarize: In this chapter, the relationship between pre- and poststimulus activity was studied. The intention to move a limb, even a paralyzed one, changes the reaction of the brain to the stimulus, possibly by altering the cortical excitability in comparison to a resting state. This effect is strong enough, that these two brain states can be discerned using the CCEPs of a single stimulus. Because the change from a resting state to a movement state is accompanied by a change in the power spectrum

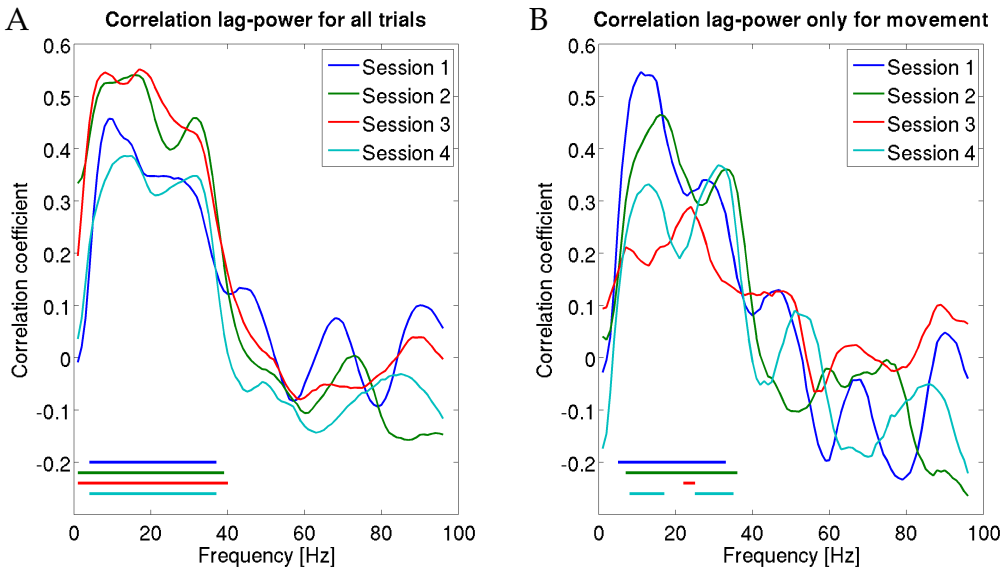

Figure 5.10.: Spearman correlation coefficient between the latency of the evoked subcomponent of P1 and the spectral power for all sessions. Significant correlations per session are marked by horizontal colored lines. **(A)**: All stimuli. **(B)**: Only stimuli during the *movement* phase.

(ERD/ERS), it was logical to look whether the CCEP amplitudes are modulated by the spectral power at the moment of stimulation as well. However, there was no direct relationship between the prestimulus spectral power of sensorimotor rhythms and the CCEP (table 5.3), a finding consistent with earlier studies on motor-evoked potentials.

6 Interaction between stimulation parameters, pre- and poststimulus activity

In the last chapter, the influence of the prestimulus activity on the evoked activity was studied for constant stimulation parameters. While the actual activity of the stimulated person at the moment of stimulation makes a difference, the analysis in section 5.5.3 has provided no indication that there is more than a very faint direct influence of the prestimulus spectral power of sensorimotor rhythms on the CCEP amplitudes. This is unfortunate, because the crucial factor whether or not the postulated closed-loop control of the evoked activity is possible is that the brain activity before the stimulus has to influence in some way the generation of the poststimulus activity. This influence has to go beyond a brain-state-dependency, because it might be sensible to contingently associate just a specific brain state with the application of stimulation, thus stimuli would be triggered only while for example the patient attempts to move. Because of this, one has to look for features of the EEG/ECoG signal which provide meaningful information about the evoked effects within a constant brain state. Thus, although the absence of a direct influence of the spectral power of sensorimotor rhythms sheds doubt on the feasibility of this particular closed-loop system, there are more possibilities to realize it which have to be investigated.

First of all, apart from sensorimotor rhythms, other parts of the spectrum could have an influence. The same holds for the waveform of the signal before the stimulus. The time domain activity in particular was very important for Brugger [23] who realized closed-loop control with features derived from the local field potential. Secondly, even if there is no direct relationship allowing the construction of a *forward model* how patterns of prestimulus activity generate the CCEP for constant stimulus parameters, there might still be an *interaction* between the prestimulus activity and the stimulation parameters. For example, Brugger [23] found that closed-loop control was only possible for a specific range of intensities, not for all. Therefore, the relationship between pre- and poststimulus activity should be studied for different stimulus intensities in an attempt to test the third hypothesis:

Hypothesis III
The prestimulus activity and the stimulation intensity interact in generating the evoked activity. Thus, the combination of pre- and poststimulus activity provides more information about the applied intensity than the poststimulus activity alone.

For this reason, experiments were conducted with the patients in which they were stimulated with varying stimulation intensities. Then, regression models were trained to infer the intensity for each individual stimulation pulse from the recorded neural activity - in a sense, to "decode" the intensity from the brain activity [174, 175]. Naturally, one would assume that the shapes of the CCEPs give the most important pieces of information about the employed intensity. If there is an influence of the prestimulus activity, even if it is an interaction with the stimulation intensity, one could detect it by analyzing the decoding results: The error in estimating the intensity when using the *direct solution* proposed by Brugger et al. [25], which combines pre- and poststimulus neural activity, should be lower than the error when using only the CCEPs as input features. Thus, two steps are needed in the analysis:

1. **Decoding from CCEPs?** One needs to show that a regression model can indeed estimate the applied stimulation intensity from the CCEPs with reasonably small error. This is not a particularly bold conjecture, because one clearly expects that there is a correlation between the intensity and the size of the evoked activity. However, this analysis is interesting by itself for several reasons, not only because it provides a baseline estimate for the decoding with combined pre- and poststimulus features: If each recording channel is processed individually, the quality of the decoding should differ between recording sites. One could speculate that this could depend on the strength of the neural connectivity between stimulation and recording site such that the decoding error might be interesting to assess effective connectivity between brain areas. Secondly, if one can show that the decoding generalizes to unknown intensities, one can think about building an open-loop stimulation system where the regression model computes an optimal intensity to evoke a certain CCEP shape.

2. **Improvement with prestimulus activity?** After that, regression models are trained on the combined pre- and poststimulus activity to perform the same task and the question is whether this leads to a reduced decoding error. If this is the case then the third hypothesis would be confirmed and closed-loop stimulation to control the evoked activity would seem feasible.

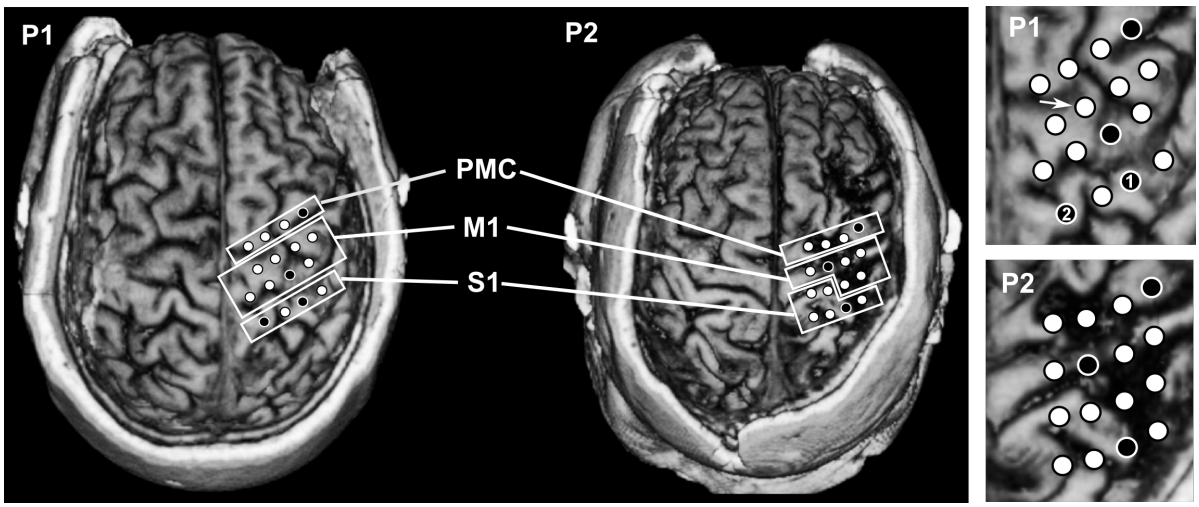

Figure 6.1.: Position of the stimulation and recording electrodes for P1 and P2. White circles denote electrodes used only for recording, while electrodes used at least once for stimulation are marked by black circles. Channel 10 of P1 is marked by the white arrow in the upper right image. Adapted from Walter et al. [175].

6.1. Experimental setup

The task as well as the recording and stimulation setup of the experiment are described in detail in section B.3. Two sessions were conducted with P1 and three with P2. In each session, the patient was stimulated with 100 repetitions of 8 different intensities in random sequence. Per session, this stimulation pattern was applied sequentially on three different stimulation electrodes, one placed over the primary somatosensory cortex (S1), one over the primary motor cortex (M1) and one over the pre-motor cortex (PMC). This configuration is shown in figure 6.1. For P2, the same three stimulation electrodes were used in all sessions, while for P1, stimulation over S1 was conducted with two different electrodes. The white number in figure 6.1 indicates which electrode was used in which session.

6.2. Feature extraction

Channels with excessively long (> 20 msec) and pronounced stimulation artifacts were removed from further analysis. Typically channels on the same strip as the stimulation electrode were affected by this. Unfortunately, this meant that due to the arrangements of the electrode strips, no effects of stimulation on somatosensory cortex (S1) could be recorded on S1 for P1 because all channels on this strip showed severe artifacts. A semi-automatic trial rejection using the variance of the post-stimulation data was employed to remove trials with channel-specific artifacts, amplifier saturation or other artifacts.

6.2.1. Poststimulus data

As shown in figure 6.2, it is reasonable to assume that the shape of the evoked waveform itself yields useful information about the applied stimulation intensity. In order to capture this shape with features suitable as input for the regression model, a binning procedure is used: First, a bandpass filter (Butterworth filter of order 2, cutoff: 5 and 500 Hz) and a notch filter at 50 Hz were applied anti-causally to the data to avoid contamination of the evoked response with the stimulation artifact. A time segment after the stimulus with length l is divided into a set of *bins* and the value of all samples within a bin is averaged. This number of samples is termed the bin width b. The advantage of the binning procedure over using the raw recorded activity is the reduced dimension of the input space and the reduction of redundancy in the input features. In order to find good settings for the binning, all permutations of values for l in the range between 20 and 500 msec in steps of 20 msec and $b \in \{1, 2, 3, 4, 5, 10, 15, 20\}$ msec have been tested. If the window length was not divisible by the bin width, the window was shortened to the next multiple of b. These settings are tested for each channel individually, because they are likely to be different due to the different shapes of the evoked activities. For the channel depicted in figure 6.2 it seems likely that a $l \leq 50$ msec is optimal.

6.2.2. Prestimulus data

Similar to the poststimulus data, meaningful features for the prestimulus activity had to be found. Brugger [23] identified the time domain activity as a useful input feature which could be improved by a projection on the principal components. Although only faint correlations between the spectral power before the stimulus and the stimulation-evoked activity could be found for resting state data (section 5.5.3), the prestimulus spectral power might still be a useful feature, too. For the extraction of prestimulus features, the bandpass filter was applied in the forward direction.

Time domain

In the time domain data, as for the poststimulus data, a binning procedure was used to capture the shape of the waveform. Due to the results of the analysis of the poststimulation data, a bin width of 1 msec was used, but the length of the prestimulus window was varied between 10 and 100 msec in steps of 10 msec.

Frequency domain

The spectral power was extracted with an autoregressive model of order 100 (determined as a model order well suited for the data by use of the ARMASA Matlab® toolbox [19]) for the frequency range of 5-100 Hz in steps of 5 Hz. The spectrum

was computed over prestimulus data windows with lengths differing between 100 and 700 msec before the stimulus in steps of 100 msec. Similar to the analysis in section 5.5.3 this was done to test for the expected trade-off between variance and immediacy of the spectrum.

6.2.3. Regression models

Regression models to infer the stimulation intensity from the time or frequency domain features were trained with the primal Support Vector Regression (SVR) algorithm [16, 26] with an ϵ-insensitive l_2-loss function. A Gaussian RBF kernel was used in order to allow for interactions between pre- and poststimulus features of the combined model. The hyperparameters - namely the regularization parameter C, the width ϵ of the loss function and the width of the kernel σ were determined using span bound optimization [34].

6.3. Evaluation of the regression models

In order to evaluate, how well a model performed in inferring the applied stimulation intensity from poststimulus features alone or the combination of pre- and poststimulus data, the root mean squared error (RMSE) and the square of Pearson's correlation coefficient r^2 between the decoded and the actual intensities were used. Models with an RMSE smaller than the step size of 1 mA were considered to be successfully trained. In a first step, 10-fold cross-validation over all trials was used to compute these measures. In each cross-validation fold, scaling factors and offsets were determined to scale the training features to the range of -1 to 1. These factors and offsets were then applied to the test data.
Secondly, in order to test whether the regression models generalize to unknown intensities, the models were trained with all instances from a subset of intensities and tested on the remaining instances from intensities unseen in the training procedure. For P1, the SVR was trained on the trials with intensities of 1, 3, 5 and 8 mA for training and tested on 2, 4, 6 and 7 mA. This was also done for the first session of P2, whereas for the second and third session, 5, 7, 9 and 12 mA were used for training and 6, 8, 10 and 11 mA for testing.

6.4. Results

The dependency of evoked responses on stimulation intensity can be seen in figure 6.2, demonstrating that there is a nonlinear relationship between the amplitude of the evoked activity and the intensity. For the depicted channel, the strongest differences are found in the first 50 msec after the stimulus.

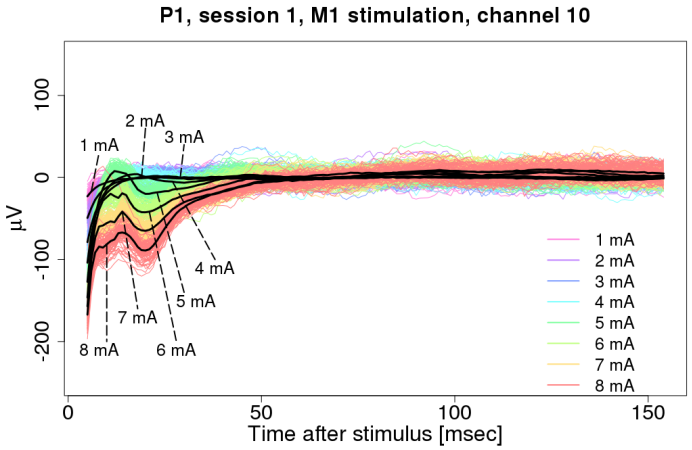

Figure 6.2.: Evoked activity on channel 10 (arrow in figure 6.1) after anodal pulses were applied to the motor cortex of P1. Colored lines: Single trials color-coded by intensity. Black solid lines: Mean evoked activity per intensity.

6.4.1. Decoding intensity from poststimulus data

An example for the results for identifying the best combination of window size and bin width for the binning procedure of post-stimulation data is depicted in figure 6.3. When estimating the applied stimulation intensity from the recorded data with the best settings for bin width and window size, the resulting RMSE of 0.26 mA indicates that the intensities are very well separable. Thus, one could argue that the connection from the brain area below the stimulation electrode to the one below the recording electrode are well connected. Indeed, both electrodes are in close vicinity (see figure 6.1). If one performs this analysis for all recording channels in a stimulation session, one might be able to use the RMSE, i.e. the measure, how well stimulation parameters are preserved in the evoked activity, as a measure of the connectivity between the stimulation and the recording area [175]. In figure 6.4, this is done for all three stimulation locations of the second session of P1. A noticeable result, especially for M1 stimulation, is that the distance to the stimulation electrode is not the only factor determining the quality of the decoding: The error is larger for electrodes frontal and lateral to the stimulation site than those parietal and medial from it.

Across all sessions, the RMSE of the estimated intensities was computed for the different brain regions. The best and averaged RMSE across all channels of each recording region is shown in table 6.1.

With the exception of stimulation over PMC and decoding over S1 and some channels on M1, for P1 a RMSE smaller than 1 mA can be reached in most cases, reproducible in both sessions. For P2, only the intensity after stimulation over M1 can be decoded with a small error on the other channels. This again is reproducible in all sessions. It seems that at least for some combinations, the relationship between

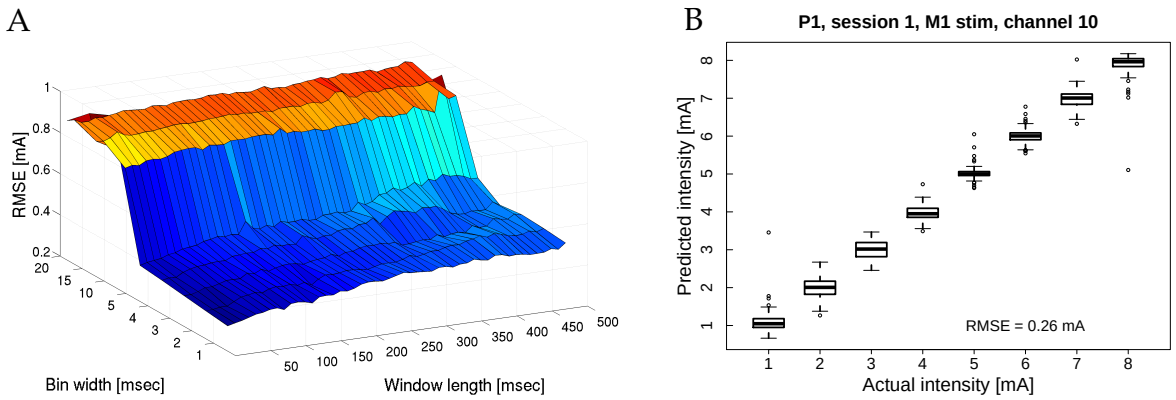

Figure 6.3.: Estimating the intensity used for the stimulation displayed in figure 6.2 from poststimulus data. **(A)**: RMSE depending on different combinations of window length and bin width. **(B)**: Estimated intensities vs. the actual intensities for the combination of window length and bin width with the lowest RMSE. Boxes encompass the 25th-75th percentile, circles denote outliers.

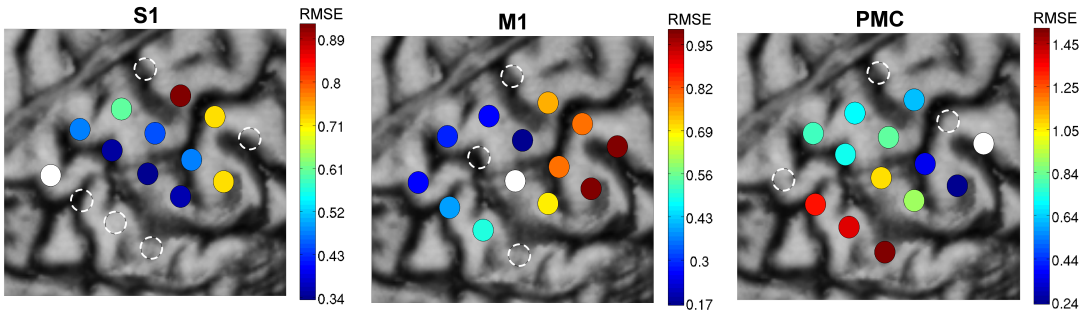

Figure 6.4.: Decoding of the intensity from all recording channels for different positions of the stimulation electrode. Second stimulation session with P1, channel positions are displayed as circles overlayed over the MRI of P1. Left: Stimulation electrode (white electrode) placed over the somatosensory cortex (S1). Middle: Stimulation electrode over M1. Right: Stimulation electrode over PMC. The RMSE of all other recording electrodes is color-coded. White dashed circles denote electrodes which were not used in the analysis, either because of strong stimulation artifacts or because they had been used as the reference electrode.

			Recording area					
			S1		M1		PMC	
Patient	**Session**	**Stim**	**mean**	**best**	**mean**	**best**	**mean**	**best**
P1	1	S1			0.42	0.29	0.67	0.51
		M1	0.42	0.40	0.47	0.27	0.69	0.43
		PMC	1.94	1.65	1.21	0.39	0.67	0.67
	2	S1			0.48	0.34	0.83	0.72
		M1	0.40	0.28	0.55	0.18	0.85	0.75
		PMC	1.43	1.35	0.71	0.24	0.64	0.64
P2	1	S1	1.99	1.49	1.83	0.85	1.45	1.28
		M1	0.63	0.49	0.53	0.46	0.55	0.50
		PMC	2.00	1.87	2.21	2.12	2.16	2.16
	2	S1	2.02	1.57	2.09	1.74	2.25	2.25
		M1	0.94	0.55	0.63	0.45	0.70	0.59
		PMC	2.03	1.70	1.98	1.52	1.84	1.51
	3	S1	1.78	1.38	1.90	0.75	1.27	1.21
		M1	0.67	0.50	0.67	0.42	0.73	0.68
		PMC	2.00	1.70	2.01	1.58	1.21	1.20

Table 6.1.: Average RMSE of the intensity estimation in mA over all channels recording from M1, S1 or PMC for different positions of the stimulation electrode (Stim) and RMSE for the channel with the lowest error per recording area. All stimulation trials were used.

stimulation intensity and the shape of the evoked activity can be captured by the regression model.

This finding opens the question, whether such a regression model might be able to predict, given a certain target shape, which stimulation intensity would be needed to evoked this target shape. This analysis can be performed with the recorded data by training the regression model on a subset of the 8 applied intensities and testing it on a disjoint set. 4 intensities were used for training and 4 for testing (see section 6.3 for the concrete values per session). The results of this analysis, measured by the average RMSE and r^2 value per brain area, are shown in table 6.2.

This table again demonstrates that, similar to the results for all intensities, the influence of the stimulation intensity on the evoked activity can be captured very well by the regression model. Furthermore, the model can generalize to unknown intensities. In Walter et al. [174] it was shown that 3-4 different training intensities are sufficient to construct models that behave robustly for novel intensities, because their estimation error is comparable to models that are trained on instances from all

			Recording area					
			S1		M1		PMC	
Patient	**Session**	**Stim**	**RMSE**	**r^2**	**RMSE**	**r^2**	**RMSE**	**r^2**
P1	1	S1			0.65	0.91	0.88	0.82
		M1	0.79	0.92	0.77	0.88	1.24	0.69
		PMC	2.06	0.00	1.36	0.49	0.69	0.88
	2	S1			0.74	0.90	1.20	0.66
		M1	0.89	0.91	0.84	0.82	1.08	0.75
		PMC	1.52	0.39	0.90	0.77	0.64	0.91
P2	1	S1	2.02	0.02	1.77	0.20	1.83	0.07
		M1	1.55	0.43	1.32	0.48	0.80	0.83
		PMC	2.00	0.01	2.04	0.00	2.16	0.02
	2	S1	1.92	0.10	2.02	0.02	2.06	0.01
		M1	1.23	0.58	0.77	0.85	0.95	0.79
		PMC	2.03	0.04	1.95	0.10	1.72	0.26
	3	S1	2.00	0.04	1.83	0.16	1.82	0.19
		M1	1.16	0.66	1.26	0.58	1.35	0.56
		PMC	2.03	0.03	1.99	0.05	1.65	0.27

Table 6.2.: Average RMSE of the intensity estimation in mA and r^2 over all channels recording from M1, S1 or PMC for different positions of the stimulation electrode (Stim). Disjoint subsets of intensities were used for training and tested. From Walter et al. [175].

available intensities. This opens up new possibilities for the optimized selection of the stimulation intensity. If one knows how the brain should react to the stimulus, one might be able to infer the optimal stimulation intensity to evoke the target shape by applying several test stimuli with different intensities, then training a regression model to estimate the intensity from the poststimulus activity. Afterward, one can use the model to compute the intensity necessary for the target activity. However, as this regression model only uses poststimulus activity, this would be a purely open-loop stimulation paradigm: Once the intensity is computed offline, it would be constant throughout the experiment. In addition, the target shape should be within the space of achievable shapes for stimulation-evoked potentials [174].

6.4.2. Influence of prestimulus activity

This experiment gives us another opportunity to test whether a closed-loop system for the control of the evoked activity is feasible. In comparison to the last chapter, the leading question this time is not whether there is a direct influence of pre- to

poststimulus activity (found to be unlikely in section 5.5.3), but whether there is an *interaction* between the prestimulus activity and the stimulation intensity in generating the poststimulus activity. If this is the case, then the open-loop system outlined in the last paragraph could be augmented to a closed-loop paradigm, where the stimulation intensity is adjusted online during the experiment in order to evoke the target shape. This would fulfill the idea of using closed-loop stimulation to reduce the variance of the evoked activity.
The feasibility of this can be tested by evaluating the regression models: If a model trained on the combination of pre- and poststimulus activity performs clearly better than a model trained only on the poststimulus activity, then there has to be relevant information encoded into the prestimulus activity. Hence, this would confirm hypothesis III. Although it has been shown in the last chapter that the influence of the prestimulus activity on the poststimulus activity is relatively small, as long as no change in the brain state occurs, this hypothesis might still hold. The reason for this is that features which are meaningless by themselves can become important for the solution of a problem if their interaction with other features provides meaningful information, as shown for example by Guyon and Elisseeff [67].
It is not clear which features of the prestimulus data might contain such relevant information. According to Brugger [23], at least for microelectrode data, the shape of the prestimulus waveform is of interest. On the other hand, as seen in the last chapter, spectral power sometimes had a significant influence on the evoked activity, hence the spectrum might be a useful feature, too. For each channel, both features were tested and combined with the poststimulus features that led to the lowest RMSE in the previous section. The length of the prestimulus window over which these features were computed was varied and again the setting with the lowest error was found using 10-fold cross-validation. In this case, however, the cross-validation was done for the combined feature set of pre- and poststimulus activity. Then, the RMSE was computed for the best setting of the preprocessing with another 10-fold CV, both for the post-. and the pre- post model, once with binning and once with spectral data. This can be considered as an example of a wrapper method for feature selection. The process resulted in a total of 169 values for each feature set, one for each combination of a recording and a stimulation electrode.

On average, the RMSE increased by 2.5 % for the spectral prestimulus features and by 2.8 % for the binning features compared to using only the poststimulus features. A Friedman test, Tukey-Cramer corrected for the three comparisons, revealed that the RMSE for poststimulus data only was significantly smaller than for the combined models ($p < 0.001$). This result does not support the hypothesis that the signal before the stimulus interacts in a meaningful way with the stimulus parameters to produce the poststimulus activity. Although a small improvement is found for some models (figure 6.5), in the majority of cases (67.5 % for binning, 77.5 % for the spec-

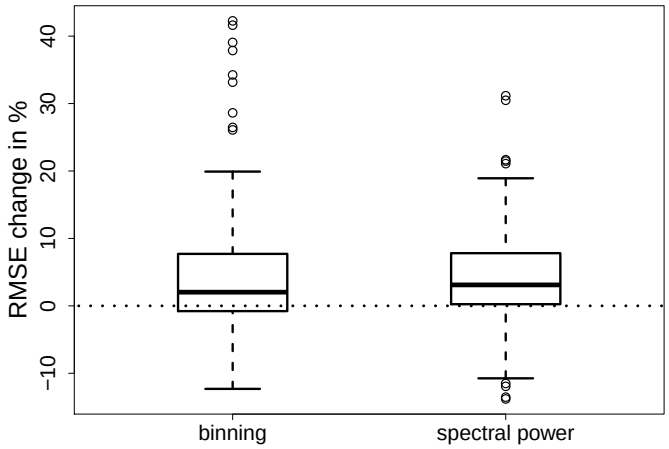

Figure 6.5.: Change in RMSE for combined pre- and poststimulus features in comparsion to models using only the poststimulus features. Each box shows the distribution of the change in percentage. Positive values indicate a higher error for the combined models. The dotted horizontal line denotes 0 %, thus no change.

tral power), the result is worse for the combined model.
For the time domain features, the smallest error was found in more than 80 % of the cases for windows with a length ≤ 50 msec with a significant positive correlation ($\rho = 0.33$, $p < 0.001$) between prestimulus window length and the intensity estimation error. Therefore, prestimulus windows longer than 100 msec seemed unnecessary to test. For the spectral features, no such correlation was found ($\rho = -0.01$, $p > 0.6$). If the prestimulus signal does not provide meaningful information for the model, this difference between time domain and frequency domain features can be explained by the fact that for the binning procedure, a longer time window means that more features are added whereas for the spectral analysis, the number of features is independent from the prestimulus window length. If the prestimulus features just add noise, an increasing number of them will lead to degrading performance.

The analysis in this chapter did not reveal any clear influence of the prestimulus activity on the CCEPs. Although the estimation error was reduced for some stimulation-recording-combinations by a small percentage, in practice the influence of the prestimulus activity is still very minor. Thus, one has to seriously doubt, given the data at hand, whether a closed-loop system that controls the shape of the evoked activity by intensity-adaptation is feasible. Of course, the absence of a relationship can not be proven and the possibility remains that either better preprocessing methods are found to extract the relevant information from the prestimulus activity, or that the negative result might be due to the patients, the electrodes and their po-

sitions or the stimulation protocol. For example, if one compares the strength of the brain-state-dependent modulations of the CCEPs and the influence of the stimulation intensity, one finds that the former are smaller than the effects induced by a change of intensity of 1 mA. As an example, one can consider the graph of the intensity-dependence of the activity of channel 10 in P1 in the first session of this stimulation experiment (figure 6.2). For an intensity of 7 mA, the strongest CCEP peak is found 20 msec after the stimulus with an average amplitude of -64.9 μV. For 6 and 8 mA, the average amplitude at this time point is -42.4 μV and -89.0 μV, respectively, thus a change of 1 mA in intensity corresponds to about 20 μV in amplitude for this particular example. If data from the first and second session of the stimulation screening experiment B.2 is taken, where P1 was stimulated with 7 mA and identical pulse shapes on the same electrode as in this experiment, the same peak in the CCEP at channel 10 with a latency of 20 msec is found. However, the average amplitude of this peak changes only between 3.5 (session 1) and 9.6 (session 2) μV between the *movement* and the *rest* state. Thus, it might be worthwhile to perform the same experiment in the future with intensity steps less than 1 mA or even a random sampling of intensities from a predefined interval. However, due to time constraints and the removal of the external connections with the implanted electrodes, such an experiment could not be conducted.

7 Discussion

The central topic of this thesis was to investigate, whether closed-loop stimulation for the facilitation of the rehabilitation of paralyzed stroke patients is feasible. Two general ideas have been proposed how closed-loop stimulation paradigms can be designed for this purpose: Firstly, brain-state-dependent stimulation, where the timing of the stimulation pulses is coupled to the output of a classifier which detects the intention of the patient to move the paralyzed limb from the brain signals. Secondly, the adaptation of stimulation intensity to the ongoing brain signal with the purpose of producing stable evoked neural activity after stimulation. These two designs have been studied in detail with severely affected stroke patients. The major findings of this thesis are:

- Algorithms for the computation of the brain signal spectrum in the presence of undesirable stimulation after-effects in the brain signal have been designed and compared.

- For the first time, brain-state-dependent stimulation (BSDS) with a continuous detection of the brain state was realized with the help of these algorithms.

- The BSDS paradigm has been shown to be applicable to patients and possible to integrate in a regular rehabilitation training.

- Experiments investigating the relationship between prestimulus and poststimulus brain activity and its interaction with stimulation parameters revealed a small but significant influence of the brain state on the processing of stimulation in the brain.

- If the patient is attempting to move the paralyzed limb, this modulation is strong enough that it can be distinguished from a relaxed state on the level of single pulses. This makes it possible to train a classifier to distinguish movement and rest solely from evoked brain activity.

- However, any direct influence of the EEG/ECoG-signal on the evoked activity before the stimulus, either in the frequency or the time domain, is likely to be very small.

- Although the stimulation intensity is well preserved in the evoked activity of distant brain areas, the interaction between the prestimulus activity and the intensity in the generation of these evoked potentials is again small.

- Hence, closed-loop stimulation to reduce the variance of the evoked brain activity does not seem promising, at least when using ECoG and epidural electrodes.

7.1. Brain-state-dependent stimulation

The BSDS protocol developed here allows a new type of experimental paradigm to investigate the reaction of the brain to cortical stimulation: Similar paradigms used so far have relied on external cues to the participant, but an online control whether the participant actually tries to fulfill the given task has not been employed. By directly decoding the brain state of the stimulated person from the brain signal, one has a tight control of the stimulation timing and can apply stimulation very specifically during the desired brain state. Thus, with this novel protocol, one can investigate whether it is possible by pairing stimulation with a certain brain state to modulate the performance of the participant in this brain state. By monitoring directly the brain signal and using it to guide the stimulation timing, this should be more successful than coupling the stimulation timing simply to external cues. Instead of using what the participant is supposed to do as input and risking that he does not do it properly, one directly uses what the participant actually does or what he wants to do. Thus the stimulation timing should be more specific with the BSDS paradigm and continuous brain state decoding.
What has been shown in this thesis is that stroke patients can control the BSDS paradigm by attempting to move the paralyzed hand. These patients trained with the paradigm first with combined EEG and TMS, then for 4 weeks using implanted epidural electrodes for recording and stimulation. Although we found slight improvements in the hand function of the patients which came to pass over the 4 weeks of the invasive phase (e.g. P1: starting from only being able to perform minimal twitches of the little finger with the left hand at the beginning of the invasive phase, he gradually developed the ability to weakly open and close the left hand voluntarily), the explorative nature of the BSDS paradigm with the cross-over design for testing different stimulation parameters (see section B.1), the number of other procedures conducted with the patients during the invasive period (e.g. other rehabilitation training, other experiments, for example for the decoding of movement-related signals) and the small number of $n = 3$ patients prevent us from drawing a conclusion about whether BSDS actually provides a benefit for the patient. This can only be tested in a randomized, controlled study with a larger number of patients. However, before such a study can be attempted, there should be more research undertaken to

get a better idea about which stimulation parameters are likely to facilitate rehabilitation. The last clinical study on brain stimulation for rehabilitation, the Northstar Everest trial [21, 79, 106, 136] used 50 or 100 Hz stimulation, but it did not yield the desired results. Furthermore, such a high stimulation frequency will not allow BSDS. For example, for 50 Hz stimulation, there is an inter-stimulus interval of 20 msec. As shown in chapter 4 the minimal gap size necessary to cover all after-effects of the stimulation which are detrimental to brain state decoding (stimulation artifact and early evoked activity) needs to be higher than 10 msec, better in the range of 50 msec, therefore no clean EEG/ECoG data would be left over for brain state decoding. As there need to be at least as many samples between successive gaps as the order or the AR model, even a gap size of 10 msec would not be sufficient to fit the model. Hence, other stimulation frequencies need to be tested for a larger trial.

7.2. Controlling the evoked activity

The analysis on the influence of prestimulus brain activity on the shape of the stimulation-evoked activity in chapter 5 and 6 do not support the hypothesis that closed-loop stimulation can reduce the variance of the evoked activity significantly. This is somewhat surprising, as it has been shown by Brugger et al. [23, 24, 25] that such a control is in principle possible. However, there are several important differences between the work of Brugger et al. [23, 24, 25] and this thesis which might account for this discrepancy:

- **Microelectrodes vs epidural electrodes/EEG**: Microelectrodes have a much higher spatial resolution than the larger electrodes employed in this work, allowing the recording of signals from single neurons. For an evoked potential to be recordable by ECoG or EEG, millions of neurons have to fire synchronously [130]. Thus, the recording in the EEG/ECoG case is much less selective than with microelectrodes.

- **Anesthetized vs awake**: The results by Brugger [23] were obtained from anesthetized rats, while the experiments reported here were conducted with awake patients. It has been previously shown, that the reaction of the brain to stimulation during sleep or anesthesia differs strongly from the reaction in awake brains [13, 54, 116]. For example, the brain switches between *up*- and *down*-states during sleep [13] and anesthesia, hence one factor in the results of Brugger [23] might be that the adaptation of the stimulation intensity was able to compensate for these state switches. Towards closed-loop stimulation for stroke rehabilitation, all stimulation pulses would need to be applied within a specific brain state. It has been speculated that at least for TMS-EEG there is only a weak direct connection between the measured brain signal and the

cortical excitability [146], possibly because the spatial resolution of the recording is too low [121]. According to the results of this study, this is similar for ECoG and epidural stimulation. Thus, once the brain-state-dependency of the stimulation effects cannot be exploited by the closed-loop system, the direct relationship between brain activity and evoked activity is too small to allow any noticeable control.

- **Controllable poststimulus time window**: In Brugger et al. [24], the amount of time after a stimulation pulse where a reduction in the variance of the evoked activity could be demonstrated was less than 10 msec. After that, no noticeable effect could be achieved. The amplifier hardware used in this work which was restricted to amplifiers certified for human use, resulted in the contamination of the recorded signal with stimulation artifacts which had a strong influence on the first $\approx$ 5 msec after the stimulus [167], thus a control was likely only for a very short amount of time. However, the hope was that the latency until evoked activity can be recorded on distant electrodes when stimulation and recording is performed with ECoG electrodes (reported by Matsumoto et al. [117] to be greater than 10 msec which was confirmed in this work) would allow us to get around this timing issue.

- **Distance between electrodes**: The electrodes used in this work were spaced 1 cm apart, while for Brugger et al. [24] this distance was only 200 μm. Thus, with the microelectrodes, very local effects were recorded, while the ECoG electrodes even recorded the effects on relatively distant electrodes. While the latter point gives a more global overview over the effects of the stimulation on the brain, it also means that the most local effects can not be recorded.

- **Stimulation intensity**: Brugger et al. [24] tested different intensity ranges and found that only the range with the smallest intensities allowed adaptive stimulation. The intensities used in this work were higher by a factor of 1000 or more. This was necessary because lower intensities, for example in the range of 1 mA, did not produce noticeable effects on any recording electrode (e.g. figure 6.2). Although the intensities used in therapeutic stimulation of patients over epidural or subdural electrodes (e.g. [20, 21, 78]) are slightly smaller than the intensities used in this work, the intensities employed in these clinical studies are still by a factor of at least 100 higher than the intensities used in Brugger et al. [24]. If there is a similar intensity-dependent effect present for stimulation over epidural electrodes which was not found due to the specific set of intensities tested in this work, the possibility of this control scheme is useless as long as the intensities are not optimal for the rehabilitation of the patients.

Thus, a direct replication of the results of the microstimulation experiments using less invasive means was unlikely.

7.3. Using stimulation-evoked activity to optimize open-loop systems

Although a closed-loop control of the stimulation-evoked activity does not seem feasible without using microelectrodes, the shape of the evoked activity still holds information which can be used to optimize open-loop stimulation systems and stroke rehabilitation. First of all, the response of the brain to stimulation in form of the evoked activity can be interpreted as a measure of the connectivity between the stimulated area and the recording area [54, 86, 117, 118, 160]. Thus, analysis of the patterns of evoked activity might help to track during the rehabilitation training of the patients whether changes in the brain connectivity associated with motor function recovery, for example between the supplementary motor area and the primary motor cortex [66] and in the medial motor area [158], occur as expected.
An indication that this is indeed the case has been demonstrated here for P1, where a renormalization of the latency of a subcomponent of evoked activity within the motor area over the course of the rehabilitation training was found. If this can be generalized to further patients, one might be able to specifically define for a patient, how the recovery-associated changes in the pattern of evoked activity will look like and derive from this a target shape to facilitate the generation of the desired changes. Although a direct closed-loop control for this desired activity is unlikely to be possible, the work described here for the decoding of the stimulation intensity from the waveform might allow to compute the stimulation parameter setting such that an open-loop stimulation systems stays close to the target activity.
The additional use of stimulation experiments where stimulation is applied during movement and during rest might be very helpful for the definition of the target activity, because it allows to identify movement-dependent patterns in the evoked activity, thus pinpointing components that are directly associated with the movement of the limb that should be restored.

7.4. Conclusion and outlook

This work has been one of the very first studies on the use of closed-loop cortical stimulation systems for human patients. Before, closed-loop stimulation has been investigated only for the treatment of epilepsy, while in all other clinical applications of stimulation, open-loop system have been employed. The same open-loop approach which seems promising for the treatment of chronic neuropathic pain, namely long pulse trains with 50 Hz frequency applied over the motor cortex, has also been transferred to stroke rehabilitation, however with contradicting results. The closed-loop protocol developed in this work, the use of brain-state-dependent stimulation, provides a new way for how to use stimulation effectively by being more specific in

the stimulation timing than all current approaches. However, the effectivity of this approach for rehabilitation needs to be proven in a controlled study with more patients. In addition, the realization of this BSDS paradigm enables the conduction of many more studies about the topic of highly specific manipulation of the brain by cortical stimulation, timed depending on the actual intentions of the stimulated subject.

The second main question of this thesis was whether it is feasible to use cortical stimulation for more than the modulation of cortical excitability, in particular whether the reaction of the brain to single stimulation pulses can be of direct use. The proposed approach of defining a target pattern of neural activity to be evoked by stimulation might have some merits, because for at least one patient there are correlates of the motor recovery to be found in the shape of the evoked activity. However, an online control of the evoked activity by adaptation of the stimulation intensity to the ongoing brain activity does not seem promising, mainly due to the weak direct link between the pre- and the poststimulus activity. But the strong relationship between the shape of the evoked activity and the applied stimulation intensity might make it possible to at least identify optimal stimulation parameters for the target activity in an open-loop setting. Whether this works in practice has to be tested with more patients.

The use of cortical stimulation for stroke rehabilitation is still in its infancy and a lot more studies with patients are needed before one can think about using cortical stimulation in clinical practice for movement recovery. Although the idea of directly modulating the brain activity in order to facilitate reorganization of the brain is enticing, it has yet to be demonstrated whether such an approach provides a benefit to the patient. If it is found that the specificity of the stimulation is an important factor, then invasive procedures with implanted electrodes, either ECoG as in this work or microelectrodes are the most promising way to go due to the lack of (spatial) specificity of current non-invasive recording and stimulation methods. This, however, means, that one has to carefully weigh the risks associated with the implantation procedure with the expected benefit for the patient. Based on the current results, the improvement with ECoG electrodes is not very large, making it difficult to advocate more implantations. On the other hand, without being able to work with more patients, one gives up the opportunity to improve the currently employed stimulation and rehabilitation paradigms to fully make use of the advantages of implanted electrodes compared to non-invasive techniques. In this work and related works, new paradigms for rehabilitation have been proposed which are at the moment not feasible without invasive recordings, for example the decoding of specific hand movements (opening hand, closing hand,...) instead of just movement versus rest. Thus, more detailed, but small scale studies similar to this, possibly with

stroke patients who have been implanted with ECoG electrodes for other reasons, for example chronic pain [65, 173], might be optimal in order to further refine the rehabilitation and stimulation paradigms and to identify a set of promising parameters. These parameters, given that the beneficial effect for rehabilitation is high enough, can then be tested in a larger patient group. In addition, animal studies might help to gain a deeper understanding about the processes involved in rehabilitation and the interaction of stimulation with the brain. In particular, the lack of a good understanding about the generation of stimulation-evoked brain activity and which parts of it provide meaningful information for stimulation paradigms needs to be overcome in order to specify how stimulation has to be applied.

A Patient characteristics

Patient	Age (y)	Sex	Months since injury	Lesion	Affected area
P1	56	M	80	Basal ganglia hemorrhage	putamen, internal capsule, insula, opercular part of inferior frontal gyrus
P2	52	M	159	MCA territory infarct (frontal)	Frontal lobe including motor cortex (M1), parietal lobe including somatosensory cortex (S1)
P3	63	F	71	Basal ganglia hemorrhage	Head of striate body, lentiform nucleus, thalamus, whole internal capsule, insula, frontal lobe

Table A.1.: Patient characteristics. All patients had an infarct in the right hemisphere (cortical and subcortical), leading to paresis of the left upper limb. Adapted from Walter et al. [172].

B Experiments

In this thesis, results from several experiments are reported. These experiments were conducted together with the Department of Neurosurgery of the University Hospital in Tübingen. This section serves as a reference to describe the individual procedures of the experiments.

B.1. Experiment I: BCI training

This section gives an overview over the BCI training experiments which were designed to support the motor recovery of the patients.

B.1.1. Task

Almost every day (excluding weekends), the patients performed one session of BCI training. Each *session* was divided into individual *runs* with each run consisting of 11 *trials*. Per session, usually about 15 runs were conducted, leading to about 160 trials per session. The participant was sitting in a chair facing a 19" monitor. The left arm of the participant was fixed with two straps, one at the forearm and one around the wrist while magnets at the fingertips connected the left hand to a commercial hand robot (Tyromotion Amadeo HTS, Graz, Austria). This device was controlled by a brain-computer interface (see section B.1.4) and moved the fingers of the inserted hand between an opened and a closed position. In the case of the stroke patients, the range of the movement was adjusted in each session [140] because it was limited by the spasticity of the patient. Each trial of the task consisted of three phases: preparation (2 sec), feedback (6 sec) and rest (8 sec). During preparation, the participant received an auditory cue but was instructed to wait with the execution until the "Go!" command was given at the start of the feedback phase. During the feedback phase, starting with a closed position of the left hand, the participant had to try to open the left hand until the end of the feedback phase. At that point, another auditory cue ("Relax!") was given. During the rest period, the hand of the participant was returned to its original closed position which took about 2-3 seconds and the participant was instructed to relax. This task design was adapted from Ramos-Murguialday et al. [138] who used it in a noninvasive BCI-guided rehabilitation

study with stroke patients, but without stimulation.

B.1.2. Electrophysiological recordings

Both EEG and ECoG were recorded with monopolar amplifiers (BrainAmp DC, BrainProducts, Munich, Germany) with a sampling rate of 1000 Hz and a high-pass filter with a cutoff frequency at 0.16 Hz. For the non-invasive sessions, 32 channels of EEG were recorded with the standard 10-10 system (Fp1, Fp2, F3, Fz, F4, FT7, FC5, FC3, FC1, FC2, FC4, FC6, FT8, C5, C3, C1, Cz, C2, C4, C6, TP7, CP5, CP3, CP1, CPz, CP2, CP4, CP6, TP8, P3, P4, POz), referenced against FCz with circular Ag-AgCl electrodes.
EMG was recorded either with a bipolar amplifier (16-channel BrainAmp ExG, BrainProducts, Munich, Germany) or a monopolar amplifier of the same type as the EEG/ECoG amplifier on both arms from flexor digitorum communis (FDC) and extensor digitorum communis (EDC). On the left arm, additionally signals from the extensor carpi ulnaris (ECU) and the extensor carpi radialis (ECR) were recorded. In some sessions, EMG from left biceps brachii (BB) and left triceps brachii (TB) were recorded as well. During monopolar recordings, the signals were referenced to an electrode on the sensory cortex and bipolarized for offline analysis.

B.1.3. Cortical stimulation

In most sessions, excluding a few sessions with sham stimulation for control, cortical stimulation was applied to the patients. When brain signals were acquired via EEG, TMS was used for stimulation, otherwise epidural electrical stimulation over the implanted electrodes was employed.

TMS

Transcranial stimuli were applied with a neuronavigated TMS device (NeXstim, Helsinki, Finland) using a biphasic figure-of-eight coil. The TMS hotspot and optimal coil angle for MEPs on EDC was located using a standardized cortical mapping procedure [177].

Epidural stimulation

For epidural stimulation, biphasic symmetric pulses with a length of 500 μs were applied monopolarly to one electrode on the grid with a STG 4008 stimulus generator (MultiChannel Systems, Reutlingen, Germany). This stimulator has a maximum output current of 16 mA, 8 independent output channels and its stimulation patterns are freely programmable via a USB interface.

Stimulation parameters

During the 4 weeks of invasive BCI training, stimulation parameters were varied from session to session in order to test different stimulation paradigms on their ability to modulate cortical excitability and plasticity. The following parameters were varied:

- **Location:** Either electrodes over premotor or primary motor cortex were used as stimulation targets. The specific electrode per cortex was chosen as that electrode with the lowest threshold for eliciting MEPs on the left hand extensor muscle EDC, i.e. the electrode covering this part of the motor cortex with the best connection to the paralyzed hand.

- **Number of pulses:** each time the stimulator was triggered, either a single pulse or a double pulse was applied. Control conditions were sham stimulation, where no stimulation was applied, and 50 Hz stimulation, where single pulses with an inter-stimulus interval of 20 msec were applied at an electrode. In the latter condition, no online signal processing of the brain signal could be performed due to the strong artifacts induced by the stimulation and thus the hand of the patient was moved passively by the orthosis. For the double pulse paradigm, two pulses were applied each time with a small, fixed inter-stimulus interval in the range of 10-20 msec. The location of the stimulation electrodes for double pulses was either: both pulses applied on the same electrode (first pulse on primary motor cortex and second pulse on the same electrode (M1/M1) or (PMC/PMC), or on different electrodes (M1/ hyperlinklink:PMCPMC or PMC/M1). In the double pulse paradigm, the first pulse served as a subthreshold conditioning pulse with only 70-75 % of the intensity of the second, suprathreshold pulse. Sub-/suprathreshold refer to the ability of a single pulse to elicit an MEP on the EDC muscle.

- **Polarity:** Stimulation was always applied monopolar, but the cortical electrode could be either the cathode or the anode. The antipole was always a 50x90 mm adhesive electrode placed on the skin of the patient below the left clavicle.

- **Intensity:** The stimulation intensity was adjusted per session for single and double pulse sessions and chosen such that it reliably evoked MEPs on the paralyzed arm without being too disruptive. If the stimulation intensity was chosen too high, the induced muscle could be very distracting or even painful for the participant, hence the intensity was set such that a small, but reliable MEP was found.

- **Contingency with brain signal:** Stimulation could be applied contingent positive to the movement intention (i.e. only when the intention to move was detected, the stimulator was triggered), contingent negative (i.e. stimulation

was only triggered while no intention to move was detected) or independent from the brain signal and the output of the brain state classifier. In all cases, a minimum inter-stimulus interval was defined (usually 500 msec) such that a new stimulus was triggered if at least the minimum inter-stimulus interval had passed since the last stimulus, and if the brain state classifier reported the correct movement state.

Before and after each BCI training session, a MEP mapping of the implanted electrodes was performed. For each electrode, an intensity threshold for the generation of MEPs on the paralyzed arm was determined by repeatedly stimulating each electrode with varying intensities. The change in threshold intensity was interpreted as a measure for the short-term modulation of the efficacy of the cortico-muscular connection (the corticospinal excitability).

B.1.4. Online signal processing

In order to make sure that the participant is actively trying to follow the task to attempt to open the hand, the hand orthosis movements were controlled with an online classificator of the EEG and the ECoG spectrum using the general-purpose brain-computer interface framework BCI2000 (http://www.bci2000.org, [150]). For all participants a classification of spectral power between movement and rest was possible in a frequency band from 16 to 22 Hz over sensorimotor cortex. For online classification, two electrodes were selected that were not strongly influenced by stimulation artifacts or signal drifts. The spectrum was estimated in a sliding window with length 500 msec with a fitted autoregressive model with order 16 for 4 spectral bins with a width of 2 Hz. In hindsight, a higher AR model order might have been more appropriate. The resulting spectral feature $f(t_i) = \sum \log(p_b(t_i))$, where p_b is the spectral power within bin b, was normalized to the mean and variance of f during rest. Because one expects that the spectral power within the β range is smaller during movement than during rest (event-related desynchronization, ERD, [179]), a negative value for the normalized f signifies ERD. The orthosis was controlled by the output of an additional smoothing step in order to reduce the variance of the spectral estimation: Only if $\sum_{j=0}^{5} c(t_i - j) f(t_i - j) < t$ with $c(t_i - j) = \begin{cases} 8 & f(t_i - j) > 0 \\ 1 & \text{else} \end{cases}$ then the movement of the hand robot was started. If the value exceeded t, the movement was stopped. The threshold value t was adjusted individually per patient and session in order to provide a challenge in each experiment.
In order to prevent stimulation artifacts and CCEPs from distorting the spectral estimation, a peak detection algorithm was used to identify the onset of stimuli and removed the strongest after-effects from the signal with linear interpolation prior to spectral estimation. Details of the integration of stimulation in the online BCI have been described in Walter et al. [172] and in chapter 4.

B.2. Experiment II: Stimulation screening

The purpose of the stimulation screening experiment was to investigate the effects of stimulation in different movement-related brain states.

B.2.1. Task

The general setup of a trial and run was the same as the one described for experiment I in section B.1.1. However, instead of the participant always being instructed to attempt to perform the hand movement, three different movement paradigms were tested:

- **Active/attempted movements:** In this paradigm, as the patients were unable to actively perform the movement, so they only had to attempt to open the hand.
- **Imagined movements:** The participants were instructed to imagine opening their hand without actually performing any movements.
- **Passive movements**: The participants were instructed to stay relaxed throughout all conditions. During the movement phase, the hand of the participants was moved passively from a closed to an opened state. This condition served as a control condition, because no change in the brain state of the participants was expected.

For all conditions, the participants received visual feedback of their muscle activity on the computer monitor they were facing. The EMG activity was measured on electrodes of the left extensor digitorum communis (EDC) and displayed in the form of a filled colored circle moving vertically in the middle of the screen. Two horizontal bars defined the target EMG activity the participants had to achieve during the feedback phase. The displayed circle was green if the EMG activity was within these limits and red if this was not the case. Participants were instructed to try to keep the circle green throughout the whole feedback phase while it should return to a 0 % level during the rest phase. Due to the impaired control of the stroke patients of EMG activity on the paralyzed hand, the target EMG level was set to a value that the patients were able to reach comfortably. This level was set commonly between 10 and 40 % of maximal extension for active movement with a range of $\pm$ 10 % and 0 - 10 % for imagined and passive movement. The purpose of this visual feedback was to encourage the patients to produce no muscle activity during *imagined* and *passive* session and to ensure a roughly constant EMG level during *active* movements. Strongly varying EMG activity during active movements would make the analysis of the elicited MEPs problematic, as muscle activity has a direct influence on their amplitude [114].
Due to time constraints, only 33 trials of active movements, 33 trials of imagined

movements and 22 trials of passive movements were conducted per session. The sequence of the trials of these movement conditions was not randomized because it might have been difficult for the patients to follow the instructions. Therefore, all trials of a movement condition were conducted successively. The sequence of the movement conditions was varied in some cases, but usually followed the pattern: First active movements, then imagined, then passive movements.

B.2.2. Electrophysiological recordings

Both EEG and ECoG were recorded with monopolar amplifiers (BrainAmp DC, BrainProducts, Munich, Germany) with a sampling rate of 1000 Hz and a high-pass filter with a cutoff frequency at 0.16 Hz. For the non-invasive sessions, 32 channels of EEG were recorded with the standard 10-10 system, referenced against FCz with circular Ag-AgCl electrodes.
EMG was recorded either with a bipolar amplifier (16-channel BrainAmp ExG, BrainProducts, Munich, Germany) or a monopolar amplifier of the same type as the EEG/ECoG amplifier. EMG was recorded on the left arm and hand from abductor pollicis brevis (APB), first dorsal interosseus (FDI), flexor digitorum communis (FDC), extensor digitorum communis (EDC), extensor carpi ulnaris (ECU), extensor carpi radialis (ECR), biceps brachii (BB) and triceps brachii (TB). During monopolar recordings, the signals were referenced to an electrode on the sensory cortex and bipolarized for offline analysis. This setup was very similar to the recording setup for the BCI training in section B.1.2, but the recording electrodes were the same in all sessions.

B.2.3. Cortical stimulation

TMS

Transcranial stimuli were applied with a neuronavigated TMS device (NeXstim, Helsinki, Finland) using a biphasic figure-of-eight coil. The TMS hotspot and optimal coil angle for MEPs on EDC was located using a standardized cortical mapping procedure [177]. The stimulation intensity was set at 110 % of the resting motor threshold. The inter-stimulus interval (ISI) of successive pulses was set to 3 seconds with a small jitter of $\pm$ 40 msec.

Epidural stimulation

For epidural stimulation we used anodal biphasic symmetric pulses with a length of 500 μs that were applied monopolarly to one electrode on the grid with a STG 4008 stimulus generator (MultiChannel Systems, Reutlingen, Germany). We used a 50x90 mm adhesive electrode under the left clavicle of the patient as cathode. We selected

the stimulation electrode on the grid as the one with the lowest intensity threshold to reliably evoke MEPs on EDC using single-pulse stimulation and held the stimulation intensity fixed within each session at a level that evoked MEPs reliably during rest. In the first session, we used for patient P1 and P2 an intensity of 7 mA and for patient P3 an intensity of 16 mA. For P2 the intensity had to be increased over the course of the following 3 sessions to 10.5, 12.5 and 14.5 mA to get stable MEPs. The pulses were given with a minimum ISI of 2 seconds with a small jitter of $\pm$ 40 msec.

B.2.4. Online signal processing

The online analysis of the brain signals and the control of the orthosis in *active* and *imagined* sessions was conducted in the same way as for the BCI training (section B.1.4). For *passive* sessions, no online processing of the brain signals was performed as the orthosis simply opened the hand of the participants passively during the feedback phase of each trial.

B.3. Experiment III: Single pulses

The purpose of this experiment was to evaluated the effects induced by different choices for the stimulation intensity on the evoked neural activity.

B.3.1. Task

In order to avoid confounding effects due to actions of the patients, the patients were instructed to lie relaxed in bed during the experiment with open eyes. The experiment was conducted with patient P1 (2 sessions) and patient P2 (3 sessions). In each session, 3 electrodes were used for the delivery of single pulse stimulation, one located on the somatosensory, one on the primary motor and one on the premotor cortex. All other electrodes were used to record the evoked neural responses.

B.3.2. Electrophysiological recordings

ECoG signals were recorded with a monopolar amplifier (BrainAmp DC, BrainProducts, Munich, Germany) with a sampling rate of 5000 Hz and a built-in low-pass filter at 1000 Hz. No high-pass filter was used to ensure that hardware filters do not interfere with the shape of the stimulation artifact and the evoked neural potentials. The signal was monitored and the built-in DC-correction of the amplifier was used if the recorded signal threatened to exceed the operating range of the amplifier ($\pm$ 3.27 mV). The ECoG data was referenced to the electrode at the fronto-medial corner of the grid.

B.3.3. Cortical stimulation

For epidural stimulation we used monopolar biphasic symmetric pulses with a length of 500 μs that were applied to one electrode on the grid with a STG4008 stimulus generator (MultiChannel Systems, Reutlingen, Germany) with a 50x90 mm adhesive electrode placed under the left clavicle of the patient acting as the antipole. This electrode also served as the ground electrode for recording. Stimulation intensities were varied in steps of 1 mA between 1 and 8 mA for P1 and the first session of P2 and between 5 and 12 mA for the second and third session of P2. We applied anodal pulses in the first sessions of both patients and the third session of P2 and cathodal pulses in the second sessions. Per session, 100 pulses were given for each intensity in randomized order, in total 800 pulses. The inter-stimulus interval was set to 1 second.

C Abbreviations

Abbreviation	Full name
AIC	Akaike Information Criterion
ALS	Amyotrophic lateral sclerosis
ANOVA	Analysis of variance
AR (model)	Autoregressive (model)
AUC	Area under the (ROC) curve
BCI	Brain-computer interface
BOLD	Blood-oxygen level dependent
BSDS	Brain-state-dependent stimulation
CCEP	Cortico-cortical evoked activity
CV	Cross-validation
DBS	Deep-brain stimulation
ECoG	Electrocorticography
EDC	Extensor digitorum communis (hand extension)
EEG	Electroencephalography
EMG	Electromyography
ERP	Event-related potential
ERD/ERS	Event-related (de-)synchronization
FFT	Fast Fourier Transform
FIFO	First in, first out
fMRI	Functional Magnetic Resonance Imaging
ICMS	Intra-cortical microstimulation
IIR filter	Infinite impulse-response filter
ISI	Inter-stimulus interval
LFP	Local field potentials
LOOE	Leave-one-out error
M1	Primary motor cortex

Abbreviation	Full name
MEA	Multielectrode array
MEG	Magnetoencephalography
MEM	Maximum Entropy Method
MEP	Motor-evoked potential
N100	Negative peak in the EEG, 100 msec after a TMS pulse
NIRS	Near-infrared spectroscopy
P1, P2, P3	Patients
PMC	Premotor cortex
PSD	Power spectral density
RBF	Radial Basis Function
RCT	Randomized controlled trial
RFE	Recursive feature elimination
RKHS	Reproducing Kernel Hilbert Space
RMSE	Root Mean Squared Error
ROC	Receiver Operating Characteristic
S1	Primary Somatosensory Cortex
S1-S7	Healthy participants
SMC	Sensorimotor cortex
SMR	Sensorimotor rhythm
SVM	Support Vector Machine
SVR	Support Vector Regression
tDCS/tACS	Transcranial direct/alternating current stimulation
TMS	Transcranial Magnetic Stimulation

Bibliography

[1] Adkins, D. L., Campos, P., Quach, D., Borromeo, M., Schallert, K., and Jones, T. a. (2006). Epidural cortical stimulation enhances motor function after sensorimotor cortical infarcts in rats. *Experimental Neurology*, 200(2):356–70.

[2] Afshar, P., Khambhati, A., Stanslaski, S., Carlson, D., Jensen, R., Linde, D., Dani, S., Lazarewicz, M., Cong, P., Giftakis, J., Stypulkowski, P., and Denison, T. (2012). A translational platform for prototyping closed-loop neuromodulation systems. *Frontiers in Neural Circuits*, 6(January):117.

[3] Akaike, H. (1974). A new look at statistical model identification. *IEEE Transactions on Automatic Control*, 19(6):716 – 723.

[4] Alonso-Alonso, M., Fregni, F., and Pascual-Leone, A. (2007). Brain stimulation in poststroke rehabilitation. *Cerebrovascular Diseases*, 24 Suppl 1(suppl 1):157–66.

[5] American Clinical Neurophysiology Society (2006). Guideline 5: Guidelines for standard electrode position nomenclature. *Journal of Clinical Neurophysiology*, 23(2):107–10.

[6] Andersen, K. K., Olsen, T. S., Dehlendorff, C., and Kammersgaard, L. P. (2009). Hemorrhagic and ischemic strokes compared: stroke severity, mortality, and risk factors. *Stroke*, 40(6):2068–72.

[7] Ang, K. K., Guan, C., Chua, K. S. G., Ang, B. T., Kuah, C. W. K., Wang, C., Phua, K. S., Chin, Z. Y., and Zhang, H. (2011). A large clinical study on the ability of stroke patients to use an EEG-based motor imagery brain-computer interface. *Clinical EEG and Neuroscience*, 42(4):253–8.

[8] Barker, A. T., Jalinous, R., and Freeston, I. L. (1985). Non-invasive magnetic stimulation of human motor cortex. *Lancet*, 1(8437):1106–7.

[9] Bashashati, A., Fatourechi, M., Ward, R. K., and Birch, G. E. (2007). A survey of signal processing algorithms in brain-computer interfaces based on electrical brain signals. *Journal of Neural Engineering*, 4(2):R32–57.

[10] Benabid, A. L., Pollak, P., Gao, D., Hoffmann, D., Limousin, P., Gay, E., Payen, I., and Benazzouz, A. (1996). Chronic electrical stimulation of the ventralis intermedius nucleus of the thalamus as a treatment of movement disorders. *Journal of Neurosurgery*, 84(2):203–14.

[11] Bender, S., Basseler, K., Sebastian, I., Resch, F., Kammer, T., Oelkers-Ax, R., and Weisbrod, M. (2005). Electroencephalographic response to transcranial magnetic stimulation in children: Evidence for giant inhibitory potentials. *Annals of Neurology*, 58(1):58–67.

[12] Berger, H. (1929). Über das Elektrenkephalogramm des Menschen. *Archiv für Psychiatrie und Nervenkrankheiten*, 87(1):527–570.

[13] Bergmann, T. O., Mölle, M., Schmidt, M. A., Lindner, C., Marshall, L., Born, J., and Siebner, H. R. (2012). EEG-Guided Transcranial Magnetic Stimulation Reveals Rapid Shifts in Motor Cortical Excitability during the Human Sleep Slow Oscillation. *Journal of Neuroscience*, 32(1):243–253.

[14] Birbaumer, N. and Cohen, L. G. (2007). Brain-computer interfaces: communication and restoration of movement in paralysis. *Journal of Physiology*, 579(Pt 3):621–36.

[15] Birbaumer, N., Ghanayim, N., Hinterberger, T., Iversen, I., Kotchoubey, B., Kübler, A., Perelmouter, J., Taub, E., and Flor, H. (1999). A spelling device for the paralysed. *Nature*, 398(6725):297–298.

[16] Bo, L., Wang, L., and Jiao, L. (2007). Recursive Finite Newton Algorithm for Support Vector Regression in the Primal. *Neural Computation*, 19(4):1082–1096.

[17] Bonnard, M., Spieser, L., Meziane, H. B., de Graaf, J. B., and Pailhous, J. (2009). Prior intention can locally tune inhibitory processes in the primary motor cortex: direct evidence from combined TMS-EEG. *The European Journal of Neuroscience*, 30(5):913–23.

[18] Bradberry, T. J., Gentili, R. J., and Contreras-Vidal, J. L. (2010). Reconstructing three-dimensional hand movements from noninvasive electroencephalographic signals. *Journal of Neuroscience*, 30(9):3432–7.

[19] Broersen, P. (2002). Automatic spectral analysis with time series models. *IEEE Transactions on Instrumentation and Measurement*, 51(2):211–216.

[20] Brown, J. (2001). Motor cortex stimulation. *Neurosurgery Focus*, 11(3):1–5.

[21] Brown, J. A., Lutsep, H. L., Weinand, M., and Cramer, S. C. (2006). Motor cortex stimulation for the enhancement of recovery from stroke: a prospective, multicenter safety study. *Neurosurgery*, 58(3):464–73.

[22] Bruckmann, S., Hauk, D., Roessner, V., Resch, F., Freitag, C. M., Kammer, T., Ziemann, U., Rothenberger, A., Weisbrod, M., and Bender, S. (2012). Cortical inhibition in attention deficit hyperactivity disorder: new insights from the electroencephalographic response to transcranial magnetic stimulation. *Brain*, 135(Pt 7):2215–30.

[23] Brugger, D. (2010). *Adaptive microstimulation for stabilizing evoked cortical potentials*. PhD thesis, University of Tübingen.

[24] Brugger, D., Butovas, S., Bogdan, M., and Schwarz, C. (2011). Real-time adaptive microstimulation increases reliability of electrically evoked cortical potentials. *IEEE transactions on bio-medical engineering*, 58(5):1483–91.

[25] Brugger, D., Butovas, S., Bogdan, M., Schwarz, C., and Rosenstiel, W. (2008). Direct and inverse solution for a stimulus adaptation problem using SVR. In *ESANN'2008 proceedings, European Symposium on Artificial Neural Networks*, number April, pages 397–402.

[26] Brugger, D., Rosenstiel, W., and Bogdan, M. (2010). Online SVR Training by Solving the Primal Optimization Problem. *Journal of Signal Processing Systems*, 65(3):391–402.

[27] Buch, E., Weber, C., Cohen, L. G., Braun, C., Dimyan, M. a., Ard, T., Mellinger, J., Caria, A., Soekadar, S., Fourkas, A., and Birbaumer, N. (2008). Think to move: a neuromagnetic brain-computer interface (BCI) system for chronic stroke. *Stroke*, 39(3):910–7.

[28] Burg, J. P. (1975). *Maximum entropy spectral analysis*. PhD thesis, Stanford University.

[29] Campbell, L. J., Sly, D. J., and O'Leary, S. J. (2012). Prediction and control of neural responses to pulsatile electrical stimulation. *Journal of Neural Engineering*, 9(2):026023.

[30] Carmena, J. M., Lebedev, M. A., Crist, R. E., O'Doherty, J. E., Santucci, D. M., Dimitrov, D. F., Patil, P. G., Henriquez, C. S., and Nicolelis, M. A. L. (2003). Learning to control a brain-machine interface for reaching and grasping by primates. *PLoS Biology*, 1(2):193–208.

[31] Casarotto, S., Määttä, S., Herukka, S.-K., Pigorini, A., Napolitani, M., Gosseries, O., Niskanen, E., Könönen, M., Mervaala, E., Rosanova, M., Soininen, H., and Massimini, M. (2011). Transcranial magnetic stimulation-evoked EEG/cortical potentials in physiological and pathological aging. *Neuroreport*, 22(12):592–7.

[32] Casarotto, S., Romero Lauro, L. J., Bellina, V., Casali, A. G., Rosanova, M., Pigorini, A., Defendi, S., Mariotti, M., and Massimini, M. (2010). EEG responses to TMS are sensitive to changes in the perturbation parameters and repeatable over time. *PloS one*, 5(4):e10281.

[33] Chang, C.-C. and Lin, C.-J. (2011). LIBSVM. *ACM Transactions on Intelligent Systems and Technology*, 2(3):1–27.

[34] Chang, M.-W. and Lin, C.-J. (2005). Leave-One-Out Bounds for Support Vector Regression Model Selection. *Neural Computation*, 17(5):1188–1222.

[35] Chapelle, O. (2007). Training a Support Vector Machine in the Primal. *Neural Computation*, 19(5):1155–78.

[36] Chapelle, O. and Vapnik, V. (1999). Model selection for support vector machines. *Advances in Neural Information Processing Systems*, (1).

[37] Chapelle, O., Vapnik, V., Bousquet, O., and Mukherjee, S. (2002). Choosing Multiple Parameters for Support Vector Machines. *Machine Learning*, 46:131–159.

[38] Chapin, J. K., Moxon, K. A., Markowitz, R. S., and Nicolelis, M. A. (1999). Real-time control of a robot arm using simultaneously recorded neurons in the motor cortex. *Nature Neuroscience*, 2(7):664–70.

[39] Cirstea, M. C., Ptito, A., and Levin, M. F. (2003). Arm reaching improvements with short-term practice depend on the severity of the motor deficit in stroke. *Experimental Brain Research*, 152(4):476–88.

[40] Cogan, S. F. (2008). Neural stimulation and recording electrodes. *Annual Review of Biomedical Engineering*, 10:275–309.

[41] Cohen, J. (1988). *Statistical Power Analysis for the Behavioral Sciences (2nd Edition)*. Routledge Academic.

[42] Collinger, J. L., Wodlinger, B., Downey, J. E., Wang, W., Tyler-Kabara, E. C., Weber, D. J., McMorland, A. J., Velliste, M., Boninger, M. L., and Schwartz, A. B. (2012). High-performance neuroprosthetic control by an individual with tetraplegia. *Lancet*, 6736(12):1–8.

[43] Cortes, C. and Vapnik, V. (1995). Support-Vector Networks. *Machine Learning*, 20:273–297.

[44] Couturier, J. L. (2005). Efficacy of rapid-rate repetitive transcranial magnetic stimulation in the treatment of depression: a systematic review and meta-analysis. *Journal of Psychiatry & Neuroscience*, 30(2):83–90.

[45] Cramer, S. C., Nelles, G., Benson, R. R., Kaplan, J. D., Parker, R. A., Kwong, K. K., Kennedy, D. N., Finklestein, S. P., and Rosen, B. R. (1997). A Functional MRI Study of Subjects Recovered From Hemiparetic Stroke. *Stroke*, 28(12):2518–2527.

[46] de Waele, S. and Broersen, P. (2000). The Burg algorithm for segments. *IEEE Transactions on Signal Processing*, 48(10):2876–2880.

[47] Di Lazzaro, V., Oliviero, A., Saturno, E., Pilato, F., Dileone, M., Sabatelli, M., and Tonali, P. a. (2004). Motor cortex stimulation for amyotrophic lateral sclerosis. Time for a therapeutic trial? *Clinical Neurophysiology*, 115(6):1479–85.

[48] Dobelle, W. H. (2000). Artificial vision for the blind by connecting a television camera to the visual cortex. *ASAIO Journal*, 46(1):3–9.

[49] Dobelle, W. H. and Mladejovsky, M. G. (1974). Phosphenes produced by electrical stimulation of human occipital cortex, and their application to the development of a prosthesis for the blind. *Journal of Physiology*, 243(2):553.

[50] Driver, J., Blankenburg, F., Bestmann, S., Vanduffel, W., and Ruff, C. C. (2009). Concurrent brain-stimulation and neuroimaging for studies of cognition. *Trends in Cognitive Sciences*, 13(7):319–327.

[51] Esser, S. K., Hill, S. L., and Tononi, G. (2005). Modeling the effects of transcranial magnetic stimulation on cortical circuits. *Journal of Neurophysiology*, 94(1):622–639.

[52] Fadiga, L., Buccino, G., Craighero, L., Fogassi, L., Gallese, V., and Pavesi, G. (1999). Corticospinal excitability is specifically modulated by motor imagery: a magnetic stimulation study. *Neuropsychologia*, 37(2):147–58.

[53] Fawcett, T. (2006). An introduction to ROC analysis. *Pattern Recognition Letters*, 27(8):861–874.

[54] Ferrarelli, F., Massimini, M., Sarasso, S., Casali, A., Riedner, B. A., Angelini, G., Tononi, G., and Pearce, R. A. (2010). Breakdown in cortical effective connectivity during midazolam-induced loss of consciousness. *PNAS*, 107(6):2681–6.

[55] Ferreri, F., Pasqualetti, P., Määttä, S., Ponzo, D., Ferrarelli, F., Tononi, G., Mervaala, E., Miniussi, C., and Rossini, P. (2011). Human brain connectivity during single and paired pulse transcranial magnetic stimulation. *NeuroImage*, 54(1):90–102.

[56] Fitzgerald, P. B., Fountain, S., and Daskalakis, Z. J. (2006). A comprehensive review of the effects of rTMS on motor cortical excitability and inhibition. *Clinical Neurophysiology*, 117(12):2584–96.

[57] Fitzsimmons, N. A., Drake, W., Hanson, T. L., Lebedev, M. A., and Nicolelis, M. A. L. (2007). Primate reaching cued by multichannel spatiotemporal cortical microstimulation. *Journal of Neuroscience*, 27(21):5593–602.

[58] Fountas, K. N. and Smith, J. R. (2007). Subdural electrode-associated complications: a 20-year experience. *Stereotactic and Functional Neurosurgery*, 85(6):264–272.

[59] Fountas, K. N., Smith, J. R., Murro, A. M., Politsky, J., Park, Y. D., and Jenkins, P. D. (2005). Implantation of a closed-loop stimulation in the management of medically refractory focal epilepsy: a technical note. *Stereotactic and functional neurosurgery*, 83(4):153–8.

[60] Ganguly, K., Dimitrov, D. F., Wallis, J. D., and Carmena, J. M. (2011). Reversible large-scale modification of cortical networks during neuroprosthetic control. *Nature Neuroscience*, 14(5):662–7.

[61] Ganguly, K., Secundo, L., Ranade, G., Orsborn, A., Chang, E. F., Dimitrov, D. F., Wallis, J. D., Barbaro, N. M., Knight, R. T., and Carmena, J. M. (2009). Cortical representation of ipsilateral arm movements in monkey and man. *The Journal of Neuroscience*, 29(41):12948–56.

[62] Georgopoulos, A., Kalaska, J. F., Caminiti, R., and Massey, J. T. (1982). On the relations between the direction of two-dimensional arm movements and cell discharge in primate motor cortex. *Journal of Neuroscience*, 2(11):1527–1537.

[63] Georgopoulos, A., Schwartz, A., and Kettner, R. (1986). Neuronal population coding of movement direction. *Science*, 233(4771):1416–1419.

[64] Gilja, V., Nuyujukian, P., Chestek, C. a., Cunningham, J. P., Yu, B. M., Fan, J. M., Churchland, M. M., Kaufman, M. T., Kao, J. C., Ryu, S. I., and Shenoy, K. V. (2012). A high-performance neural prosthesis enabled by control algorithm design. *Nature Neuroscience*, 15(12):1752–7.

[65] Gomez-Rodriguez, M., Peters, J., Hill, J., Schölkopf, B., Gharabaghi, A., and Grosse-Wentrup, M. (2011). Closing the sensorimotor loop: haptic feedback facilitates decoding of motor imagery. *Journal of Neural Engineering*, 8(3):036005.

[66] Grefkes, C. and Fink, G. R. (2011). Reorganization of cerebral networks after stroke: new insights from neuroimaging with connectivity approaches. *Brain*, 134(Pt 5):1264–76.

[67] Guyon, I. and Elisseeff, A. (2003). An Introduction to Variable and Feature Selection. *Journal of Machine Learning Research*, 3:1157–1182.

[68] Guyon, I., Weston, J., and Barnhill, S. (2002). Gene selection for cancer classification using support vector machines. *Machine Learning*, pages 389–422.

[69] Hampson, R. E., Gerhardt, G. A., Marmarelis, V., Song, D., Opris, I., Santos, L., Berger, T. W., and Deadwyler, S. A. (2012a). Facilitation and restoration of cognitive function in primate prefrontal cortex by a neuroprosthesis that utilizes minicolumn-specific neural firing. *Journal of Neural Engineering*, 9(5):056012.

[70] Hampson, R. E., Song, D., Chan, R. H. M., Sweatt, A. J., Riley, M. R., Goonawardena, A. V., Marmarelis, V. Z., Gerhardt, G. A., Berger, T. W., and Deadwyler, S. A. (2012b). Closing the loop for memory prosthesis: detecting the role of hippocampal neural ensembles using nonlinear models. *IEEE Transactions on Neural Systems and Rehabilitation Engineering*, 20(4):510–25.

[71] Hansen, N. L. and Nielsen, J. B. (2004). The effect of transcranial magnetic stimulation and peripheral nerve stimulation on corticomuscular coherence in humans. *Journal of Physiology*, 561(Pt 1):295–306.

[72] Harris-Love, M. L. and Cohen, L. G. (2006). Noninvasive cortical stimulation in neurorehabilitation: a review. *Archives of Physical Medicine and Rehabilitation*, 87(12 Suppl 2):S84–93.

[73] Hashimoto, R. and Rothwell, J. C. (1999). Dynamic changes in corticospinal excitability during motor imagery. *Experimental brain research*, 125(1):75–81.

[74] Häusler, U. H., Lutzenberger, W., and Birbaumer, N. (1995). Simultaneous recording of slow brain potentials and transcranial magnetix stimulation of hand area in human motor cortex. *Neuroscience Letters*, 200:183–186.

[75] Hebb, D. O. (1949). *The organization of behaviour*. Wiley & Sons.

[76] Hochberg, L. R., Bacher, D., Jarosiewicz, B., Masse, N. Y., Simeral, J. D., Vogel, J., Haddadin, S., Liu, J., Cash, S. S., van der Smagt, P., and Donoghue, J. P. (2012). Reach and grasp by people with tetraplegia using a neurally controlled robotic arm. *Nature*, 485(7398):372–5.

[77] Hochberg, L. R., Serruya, M. D., Friehs, G. M., Mukand, J. A., Saleh, M., Caplan, A. H., Branner, A., Chen, D., Penn, R. D., and Donoghue, J. P. (2006). Neuronal ensemble control of prosthetic devices by a human with tetraplegia. *Nature*, 442(7099):164–171.

[78] Holsheimer, J., Nguyen, J.-P., Lefaucheur, J.-P., and Manola, L. (2007). Cathodal, anodal or bifocal stimulation of the motor cortex in the management of chronic pain? *Acta Neurochirurgica. Supplement*, 97(Pt 2):57–66.

[79] Huang, M., Harvey, R. L., Stoykov, M. E., Ruland, S., Weinand, M., Lowry, D., and Levy, R. (2008). Cortical stimulation for upper limb recovery following ischemic stroke: a small phase II pilot study of a fully implanted stimulator. *Topics in stroke rehabilitation*, 15(2):160–72.

[80] Hummel, F., Celnik, P., Giraux, P., Floel, A., Wu, W.-H., Gerloff, C., and Cohen, L. G. (2005). Effects of non-invasive cortical stimulation on skilled motor function in chronic stroke. *Brain*, 128(Pt 3):490–9.

[81] Hummel, F. and Cohen, L. (2006). Non-invasive brain stimulation: a new strategy to improve neurorehabilitation after stroke? *The Lancet Neurology*, 5(8):708–712.

[82] Hunter, S. and Crome, P. (2002). Hand function and stroke. *Reviews in Clinical Gerontology*, 12(01).

[83] Ilmoniemi, R. and Kičić, D. (2010). Methodology for combined TMS and EEG. *Brain Topography*, 22(4):233–248.

[84] Jackson, A., Mavoori, J., and Fetz, E. (2006). Long-term motor cortex plasticity induced by an electronic neural implant - supplementary. *Nature*, 444(7115):56–60.

[85] Jensen, O., Bahramisharif, A., Oostenveld, R., Klanke, S., Hadjipapas, A., Okazaki, Y. O., and van Gerven, M. A. J. (2011). Using brain-computer interfaces and brain-state dependent stimulation as tools in cognitive neuroscience. *Frontiers in Psychology*, 2(May):1–11.

[86] Johnson, J. S., Kundu, B., Casali, A. G., and Postle, B. R. (2012). Task-dependent changes in cortical excitability and effective connectivity: A combined TMS-EEG study. *Journal of Neurophysiology*, (February):2383–2392.

[87] Kakei, S., Hoffman, D. S., and Strick, P. L. (1999). Muscle and movement representations in the primary motor cortex. *Science*, 285(5436):2136–9.

[88] Kammer, T. and Thielscher, A. (2003). Physikalische und physiologische Grundlagen der transkraniellen Magnetstimulation. *Nervenheilkunde*, 4:168–176.

[89] Kantak, S. S., Stinear, J. W., Buch, E. R., and Cohen, L. G. (2011). Rewiring the Brain: Potential Role of the Premotor Cortex in Motor Control, Learning, and Recovery of Function Following Brain Injury. *Neurorehabilitation and Neural Repair*, 26(3):282–292.

[90] Kay, S. and Marple, S. (1981). Spectrum analysis - A modern perspective. *Proceedings of the IEEE*, 69(11):1380–1419.

[91] Kiers, L., Clouston, P., Chiappa, K. H., and Cros, D. (1995). Assessment of cortical motor output: compound muscle action potential versus twitch force recording. *Electroencephalography and Clinical Neurophysiology*, 97(2):131–9.

[92] Kinoshita, M., Ikeda, A., Matsuhashi, M., Matsumoto, R., Hitomi, T., Begum, T., Usui, K., Takayama, M., Mikuni, N., Miyamoto, S., Hashimoto, N., and Shibasaki, H. (2005). Electric cortical stimulation suppresses epileptic and background activities in neocortical epilepsy and mesial temporal lobe epilepsy. *Clinical Neurophysiology*, 116(6):1291–9.

[93] Kinoshita, M., Ikeda, A., Matsumoto, R., Begum, T., Usui, K., Yamamoto, J., Matsuhashi, M., Takayama, M., Mikuni, N., Takahashi, J., Miyamoto, S., and Shibasaki, H. (2004). Electric stimulation on human cortex suppresses fast cortical activity and epileptic spikes. *Epilepsia*, 45(7):787–91.

[94] Kobayashi, M., Hutchinson, S., Schlaug, G., and Pascual-Leone, A. (2003). Ipsilateral motor cortex activation on functional magnetic resonance imaging during unilateral hand movements is related to interhemispheric interactions. *NeuroImage*, 20(4):2259–70.

[95] Kohavi, R. and John, G. H. (1997). Wrappers for feature subset selection. *Artificial Intelligence*, 97(97):273–324.

[96] Kolominsky-Rabas, P. L., Heuschmann, P. U., Marschall, D., Emmert, M., Baltzer, N., Neundörfer, B., Schöffski, O., and Krobot, K. J. (2006). Lifetime Cost of Ischemic Stroke in Germany: Results and National Projections From a Population-Based Stroke Registry: The Erlangen Stroke Project. *Stroke*, 37(5):1179–1183.

[97] Komssi, S., Aronen, H. J., Huttunen, J., Kesäniemi, M., Soinne, L., Nikouline, V. V., Ollikainen, M., Roine, R. O., Karhu, J., Savolainen, S., and Ilmoniemi, R. J. (2002). Ipsi- and contralateral EEG reactions to transcranial magnetic stimulation. *Clinical Neurophysiology*, 113(2):175–84.

[98] Komssi, S., Kähkönen, S., and Ilmoniemi, R. J. (2004). The effect of stimulus intensity on brain responses evoked by transcranial magnetic stimulation. *Human Brain Mapping*, 21(3):154–64.

[99] Kubánek, J., Miller, K. J., Ojemann, J. G., Wolpaw, J. R., and Schalk, G. (2009). Decoding flexion of individual fingers using electrocorticographic signals in humans. *Journal of Neural Engineering*, 6(6):066001.

[100] Kübler, A., Nijboer, F., Mellinger, J., Vaughan, T. M., Pawelzik, H., Schalk, G., McFarland, D. J., Birbaumer, N., and Wolpaw, J. R. (2005). Patients with ALS can use sensorimotor rhythms to operate a brain-computer interface. *Neurology*, 64(10):1775–1777.

[101] Kundu, B., Sutterer, D. W., Emrich, S. M., and Postle, B. R. (2013). Strengthened effective connectivity underlies transfer of working memory training to tests of short-term memory and attention. *The Journal of neuroscience : the official journal of the Society for Neuroscience*, 33(20):8705–15.

[102] Kwakkel, G., Kollen, B. J., van der Grond, J., and Prevo, A. J. H. (2003). Probability of regaining dexterity in the flaccid upper limb: impact of severity of paresis and time since onset in acute stroke. *Stroke*, 34(9):2181–6.

[103] Langhorne, P., Coupar, F., and Pollock, A. (2009). Motor recovery after stroke: a systematic review. *Lancet Neurology*, 8(8):741–54.

[104] Lefaucheur, J.-P. and de Andrade, D. C. (2009). Intraoperative neurophysiologic mapping of the central cortical region for epidural electrode placement in the treatment of neuropathic pain by motor cortex stimulation. *Brain Stimulation*, 2(3):138–148.

[105] Levin, M. F., Kleim, J. A., and Wolf, S. L. (2009). What do motor "recovery" and "compensation" mean in patients following stroke? *Neurorehabilitation and neural repair*, 23(4):313–9.

[106] Levy, R., Ruland, S., Weinand, M., Lowry, D., Dafer, R., and Bakay, R. (2008). Cortical stimulation for the rehabilitation of patients with hemiparetic stroke: a multicenter feasibility study of safety and efficacy. *Journal of Neurosurgery*, 108(4):707–14.

[107] Li, S., Stevens, J. A., and Rymer, W. Z. (2009). Interactions between imagined movement and the initiation of voluntary movement: a TMS study. *Clinical Neurophysiology*, 120(6):1154–1160.

[108] Liepert, J., Bauder, H., Miltner, W., Taub, E., and Weiller, C. (2000). Treatment-induced cortical reorganization after stroke in humans. *Stroke*, 31(6):1210–1216.

[109] Lima, M. C. and Fregni, F. (2008). Motor cortex stimulation for chronic pain: systematic review and meta-analysis of the literature. *Neurology*, 70(24):2329–37.

[110] Liu, J., Khalil, H. K., and Oweiss, K. G. (2011). Neural Feedback for Instantaneous Spatiotemporal Modulation of Afferent Pathways in Bi-Directional Brain–Machine Interfaces. *IEEE Transactions on Neural Systems and Rehabilitation Engineering*, 19(5):521–533.

[111] Lomb, N. R. (1976). Least-squares frequency analysis of unequally spaced data. *Astrophysics and Space Science*, 39(2):447–462.

[112] Lotte, F., Congedo, M., Lécuyer, A., Lamarche, F., and Arnaldi, B. (2007). A review of classification algorithms for EEG-based brain–computer interfaces. *Journal of Neural Engineering*, 4(2):R1–R13.

[113] Mackay, J. and Mensah, G. (2004). *The Atlas of Heart Disease and Stroke*. World Health Organization.

[114] MacKinnon, C. D. and Rothwell, J. C. (2000). Time-varying changes in corticospinal excitability accompanying the triphasic EMG pattern in humans. *The Journal of physiology*, 528(Pt 3):633–45.

[115] Marzullo, T. C., Lehmkuhle, M. J., Gage, G. J., and Kipke, D. R. (2010). Development of Closed-Loop Neural Interface Technology in a Rat Model: Combining Motor Cortex Operant Conditioning With Visual Cortex Microstimulation. *IEEE Transactions on Neural Systems and Rehabilitation Engineering*, 18(2):117–126.

[116] Massimini, M., Ferrarelli, F., Huber, R., Esser, S. K., Singh, H., and Tononi, G. (2005). Breakdown of cortical effective connectivity during sleep. *Science*, 309(5744):2228–32.

[117] Matsumoto, R., Nair, D. R., LaPresto, E., Bingaman, W., Shibasaki, H., and Lüders, H. O. (2007). Functional connectivity in human cortical motor system: a cortico-cortical evoked potential study. *Brain*, 130(Pt 1):181–97.

[118] Matsumoto, R., Nair, D. R., LaPresto, E., Najm, I., Bingaman, W., Shibasaki, H., and Lüders, H. O. (2004). Functional connectivity in the human language system: a cortico-cortical evoked potential study. *Brain*, 127(Pt 10):2316–30.

[119] McFarland, D. J. and Wolpaw, J. R. (2008). Sensorimotor rhythm-based brain-computer interface (BCI): model order selection for autoregressive spectral analysis. *Journal of Neural Engineering*, 5(2):155–62.

[120] Miller, K. J., Zanos, S., Fetz, E. E., den Nijs, M., and Ojemann, J. G. (2009). Decoupling the cortical power spectrum reveals real-time representation of individual finger movements in humans. *Journal of Neuroscience*, 29(10):3132–7.

[121] Mitchell, K., Baker, M. R., and Baker, S. N. (2007). Muscle responses to transcranial stimulation in man depend on background oscillatory activity. *Journal of Physiology*, 583(Pt 2):567–579.

[122] Morbidi, F., Garulli, A., Prattichizzo, D., Rizzo, C., Manganotti, P., and Rossi, S. (2007). Off-line removal of TMS-induced artifacts on human electroencephalography by Kalman filter. *Journal of Neuroscience Methods*, 162(1-2):293–302.

[123] Morishima, Y., Akaishi, R., Yamada, Y., Okuda, J., Toma, K., and Sakai, K. (2009). Task-specific signal transmission from prefrontal cortex in visual selective attention. *Nature Neuroscience*, 12(1):85–91.

[124] Morrell, M. J. (2011). Responsive cortical stimulation for the treatment of medically intractable partial epilepsy. *Neurology*, 77(13):1295–304.

[125] Nakayama, H., Jø rgensen, H. S., Raaschou, H. O., and Olsen, T. S. (1994). Recovery of upper extremity function in stroke patients: the Copenhagen Stroke Study. *Archives of physical medicine and rehabilitation*, 75(4):394–8.

[126] Nguyen, J. P., Lefaucheur, J. P., Decq, P., Uchiyama, T., Carpentier, A., Fontaine, D., Brugières, P., Pollin, B., Fève, A., Rostaing, S., Cesaro, P., and Keravel, Y. (1999). Chronic motor cortex stimulation in the treatment of central and neuropathic pain. Correlations between clinical, electrophysiological and anatomical data. *Pain*, 82(3):245–51.

[127] Niedermeyer, E. and Lopes da Silva, F. (2004). *Electroencephalography: Basic Principles, Clinical Applications, and Related Fields*. Lippincott Williams & Wilkins.

[128] Nikulin, V. V., Kicić, D., Kähkönen, S., and Ilmoniemi, R. J. (2003). Modulation of electroencephalographic responses to transcranial magnetic stimulation: evidence for changes in cortical excitability related to movement. *The European Journal of Neuroscience*, 18(5):1206–12.

[129] Nowak, D. A., Grefkes, C., Ameli, M., and Fink, G. R. (2009). Interhemispheric competition after stroke: brain stimulation to enhance recovery of function of the affected hand. *Neurorehabilitation and Neural Repair*, 23(7):641–656.

[130] Nunez, P. L. and Srinivasan, R. (2006). *Electric Fields of the Brain: The Neurophysics of EEG*. Oxford University Press, Inc., 2 edition.

[131] O'Doherty, J. E., Lebedev, M. A., Hanson, T. L., Fitzsimmons, N. A., and Nicolelis, M. A. L. (2009). A brain-machine interface instructed by direct intracortical microstimulation. *Frontiers in Integrative Neuroscience*, 3(September):1–10.

[132] Ostrowsky, K., Magnin, M., Ryvlin, P., Isnard, J., Guenot, M., and Mauguière, F. (2002). Representation of pain and somatic sensation in the human insula: a study of responses to direct electrical cortical stimulation. *Cerebral Cortex*, 12(4):376–85.

[133] Pardey, J., Roberts, S., and Tarassenko, L. (1996). A review of parametric modelling techniques for EEG analysis. *Medical Engineering & Physics*, 18(1):2–11.

[134] Penfield, W. and Jasper, H. (1954). *Epilepsy and the Functional Anatomy of the Human Brain*. Churchill.

[135] Pfurtscheller, G. and Lopes da Silva, F. H. (1999). Event-related EEG/MEG synchronization and desynchronization: basic principles. *Clinical Neurophysiology*, 110(11):1842–57.

[136] Plow, E. B., Carey, J. R., Nudo, R. J., and Pascual-Leone, A. (2009). Invasive cortical stimulation to promote recovery of function after stroke: a critical appraisal. *Stroke*, 40(5):1926–31.

[137] Pogosyan, A., Gaynor, L. D., Eusebio, A., and Brown, P. (2009). Boosting cortical activity at Beta-band frequencies slows movement in humans. *Current Biology*, 19(19):1637–1641.

[138] Ramos-Murguialday, A., Broetz, D., Rea, M., Läer, L., Yilmaz, O., Brasil, F. L., Liberati, G., Curado, M. R., Garcia-Cossio, E., Vyziotis, A., Cho, W., Agostini, M., Soares, E., Soekadar, S., Caria, A., Cohen, L. G., and Birbaumer, N. (2013a). Brain-machine-interface in chronic stroke rehabilitation: A controlled study. *Annals of Neurology*, 74(1):100–108.

[139] Ramos-Murguialday, A., Garcia-Cossio, E., Walter, A., Cho, W., Broetz, D., Bogdan, M., Cohen, L. G., and Birbaumer, N. (2013b). Detecting paretic arm motions intention through muscle activity decoding in severe chronic stroke. *Brain*, (Submitted).

[140] Ramos-Murguialday, A., Schürholz, M., Caggiano, V., Wildgruber, M., Caria, A., Hammer, E. M., Halder, S., and Birbaumer, N. (2012). Proprioceptive Feedback and Brain Computer Interface (BCI) Based Neuroprostheses. *PloS one*, 7(10):e47048.

[141] Rebesco, J. M. and Miller, L. E. (2011). Enhanced detection threshold for in vivo cortical stimulation produced by Hebbian conditioning. *Journal of Neural Engineering*, 8(1):016011.

[142] Rebesco, J. M., Stevenson, I. H., Körding, K. P., Solla, S. A., and Miller, L. E. (2010). Rewiring neural interactions by micro-stimulation. *Frontiers in Systems Neuroscience*, 4(August):1–15.

[143] Rolston, J. D., Desai, S. A., Laxpati, N. G., and Gross, R. E. (2011). Electrical stimulation for epilepsy: experimental approaches. *Neurosurgery clinics of North America*, 22(4):425–42, v.

[144] Romei, V., Brodbeck, V., Michel, C., Amedi, A., Pascual-Leone, A., and Thut, G. (2008). Spontaneous fluctuations in posterior alpha-band EEG activity reflect variability in excitability of human visual areas. *Cerebral Cortex*, 18(9):2010–8.

[145] Rosanova, M., Casali, A., Bellina, V., Resta, F., Mariotti, M., and Massimini, M. (2009). Natural frequencies of human corticothalamic circuits. *Journal of Neuroscience*, 29(24):7679–7685.

[146] Rosanova, M., Gosseries, O., Casarotto, S., Boly, M., Casali, A. G., Bruno, M.-A., Mariotti, M., Boveroux, P., Tononi, G., Laureys, S., and Massimini, M. (2012). Recovery of cortical effective connectivity and recovery of consciousness in vegetative patients. *Brain*, 135:1308–1320.

[147] Rouse, A. G., Stanslaski, S. R., Cong, P., Jensen, R. M., Afshar, P., Ullestad, D., Gupta, R., Molnar, G. F., Moran, D. W., and Denison, T. J. (2011). A chronic generalized bi-directional brain-machine interface. *Journal of Neural Engineering*, 8(3):036018.

[148] Rzesnitzek, L., Wächter, T., Krüger, R., Gharabaghi, A., and Plewnia, C. (2011). Suppression of extrapyramidal side effects of doxepin by thalamic deep brain stimulation for Tourette syndrome. *Neurology*, 77(18):1708–9.

[149] Schalk, G., Kubánek, J., Miller, K. J., Anderson, N. R., Leuthardt, E. C., Ojemann, J. G., Limbrick, D., Moran, D., Gerhardt, L. a., and Wolpaw, J. R. (2007). Decoding two-dimensional movement trajectories using electrocorticographic signals in humans. *Journal of Neural Engineering*, 4(3):264–75.

[150] Schalk, G., McFarland, D. J., Hinterberger, T., Birbaumer, N., and Wolpaw, J. R. (2004). BCI2000: a general-purpose brain-computer interface (BCI) system. *IEEE Transations on Biomedical Engineering*, 51(6):1034–1043.

[151] Schmidt, E. M., Bak, M. J., Hambrecht, F. T., Kufta, C. V., O'Rourke, D. K., and Vallabhanath, P. (1996). Feasibility of a visual prosthesis for the blind based on intracortical microstimulation of the visual cortex. *Brain*, 119(2):507–22.

[152] Schölkopf, B. and Smola, A. J. (2001). Learning with Kernels: Support Vector Machines, Regularization, Optimization, and Beyond.

[153] Schulz, H., Ubelacker, T., Keil, J., Müller, N., and Weisz, N. (2013). Now I am Ready–Now I am not: The Influence of Pre-TMS Oscillations and Corticomuscular Coherence on Motor-Evoked Potentials. *Cerebral cortex*.

[154] Slutzky, M. W., Jordan, L. R., Krieg, T., Chen, M., Mogul, D. J., and Miller, L. E. (2010). Optimal spacing of surface electrode arrays for brain-machine interface applications. *Journal of Neural Engineering*, 7(2):26004.

[155] Spüler, M., Walter, A., Rosenstiel, W., and Bogdan, M. (2013). Spatial filtering based on Canonical Correlation analysis improves classification of evoked or event-related potentials in EEG data. *IEEE Transactions on Neural Systems and Rehabilitation Engineering*, Accepted.

[156] Stacey, W. C. and Litt, B. (2008). Technology insight: neuroengineering and epilepsy-designing devices for seizure control. *Nature Clinical Practice. Neurology*, 4(4):190–201.

[157] Stagg, C. J., Bachtiar, V., O'Shea, J., Allman, C., Bosnell, R. a., Kischka, U., Matthews, P. M., and Johansen-Berg, H. (2011). Cortical activation changes underlying stimulation-induced behavioural gains in chronic stroke. *Brain*, (2011):276–284.

[158] Strens, L., Asselman, P., Pogosyan, A., and Loukas, C. (2004). Corticocortical coupling in chronic stroke. *Neurology*, 63(3):475–484.

[159] Tenore, F. V. G., Ramos, A., Fahmy, A., Acharya, S., Etienne-Cummings, R., and Thakor, N. V. (2009). Decoding of individuated finger movements using surface electromyography. *IEEE Transactions on Bio-medical Engineering*, 56(5):1427–34.

[160] Terada, K., Usui, N., Umeoka, S., Baba, K., Mihara, T., Matsuda, K., Tottori, T., Agari, T., Nakamura, F., and Inoue, Y. (2008). Interhemispheric connection of motor areas in humans. *Journal of Clinical Neurophysiology*, 25(6):351–6.

[161] Teskey, G. C., Flynn, C., Goertzen, C. D., Monfils, M. H., and Young, N. A. (2003). Cortical stimulation improves skilled forelimb use following a focal ischemic infarct in the rat. *Neurological Research*, 25(8):794–800.

[162] Tsubokawa, T., Katayama, Y., Yamamoto, T., Hirayama, T., and Koyama, S. (1991). Chronic motor cortex stimulation for the treatment of central pain. *Acta Neurochirurgica Supplement*, 52:137–139.

[163] Valentin, A., Arunachalam, R., Mesquita-Rodrigues, A., Garcia Seoane, J. J., Richardson, M. P., Mills, K. R., and Alarcon, G. (2008). Late EEG responses triggered by transcranial magnetic stimulation (TMS) in the evaluation of focal epilepsy. *Epilepsia*, 49(3):470–80.

[164] Van Der Werf, Y. D. and Paus, T. (2006). The neural response to transcranial magnetic stimulation of the human motor cortex. I. Intracortical and cortico-cortical contributions. *Experimental Brain Research*, 175(2):231–245.

[165] van Elswijk, G., Maij, F., Schoffelen, J.-M., Overeem, S., Stegeman, D. F., and Fries, P. (2010). Corticospinal beta-band synchronization entails rhythmic gain modulation. *Journal of Neuroscience*, 30(12):4481–4488.

[166] Vapnik, V. and Chapelle, O. (2000). Bounds on Error Expectation for Support Vector Machines. In *Advances in Large Margin Classifiers*, volume 12, pages 2013–36.

[167] Veniero, D., Bortoletto, M., and Miniussi, C. (2009). TMS-EEG co-registration: on TMS-induced artifact. *Clinical Neurophysiology*, 120(7):1392–1399.

[168] Vidaurre, C. and Blankertz, B. (2010). Towards a cure for BCI illiteracy. *Brain Topography*, 23(2):194–8.

[169] Wagner, T., Fregni, F., Eden, U., and Ramos-Estebanez, C. (2006). Transcranial magnetic stimulation and stroke: a computer-based human model study. *NeuroImage*, 30:857–870.

[170] Wagner, T., Valero-Cabre, A., and Pascual-Leone, A. (2007). Noninvasive human brain stimulation. *Annual Review of Biomedical Engineering*, 9(April):527–65.

[171] Walter, A., Bensch, M., Brugger, D., Rosenstiel, W., Bogdan, M., Birbaumer, N., and Gharabaghi, A. (2009). BCCI - a bidirectional cortical communication interface. In *Proceedings of the International Joint Conference on Computational Intelligence*, pages 440–445, Funchal, Madeira.

[172] Walter, A., Murguialday, A. R., Spüler, M., Naros, G., Leão, M. T., Gharabaghi, A., Rosenstiel, W., Birbaumer, N., and Bogdan, M. (2012a). Coupling BCI and cortical stimulation for brain-state-dependent stimulation: methods for spectral estimation in the presence of stimulation after-effects. *Frontiers in Neural Circuits*, 6(87).

[173] Walter, A., Naros, G., Roth, A., Rosenstiel, W., Gharabaghi, A., and Bogdan, M. (2012b). A brain-computer interface for chronic pain patients using epidural ECoG and visual feedback. In *Proceedings of the 2012 IEEE 12th International conference on Bioinformatics & Bioengineering (BIBE)*, number November, pages 380–385, Larnaca, Cyprus.

[174] Walter, A., Naros, G., Spüler, M., Gharabaghi, A., Rosenstiel, W., and Bogdan, M. (2013a). Decoding stimulation intensity from evoked ECoG activity. *Neurocomputing*, Accepted.

[175] Walter, A., Naros, G., Spüler, M., Gharabaghi, A., Rosenstiel, W., and Bogdan, M. (2013b). Decoding stimulation intensity from evoked ECoG activity using support vector regression. In *Proceedings of the ESANN 2013*, pages 321–326, Bruges, Belgium.

[176] Walter, A., Naros, G., Spüler, M., Rosenstiel, W., Gharabaghi, A., and Bogdan, M. (2013c). Dynamics of a Stimulation-evoked ECoG Potential During Stroke Rehabilitation - A Case Study. In *NEUROTECHNIX 2013 - International Congress on Neurotechnology, Electronics and Informatics*, pages 241–248, Vilamoura, Portugal.

[177] Wassermann, E., Epstein, C., and Ziemann, U. (2008). *Oxford Handbook of Transcranial Stimulation (Oxford Handbooks)*. Oxford University Press, USA.

[178] Weiss, D., Breit, S., Wächter, T., Plewnia, C., Gharabaghi, A., and Krüger, R. (2011). Combined stimulation of the substantia nigra pars reticulata and the subthalamic nucleus is effective in hypokinetic gait disturbance in Parkinson's disease. *Journal of Neurology*, 258(6):1183–5.

[179] Wolpaw, J. R., Birbaumer, N., McFarland, D. J., Pfurtscheller, G., and Vaughan, T. M. (2002). Brain-computer interfaces for communication and control. *Clinical Neurophysiology*, 113(6):767–791.

[180] Woody, C. D. (1967). Characterization of an adaptive filter for the analysis of variable latency neuroelectric signals. *Medical & Biological Engineering*, 5(6):539–554.

[181] Yanagisawa, T., Hirata, M., Saitoh, Y., Goto, T., Kishima, H., Fukuma, R., Yokoi, H., Kamitani, Y., and Yoshimine, T. (2011). Real-time control of a prosthetic hand using human electrocorticography signals. *Journal of Neurosurgery*, 114(6):1715–22.